

Spring 2002

Behavior of nano-engineered platelets in a coronary artery stenosis model

Hua Ai

Follow this and additional works at: <https://digitalcommons.latech.edu/dissertations>

 Part of the [Biomedical Engineering and Bioengineering Commons](#)

INFORMATION TO USERS

This manuscript has been reproduced from the microfilm master. UMI films the text directly from the original or copy submitted. Thus, some thesis and dissertation copies are in typewriter face, while others may be from any type of computer printer.

The quality of this reproduction is dependent upon the quality of the copy submitted. Broken or indistinct print, colored or poor quality illustrations and photographs, print bleedthrough, substandard margins, and improper alignment can adversely affect reproduction.

In the unlikely event that the author did not send UMI a complete manuscript and there are missing pages, these will be noted. Also, if unauthorized copyright material had to be removed, a note will indicate the deletion.

Oversize materials (e.g., maps, drawings, charts) are reproduced by sectioning the original, beginning at the upper left-hand corner and continuing from left to right in equal sections with small overlaps.

Photographs included in the original manuscript have been reproduced xerographically in this copy. Higher quality 6" x 9" black and white photographic prints are available for any photographs or illustrations appearing in this copy for an additional charge. Contact UMI directly to order.

ProQuest Information and Learning
300 North Zeeb Road, Ann Arbor, MI 48106-1346 USA
800-521-0600

UMI[®]

BEHAVIOR OF NANO-ENGINEERED PLATELETS IN
A CORONARY ARTERY STENOSIS MODEL

by

Hua Ai, B.M

A Dissertation Presented in Partial Fulfillment
of the Requirements for the Degree
Doctor of Philosophy

COLLEGE OF ENGINEERING AND SCIENCE
LOUISIANA TECH UNIVERSITY

May 2002

UMI Number: 3043600

UMI[®]

UMI Microform 3043600

Copyright 2002 by ProQuest Information and Learning Company.
All rights reserved. This microform edition is protected against
unauthorized copying under Title 17, United States Code.

ProQuest Information and Learning Company
300 North Zeeb Road
P.O. Box 1346
Ann Arbor, MI 48106-1346

LOUISIANA TECH UNIVERSITY

THE GRADUATE SCHOOL

April 17, 2002

Date

We hereby recommend that the dissertation prepared under our supervision

by Hua Ai

entitled Behavior of Nano-Engineered Platelets in a Coronary Artery

Stenosis Model

be accepted in partial fulfillment of the requirements for the degree of

Doctor of Philosophy in Biomedical Engineering

Steven Jones
Supervisor of Thesis Research

Stan Nappa
Head of Department

Biomedical Engineering
Department

Recommendation concurred in:

Roger Schubert

Stan Nappa

David Mills

G. H. H.

Advisory Committee

Approved: Bala Samarasekera
Director of Graduate Studies

Approved: William M. Melonathy
Director of the Graduate school

Leslie Grice
Dean of the College

GS Form 13
(1/00)

ABSTRACT

Cardiovascular disease is the leading cause of death in North America. Cardiac infarction caused by thrombus plaque rupture can often lead to sudden death. Arterial stenosis caused by atherosclerosis is an important precursor leading to thrombus formation. Shear stress, abnormal lipid metabolism, and subendothelial layer exposure are the major contributors to arterial thrombus formation. Platelet activation by the above factors, followed by adhesion is the basic sequence in thrombus formation.

Platelets were encapsulated with nanofilm in order to reduce platelet activation and adhesion under high shear stress. Polyions, nanoparticles and immunoglobulins were assembled in nano-organized shells on fixed bovine platelets through the electrostatic layer-by-layer (LbL) self-assembly technique. The coverage of 78-nm silica and 45-nm fluorescent nanospheres on platelets was studied under TEM or fluorescence microscopes. An IgG-layer was adsorbed on platelets in alternation with poly(styrenesulfonate), and its specific immune-recognition and targeting with fluorescent anti-IgG-FITC were demonstrated. Not only limited to fixed platelets, live platelets were also coated with polyions with a outermost layer of heparin. Most platelets were alive and not activated after the coating procedure and no obvious cytotoxicity was observed.

A coronary artery stenosis silicone model was built to test encapsulated platelet function under high shear stress generated by the stenosis. In the platelet activation study,

encapsulated platelets released less TXB₂ compared with unmodified platelets. Platelets with heparin coating were not that easily adhered onto collage substrate in silicone model after the flow experiment. The heparin shell might block the possible binding reactions between collagen and platelet surface glycoproteins.

In conclusion, the nano-engineered platelets expressed less activation and adhesion under high shear stress.

DEDICATION

This work is dedicated to
my mother Zuming Jiang,
my father Rudi Ai,
and my wife Ming Fang

TABLE OF CONTENTS

ABSTRACT.....	iii
DEDICATION.....	v
LIST OF TABLES.....	xi
LIST OF FIGURES.....	xii
ACKNOWLEDGMENTS.....	xvi
CHAPTER 1 Introduction.....	1
1.1 Introduction	1
1.2 Background and Significance.....	3
1.2.1 Coronary Artery Stenosis.....	3
1.2.2 The Role of Platelet Glycoproteins in Platelet Activation, Aggregation and Adhesion	6
1.2.3 Thromboxane B ₂ : An Indicator of Platelet Activation.....	13
1.2.4 Shear Stress Plays Important Roles in Platelet Activation and Adhesion	14
1.2.5 Nitric Oxide Released from Endothelial Cells.....	16
1.3 The Layer-by-Layer Self-Assembly Technique	18
1.3.1 Introduction	18
1.3.2 Biocompatible Ultrathin Films.....	21
1.3.3 Encapsulation of Micro/Nanotemplates	25
1.4 Hypothesis and Specific Aims.....	28

1.4.1 Hypothesis.....	28
1.4.2 Study Objectives	28
CHAPTER 2 MATERIALS AND METHODS	31
2.1 Introduction	31
2.2 Coronary Artery Stenosis Silicone Model.....	32
2.2.1 Model Geometry	32
2.2.2 Casting the Coronary Artery Stenosis Model	33
2.3 Silicone Surface Modification through Micro/Nano-Film Coating	35
2.3.1 Gelatin-Glutaraldehyde Crosslinking on a Flat Silicone Rubber Substrate.....	35
2.3.1.1 Silicone Rubber Substrate.....	35
2.3.1.2 Gelatin Crosslinking Methods.....	35
2.3.1.3 Gelatin Film Thickness.....	36
2.3.1.4 Cell Culture.....	37
2.3.1.5 Measurement of Contact Angle.....	37
2.3.1.6 Viscosity Study.....	37
2.3.2 Coating Biocompatible Nanofilm on a Flat Silicone Rubber Substrate	38
2.3.2.1 Coating PEI/PSS Multilayers on PDMS.....	39
2.3.2.2 Coating PEI/Gelatin Multilayers on Silicone Rubber.....	40
2.3.2.3 Coating PDL/Gelatin Multilayers on Silicone Rubber.....	41
2.3.2.4 Coating PSS/Collagen Multilayers on Silicone Rubber.....	41
2.3.2.5 Measurement of Contact Angle.....	42
2.3.2.6 Monitoring the Thickness of a Nanofilm.....	42
2.3.3 Coating a Collagen Nanofilm onto the Inner Surface of a Silicone Model	42

2.3.4 Seeding Endothelial Cells onto the Gelatin Nanofilm Coated on the Silicone Rubber Substrate	44
2.3.4.1 Cell Adhesion and Growth on PEI/Gelatin Nanofilm.....	44
2.3.4.2 Cell Adhesion and Growth on PDL/Gelatin Nanofilm.....	45
2.3.5 Seeding Endothelial Cells on the Inner Surface of Silicone Model	46
2.4 Nano-Encapsulation of Platelets.....	48
2.4.1 Nano-Encapsulation of Fixed Platelets	48
2.4.1.1 Reagents and Materials.....	49
2.4.1.2 Platelets.....	49
2.4.1.3 Instrumentation.....	49
2.4.1.4 Platelets Nano-Assembly.....	49
2.4.2 Nano-Encapsulation of Live Platelets	52
2.4.2.1 Platelets Live/Dead Viability and Cytotoxicity Analysis.....	53
2.4.2.2 Labeling Procedure.....	53
2.5 Model Setup.....	54
2.6 Thromboxane B ₂ Measurement through ELISA	56
2.6.1 Contents of the Assay System.....	56
2.6.2 Enzymeimmunoassay Procedure.....	58
2.6.2.1 Reagent Preparation.....	59
2.6.2.2 Preparation of Working Standards.....	59
2.6.2.3 Assay Protocol.....	60
2.6.2.4 Calculation of Results.....	61
2.7 Platelet Adhesion Test.....	60
2.8 Nitric Oxide Fluorescence Sensor	61

2.9 Data Analysis.....	63
CHAPTER 3 RESULTS	64
3.1 Silicone Surface Modification for Endothelial Cell Adhesion and Growth.....	64
3.1.1 Gelatin-Glutaraldehyde Crosslinking on Silicone	64
3.1.1.1 Gelatin Film Thickness.....	64
3.1.1.2 Contact Angle.....	65
3.1.1.3 Viscosity Study.....	66
3.1.1.4 Endothelial Cell Adhesion and Growth.....	68
3.1.2 Coating a Biocompatible Nanofilm on Silicone Rubber.....	70
3.1.2.1 Contact Angle Measurements.....	71
3.1.2.2 Nanofilm Thickness.....	72
3.1.2.3 Endothelial Cell Adhesion and Growth on Gelatin Nanofilm.....	76
3.2 Nano-Encapsulation of Platelets.....	77
3.2.1 Nano-Encapsulation of Fixed Platelets	77
3.2.1.1 Elaboration of the Polyion/Nanoparticle/Immunoglobulin Assembly on a Plane Surface.....	77
3.2.1.2 Assembly of POlyion/Nanoparticle/Antibody Coating on Platelets.....	81
3.2.2 Nano-Encapsulation of Live Platelets.....	85
3.2.2.1 Elaboration of the Polyion/Heparin Assembly on the Plane Surface.....	85
3.3 Thromboxane B ₂ Measurement through ELISA	89
3.4 Platelet Adhesion Test in the Stenosis Model	91
3.5 Nitric Oxide Release from the Endothelial Cells	92
CHAPTER 4 DISCUSSION.....	97
4.1 Introduction	97

4.2 Micro/Nanofilm Coated on a Silicone Substrate.....	98
4.3 Nano-Encapsulation of Platelets.....	100
4.3.1 Nano-Encapsulation of Fixed Platelets	100
4.3.2 Nano-Encapsulation of Live Platelets	101
4.4 Thromboxane B ₂ Release from Platelets	102
4.5 Platelet adhesion.....	103
4.6 Measuring Nitric Oxide Release from Endothelial Cells.....	104
CHAPTER 5 CONCLUSIONS AND RECOMMENDATIONS	105
5.1 Conclusions	105
5.1.1 Micro/Nano-Film Coating.....	105
5.1.2 Nano-Encapsulation of Platelets	106
5.2 Recommendations	107
REFERENCES	109

LIST OF TABLES

Table 1.1 Adhesion Receptors on Platelets.....	8
Table 2.1 Thromboxane B2 Enzymeimmunoassay Protocol (volume unit: μ l)	59
Table 3.1 The Thickness of Gelatin/GA Crosslinked Films.....	64

LIST OF FIGURES

Figure 1.1 SEM of activated platelets (George, 2000)	6
Figure 1.2 Integrin signaling (from Shattil, 1998).....	9
Figure 1.3 The pathway of thromboxane B ₂	14
Figure 1.4 Range of wall shear stress magnitude (modified from Malek, 1999)	15
Figure 2.1 The core of the stenosis model	32
Figure 2.2 The 3-D view of the stenosis model.....	32
Figure 2.3 The stenosis model of coronary artery	34
Figure 2.4 Two methods of gelatin/GA crosslinking on a silicone rubber substrate.....	36
Figure 2.5 Coating PEI/PSS film on silicone rubber substrate.....	40
Figure 2.6 Coating PSS/Collagen film on PDMS substrate	42
Figure 2.7 Cross-sectional view of a collagen nanofilm coated on the inner surface of a silicone model.	44
Figure 2.8 Seeding endothelial cells on PEI/Gelatin nanofilm coated on silicone rubber substrate.....	45
Figure 2.9 Seeding endothelial cells on PDL/Gelatin nanofilm coated on silicone rubber substrate.....	46
Figure 2.10 The cross-section view of a silicone model with inner surface coverage of endothelial cells.....	47
Figure 2.11 Culture endothelial cells in a flow system.....	48
Figure 2.12 Scheme of three methods of an assembly to functionalize platelet shells....	50

Figure 2.13 Anti-bovine IgG-FITC encapsulated platelets targeting to the IgG coated area.	51
Figure 2.14 Live platelets assembly.....	52
Figure 2.15 The setup of a stenosis model in a flow system	56
Figure 2.16 TXB ₂ measurement through ELISA (modified from BIOTRAK, 1994)	57
Figure 2.17 Reaction scheme for the detection of nitric oxide (NO) by DAF-FM and DAF-FM diacetate.	61
Figure 2.18 Regions of endothelial cells used for NO release measurement	62
Figure 3.1 Contact angles of different surfaces. The contact angle on the unmodified silicone rubber is $107 \pm 1.1^\circ$	66
Figure 3.2 Viscosity measurements of different gelatin solutions.....	67
Figure 3.3a Cells attached on method I (GA: 0.08%) modified surface at 72 hours.....	69
Figure 3.3b Cells attached on method I (GA: 0.04%) modified surface.....	69
Figure 3.3c Cells attached on method I (GA: 0.02%) modified surface.....	69
Figure 3.4 Cells attached on method II modified surface at 72 hours	70
Figure 3.5 Cells attached on silicone rubber surface at 72 hours	70
Figure 3.6 Contact angle measurements vs adsorption layers	71
Figure 3.7 Contact angle measurements during the coating procedure	72
Figure 3.8 (PEI/PSS) ₆ film growth vs frequency shift.....	73
Figure 3.9 PEI/gelatin film thickness vs adsorption layers.....	74
Figure 3.10 PDL/gelatin film frequency shift/thickness vs adsorption layers.....	75
Figure 3.11 Bovine coronary artery endothelial cells attached on a (PEI/PSS) ₂ + (PDL/gelatin) ₅ nanofilm.....	77
Figure 3.12 Film thickness of each assembly layer for (PDDA/PSS)(PDDA/Silica) ₂ /PDDA and (PDDA/PSS)(PDDA/FN) ₂ /PDDA.	78

Figure 3.13 Adsorption density of each assembly layer for IgG and anti IgG coatings...	79
Figure 3.14 Assembly procedure of (PDDA/IgG) ₅ + Anti-IgG.....	80
Figure 3.15a A bovine platelet (TEM image × 21K).....	81
Figure 3.15b Four platelets coated with 78 nm silica shell with composition PDDA/PSS/PDDA+(Silica/PDDA) ₂ (TEM×1.65k).....	82
Figure 3.15c A magnified image of a platelet (arrow) from (b) (TEM×21k).....	82
Figure 3.16a Platelets coated with 45 nm fluorescence nanospheres. (Magnification: 1K).....	83
Figure 3.16b Platelets assembled with bovin IgG and labeled with anti-bovin IgG-FITC.....	83
Figure 3.17 Anti-IgG shelled platelets targeted to an area based on anti-IgG-FITC recognition of IgG covered regions.....	84
Figure 3.18 Frequency shift/film thickness vs adsorption layers of PDDA/heparin multilayers.....	85
Figure 3.19 Platelets after encapsulation and labeled with LIVE/DEAD cell viability/cytotoxicity sensor under fluorescence microscope at 0 min.	86
Figure 3.20 Platelets after encapsulation under fluorescence microscope at 30 min.	87
Figure 3.21 Live/dead platelet emission at different wavelengths.	87
Figure 3.22 Fluorescence signal of dead platelets at 617 nm when excited at 528 nm	88
Figure 3.23 fluorescence intensity of live and dead platelets	89
Figure 3.24 The Thromboxane B2 standard curve	90
Figure 3.25 The level of TXB ₂ released from shelled and non-shelled platelets	90
Figure 3.26 The fluorescence intensity of non-shelled platelets.....	91
Figure 3.27 Percentage of shelled and non-shelled platelets adhesion to the collagen nanofilm	92
Figure 3.28 Fluorescence intensity of cells without DAF-FM diacetate labeling.....	93
Figure 3.29a Fluorescence intensity of NO release at region 1	94

Figure 3.29b Fluorescence intensity of NO release at region 2.....	94
Figure 3.29c Fluorescence intensity of NO release at region 3.....	95
Figure 3.29d Fluorescence intensity of NO release at region 4.....	95
Figure 3.30 Fluorescence intensity of NO release at all regions	96

ACKNOWLEDGMENTS

I want to thank my mentor, Dr. Steven A. Jones, for his guidance and support during the course of this research. I would also like to thank my committee Drs. David K. Mills, Huaijin Gu, Roy Schubert, and Stan Napper for the help, guidance, and laboratory supplies.

I want to thank Dr. Yuri M. Lvov for his willingness to answer questions, provision for laboratory equipment and supplies, and his instruction in layer-by-layer self-assembly technique. Dr. Xiaoxi Qiao (LSU Medical Center) helped me with transmission electron microscopy. Dr. Jonathan S. Alexander (LSU Medical Center) gave me important guidance in tissue engineering. Dr. Barbara J. Ballermann (Johns Hopkins Medical School) gave me important guidance in silicone surface modification.

Numerous other people also deserve a word of thanks. Dr. William Green, Dr. Mark Murphy, and Mr. Benny Hennen who assisted me with blood collection for the project. Their cooperation and expertise are much appreciated. Mr. Shawn Moncrief, Mr. Jimmy Cook, and Mr. Murray Rasbury helped me with the silicone model building.

CHAPTER 1

INTRODUCTION

1.1 Introduction

Platelets possess unique features that facilitate their functions in the hemostasis. Among these are the ability to secrete multiple substances, such as adenosine diphosphate (ADP), serotonin, and thromboxane A₂ (TXA₂) that recruit other platelets to a forming thrombus through a dramatic positive feedback mechanism. Platelets are also able to express membrane receptors for thrombin, von Willebrand factor (vWF), fibrinogen, and other proteins that support adhesion and aggregation in a way that enhanced by hemodynamic shear stress (Baumgartner *et al.*, 1980). They also support a mechanism for uptake of serotonin (Glynn, 1973). Platelet thrombus contributes to the development of atherosclerosis (Duguid *et al.*, 1985), directly causes myocardial infarction (Fuster *et al.*, 1985; Fuster *et al.*, 1990; Mustard *et al.*, 1990). Because of the unique features of platelets and the importance of platelets to cardiovascular health and pathology, it is of interest to examine the possibility of modifying these cells, either as a therapy for diseases caused or exacerbated by platelets, or as a means to provide them with new functions, such as drug delivery or biochemical sensing.

A type of platelet modification is already being used as a therapy for patients who have coronary artery disease. It involves the use of an antibody to the membrane receptor, GPIIb-IIIa, that is responsible for adhesion of platelets in a high shear stress environment, such as that found in an arterial stenosis (Hanson *et al.*, 1988). This method works through the injection of a monoclonal antibody (e.g., abciximab) to the receptor into the body. An alternative is to extract platelets, modify them *in vitro*, and then return them to the circulation. If such a method is to be useful, it must take advantage of the unique properties of platelets, such as their ability to actively secrete agents upon activation. An example is the use of platelets as a drug delivery device. The advantage of platelet is that the platelet, when activated, actively secretes the drug at the targeted location, rather than slowly and passively releasing the drug.

Recently a method has been developed by Iler (1966) in which a thin (nanoscale) film can be adsorbed onto a surface through the sequential exposure of the surface to solutions of alternately charged colloidal particles and proteins. The technique is particularly useful because of its applicability to any charged surface and its ability to radically change surface properties without substantially increasing the size of the object being modified. For example, the release rate of a dye (Antipov, 2001) or drug microcrystals (Qiu, 2001; Ai, 2002b) can be controlled through nano-encapsulation, and because the coating is thin, the size of the resulting microcapsule is small enough to be injected.

Platelets have been successfully encapsulated with polyions, antibodies, and nanoparticles (Ai, 2002a). The shell formed on platelets may block agonists from reaching platelet receptors, thus reducing platelet activation or adhesion. Similarly, the

secretion of agonists from platelets can be controlled by the shell. Localized targeting of platelets can be achieved if the surface is coated with anti-IgG.

In an effort for researcher to understand how nano-engineered platelets react to high shear stress caused by an arterial stenosis, platelets have been encapsulated by the layer-by-layer technique and their behavior was examined in an *in vitro* silicone coronary artery stenosis model. Platelet activation and adhesion, and the NO release from endothelial cells were examined. Blood Thromboxane B₂ (TXB₂) was measured by enzyme-linked immunosorbent assay (ELISA) as a measure of overall platelet activation. Platelet adhesion to a collagen substrate on the inner surface of the silicone model was quantified through fluorescence tagging. The amount of NO release from endothelial cells was measured with a cell membrane permeable fluorescence sensor. The overall purpose of this study was to determine whether nano-encapsulated platelets express less activation and adhesion than unencapsulated platelets under the high shear stress generated by the stenosis.

1.2 Background and Significance

1.2.1 Coronary Artery Stenosis

Cardiovascular disease is the leading cause of death in North America (Malek *et al.*, 1999). Cardiac infarction induced by thrombus plaques can often cause sudden death (Fuster *et al.*, 1985; Fuster *et al.*, 1990; Mustard *et al.*, 1990), and arterial stenosis caused by atherosclerosis is an important step leading to thrombus formation (Malek *et al.*, 1999). The National Health and Nutrition Examination Survey III (NHANES III) reports that 60,800,000 Americans have one or more types of cardiovascular disease (CVD).

Among these patients, about 20.4% have coronary heart disease, 12% have myocardial infarction, and 10.5% have angina pectoris. The hemodynamic environment and biochemical factors affected by the existing stenosis are of great importance in further formation of thrombus (Goto *et al.*, 1998; Badimon *et al.*, 1986; Malek *et al.*, 1999; Weigensberg *et al.*, 1975; Murata *et al.*, 1969; Honour *et al.*, 1978; Sekimoto, 1980; Naqvi *et al.*, 1999). Hemodynamic wall shear stress is important for platelet activation, subsequent adhesion and aggregation (Malek *et al.*, 1999). While arterial stenosis caused by atherosclerosis is an important precursor to thrombus formation, no direct relationship has been shown between stenosis severity and acute coronary thrombosis or restenosis from past studies (Ambrose, 1988; Ellis, 1989a); some patients who had myocardial infarction might not have serious stenosis (Ambrose, 1988; Little, 1996). Therefore, it is important to understand the relationship between stenosis and thrombus formation if the mechanics for myocardial infarction is to be fully understood. The pathogenesis of thrombosis consists of two processes: atherosclerosis and thrombosis (Prentice, 1990). The mechanism for thrombus formation is complicated, and many mechanical and biochemical factors are involved. Shear stress (Goto, 1998; Badimon, 1986; Malek, 1999), abnormal lipid metabolism (Weigensberg, 1975; Murata, 1969; Honour, 1978; Sekimoto, 1980; Naqvi, 1999), and subendothelial layer exposure (Weiss, 1986; Badimon, 1986; Badimon, 1988) are the major contributors to arterial thrombus formation. Platelet activation by the above factors, followed by adhesion, is the basic sequence in thrombus formation. Under pathologic conditions, ruptured plaques and high shear stress at sites of stenosis may induce formation of platelet-rich thrombi that become

life-threatening when they occlude the vascular lumen and block blood flow (Fuster, 1992a; Fuster, 1992b).

Many previous studies have shown platelet adhesion on damaged endothelial cells (Dewitz *et al.*, 1978; Moritz *et al.*, 1988; Belval *et al.*, 1984; Ikeda *et al.*, 1991; Huang *et al.*, 1993), but thrombus formation has rarely been observed on an intact endothelium (Rosenblum, 1997). Nitric oxide (NO), an important intracellular and intercellular messenger released from endothelial cells, can prevent platelet activation and adhesion (Mellion *et al.*, 1981; Salvemini *et al.*, 1989). Less release of NO at downstream locations from stenosis may increase the adhesion of activated platelets.

Coronary angioplasty, thrombolysis, or a combination of these therapies, are commonly used in the treatment of coronary stenosis. Coronary Artery Bypass Graft (CABG) Surgery is also a popular method to relieve symptoms (Arcidi, 1988). Coronary angioplasty is an effective and popular treatment for acute myocardial infarction (Ellis, 1989b; Steg, 1999; Grines, 1999; Lane, 2000; Bar, 2000) and coronary stenosis (Borrione, 1993; Conti, 1991; Liska, 1999; Shin, 1999). Restenosis after the angioplasty procedure (Buchwald, 1990; Klein, 1990; Schwartz, 1990; Marzocchi, 1991), and bleeding side effects caused by thrombolysis are not uncommon (Cohen, 1998; de Bono, 1993; Erlemeier, 1989). Polymorphism of platelet glycoproteins (Abbate, 1998; Bottiger, 1999; Kastrati, 1999), higher platelet aggregation (Goel, 1997), and platelet-vessel wall interaction (Hoylaerts, 1997) are all involved in restenosis. CABG failure was also reported due to different factors (Pitrowski, 1991; Yang, 1997; Rasmussen, 1997). Endothelial nitric oxide synthase (eNOS) gene delivery has been used as a method for the treatment endothelial cell dysfunction (Lake, 1999; Sato, 2000). Blood vessel relaxation

(Lake, 1999) and smooth muscle cell growth inhibition (Sato, 2000) were achieved through gene transfer to endothelial cells. This is a promising approach but requires substantial work before it can be applied clinically.

1.2.2 The Role of Platelet Glycoproteins in Platelet Activation, Aggregation and Adhesion

Platelets have several effects in the cardiovascular system, including blood vessel repair, clot formation, clot retraction, clot dissolution, vasodilation, and vasoconstriction. When activated, platelets change from the normal disc shape to a compact sphere with long dendritic extensions facilitating adhesion (Figure 1.1). Also, the activated platelet surface membrane area increases about 60% after activation (Born, 1970). This fact increases the probabilities that the platelet will attach to the subendothelial matrix or adhere to other platelets. Fibronectin, collagen fibers, vitronectin, and VWF in the subendothelial matrix are the targets for those surface glycoproteins to bind.



Figure 1.1 SEM of activated platelets (George, 2000)

Platelet adhesion to endothelial cells can be induced by thrombin (Venturini, 1992), collagen (Ross, 1995b), shear stress (Huang, 1993), and many other factors. When activated, platelets will adhere to a damaged endothelial cell layer (Badimon, 1986; Hoylaerts, 1997). But platelet adhesion and aggregation without endothelial denudation or exposure of basal lamina and/or collagen has also been reported (Rosenblum, 1996).

Platelets are disk-shaped cells with diameters from 2 to 4 microns and volumes from 5 to 7.5 μm^3 and derived from megakaryocyte cytoplasm fragments. Generally, two types of granules are in platelet cytoplasm, α lysosomal granules and dense granules. Partial release of acid hydrolases from lysosome-like organelles has also been reported (Holmsen, 1992). The α granules secrete adhesive proteins such as von Willebrand factor (VWF), platelet-derived growth factor (PDGF), platelet factor 4 (PF-4), fibronectin, thrombospondin and fibrinogen, and plasma proteins such as albumin and IgG (Sander, 1983; Stenberg, 1984; Kaplan, 1979a; Kaplan, 1979b). While very dense granules secrete serotonin (White, 1968), ADP, and Calcium (blood coagulation factor IV) (George, 2000). The membranes of platelets, mainly composed of lipids and glycoproteins, are of special interests in the platelet activity study. This cell coat, about 150 to 200 nm thick (Zucker-Franklin, 1990), prevents platelet adhesion to a normal endothelial layer and helps platelets attach to a damaged cell layer (Guyton, 1996; Faull, 1994). There are at least 30 distinguishable glycoproteins on the platelet surface (Holmsen, 1990). Some glycoproteins, together with platelet endothelial cell adhesion molecule 1 (PECAM-1) and P-selectin, are important adhesion receptors on platelets (Table. 1.1).

Table 1.1 Adhesion Receptors on Platelets*

Gene family	Receptor	Ligand	Number/cell
Integrin	$\alpha_{IIb}\beta_3$ (GPIIb-IIIa)	Fibrinogen, vWF, Vn, Fn	80,000
	$\alpha_V\beta_3$ (GPV-IIIa)	Fibrinogen, vWF, Vn, Fn, OP	250
	$\alpha_2\beta_1$ (GPII-Ib β)	Collagen	<1,000
	$\alpha_5\beta_1$ (GPV-Ib β)	Fn	<1,000
	$\alpha_6\beta_1$ (GPVI-Ib β)	Laminin	<1,000
Leucine-rich motif	GP Ib-IX	VWF	25,000
Immunoglobulin	PECAM-1	PECAM-1, GAGs	5,000
Selectin	P-selectin	CHO on WBC	10,000

*: Modified from Shattil *et al.*, 1994.

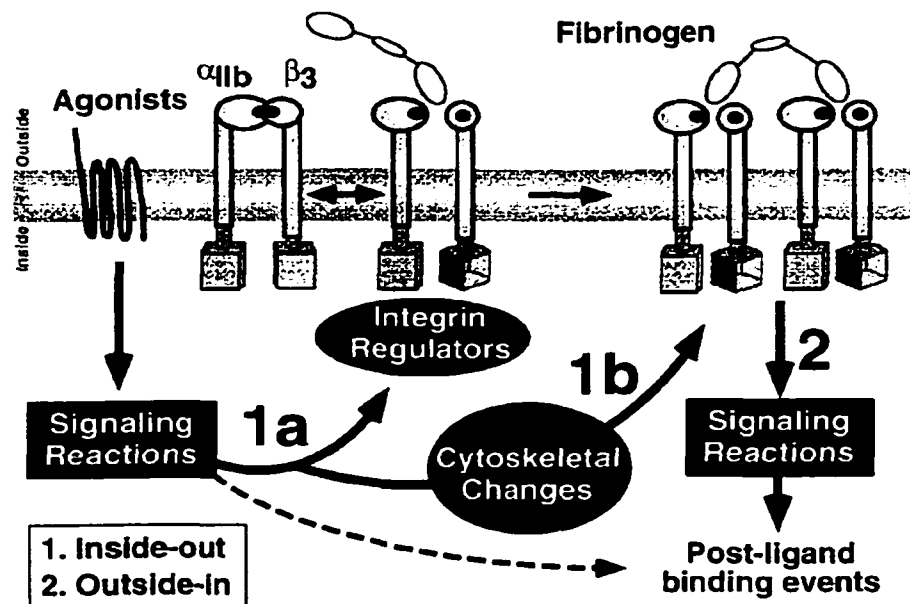
Vn: vitronectin; Fn: fibronectin; OP: osteopontin; GAGs: glycosaminoglycans;

PECAM-1: platelet endothelial cell adhesion molecule; CHO: sialylated and fucosylated carbohydrates displayed on specific membrane proteins

GPIIb-IIIa is the most important glycoprotein in platelet aggregation and adhesion (Jennings, 1986; Pytela, 1986; Plow, 1984). GPIIb-IIIa is an integrin that consists of a two-chain α unit bound noncovalently to a single-chain β unit (Shattil, 1998). It is the most abundant surface glycoprotein (Holmsen, 1990), with 80,000 receptors on the platelet surface (Wagner, 1996), and it requires a conformational change during platelet activation to express receptor function, mainly for fibrinogen (Shattil, 1985; Shattil, 1997; Shattil, 1998). GPIIb-IIIa also attaches to vWF (Ruggeri, 1982), fibronectin (Ginsberg, 1983), and vitronectin (Fitzgerald, 1987; Fijnheer, 1990). Activated platelets express about 45,000 to 50,000 GPIIb-IIIa receptors on the surface, which is 56.2% to 62.5% of the total resting receptors (Shattil, 1985; Abrams, 1991). Peptides containing the amino acid sequence Arg-Gly-Asp (RGD), a sequence present at two locations in the α chain of fibrinogen, can be recognized by GPIIb-IIIa in the binding process (Bennett, 1988). This binding is activation-independent (Lam, 1987; Frelinger, 1988). Accurate information on the amount of expressed GPIIb-IIIa aids in the analysis of platelet activation. Several methods have been applied in past studies, but flow cytometry is

widely used and has proved to be effective (Abrams, 1990; Andrews, 1996; Konstantopoulos, 1995; Lindahl, 1992; Michelson, 2000; Warkentin, 1990; Yano, 1994).

To better explain the working principle of GPIIb-IIIa in platelet activation, integrin signaling was proposed (Shattil, 1998). Integrin signaling includes inside-out signaling and outside-in signaling. Inside-out signaling denotes those reactions initiated by the binding of one or more agonists to their plasma membrane receptors, leading to the conversion of GPIIb-IIIa from a low-affinity/avidity receptor to a high-affinity/avidity receptor (Shattil, 1998). Outside-in signaling triggers a number of postligand binding events and these require cooperative signaling between GPIIb-IIIa and agonist receptors. The integrin signaling is illustrated in Figure 1.2. Affinity modulation is depicted hypothetically as a signal-induced rotation of the IIIa subunit to generate and unmask fibrinogen binding sites in the extracellular domains of GPIIb-IIIa (Shattil, 1998).



1a: inside-out signaling increases the affinity of GPIIb-IIIa

1b: inside-out signaling increases the avidity of GPIIb-IIIa

Figure 1.2 Integrin signaling (from Shattil, 1998)

Other glycoproteins are also of great importance in platelet activation, aggregation and adhesion. GPIX, a 17-kDa to 22-kDa single-chain platelet membrane glycoprotein, can noncovalently bind with GPIb and GPV to form GPIb-IX-V complex (Du, 1987; Modderman, 1992). This glycoprotein plays important functions in normal platelet activation and adhesion (Hourdille, 1990; Ruggeri, 1991). The GPIb-IX-V complex contains a VWF binding site that mediates the activation-independent, shear-dependent adhesion of platelets to the exposed vascular subendothelial layer (Du et al., 1987; Fox et al., 1988; Hickey et al., 1989; Ruggeri et al., 1991; Modderman et al., 1992; Michelson et al., 1991). PECAM-1, a 130-kDa to 140-kDa single-chain integral membrane protein, functions as a vascular cell adhesion molecule, also involved in thrombosis (Albelda et al., 1991; Horak et al., 1992). P-selectin, also known as platelet activation-dependent granule-external membrane (PADGEM) protein (Hsu-Lin et al., 1984) or granule membrane protein (GMP-140) (Stenberg et al., 1985), is a 140-kdalton single-chain polypeptide (McEver, 1990).

Fibrinogen (blood coagulation factor I), a 340-kDa glycoprotein (Caspary et al., 1957), is present in platelet α granules. While endothelial cells do not synthesize fibrinogen, and fibrinogen is not normally present in the subendothelial layer, fibrinogen is present in the subendothelium of healing blood vessels (Clark *et al.*, 1984; Fujikawa *et al.*, 1984). This glycoprotein is considered an interplatelet linkage after platelet activation and the conformational change of GPIIb-IIIa (Hawiger, 1991).

The large multimeric glycoprotein vWF contains a variable number of subunits. It is contained in platelet α granules and synthesized and secreted by endothelial cells (Jaffe, 1974; Wagner, 1984; McCarroll, 1985). The concentration of VWF in the plasma

is about 7-10 $\mu\text{g/ml}$ (Girma, 1986). VWF functions as a molecular anchor between the subendothelium and platelets (Hawiger, 1991). It binds to the subendothelium, changes in conformation, and is then able to interact with GPIb (Sixma, 1991). VWF deposited in the subendothelium is responsible for up to 40% of normal adhesion, and the action of VWF is seen at high shear rates (Sixma, 1991). VWF binds at the cell surface interface between platelets (Senogles, 1983), which can promote further platelet aggregation.

Collagen fibers are one of three principal connective tissue fibers widely distributed in the body. Nineteen different types (Kehrel, 1995) of collagen have been identified, and each collagen molecule is composed of three polypeptide α chains in a helical configuration (Ross, 1995a). At least nine of the different collagens – type I, III, IV, V, VI, VIII, XII, XIII, XIV are found in the vessel wall (Kehrel, 1995). Collagen is exposed when the endothelium is damaged. The interaction of platelets with collagen is complex because the collagen monomer has no affinity to platelets, while collagen fibrils and immobilized collagen bind strongly to platelets (Moroi, 1997). Many studies have shown that platelets can attach to collagen in a flow condition (van Zanten, 1996; Huang, 1998; Mazzucato, 1999; Moroi, 1996; Ross, 1995b; Saelman, 1995).

Collagen types I, III, V and VI can induce α -granule secretion and up-regulation of cell surface GPIIb-IIIa (Alberio, 1998). Platelet adhesion and aggregation on collagen VI are different in shear rate dependence from collagen I; collagen VI and vWF may play a role under low shear rates (Ross, 1995b). Chiang *et al.* (1993) suggested that type I and type III collagens interact with platelets at separate sites. Platelet adhesion to collagen type III is strongly but not completely determined by the adhesive properties of vWF

(Wu, 1996). Collagen type IV is a sheet-forming collagen and a major constituent of the vessel wall. It is a reactive collagen for platelets (Henrita, 1996).

Platelet glycoproteins are the major receptors for collagen attachment. Collagen-platelet interaction, occurring in hemostasis and thrombosis, is a two-step process of adhesion and activation involving the sequential recognition of distinct receptors (Barnes, 1998). The normal platelet adhesion to collagen is mediated through the binding to vWF to collagen and to both GPIb and GPIIb-IIIa on the platelet membrane (Fressinaud, 1988). Adhesion involves first the reversible recognition of collagen-bound VWF by the platelet receptor complex α IIb β 1, which binds to a specific sequences in collagen in which the GER motif appears important (Barnes, 1998). It was suggested that both the α IIb β 1 integrin and GPVI are involved in inside-out signaling leading to activation of GPIIb-IIIa complex after platelet adhesion to collagen and generation of TXA₂ may further enhance expression of activated GPIIb-IIIa (Nakamura, 1999).

GPIV (CD36) does not play a major role in collagen-dependent platelet signal transduction (Daniel, 1994). Integrin GPIa-IIa is a major platelet receptor for collagen (Estavillo, 1999). But it is shown that the α (2)-I domain can prevent platelet adhesion to a collagen surface exposed to flowing blood under low shear stress (Estavillo, 1999).

Other factors are also related to collagen-platelet interactions. It was suggested that platelet-activating factor (PAF) plays an important role in collagen-induced whole blood aggregation (Oura, 1994). Collagen fibers could inhibit platelet membrane adenylate cyclase in a dose-dependent manner (Farndale, 1992).

1.2.3 Thromboxane B₂: An Indicator of Platelet Activation

Thromboxanes also play important roles in platelet activation and aggregation. The pathway of thromboxane B₂ is illustrated as in the Figure 1.3. During platelet activation arachidonic acid is liberated from certain glycerophospholipids (Holmsen, 1990b). PGG₂ and PGH₂ are subsequently converted from arachidonic acid. PGG₂ and PGH₂ are unstable in an aqueous environment (half-life time: $T_{1/2} = 300$ s) and may be converted nonenzymatically to the stable prostaglandins (Smith, 1987a). Thromboxane A₂ is derived from PGH₂ by thromboxane synthase. The half-life time of TXA₂ is about 32 seconds (Samuelsson, 1976). TXA₂, a potent platelet agonist and vasoconstrictor (Smith, 1987b), can promote further platelet aggregation. Thromboxane B₂, converted from thromboxane A₂, is an indicator of TXA₂ production with a half-life time 20 ~ 30 minutes (McCann, 1981; Fitzpatrick, 1977). Intact endoperoxides, PGE₂, and PGF_{2 α} account for only a very small part of the transformation via the cyclooxygenase pathway, the main products being C₁₇-hydroxy acid (HHT) and TXB₂ (Samuelsson, 1976). It was found that aggregation of washed platelets by thrombin was accompanied by release of large amounts of end products such as TXB₂ from arachidonic acid metabolism (Hamberg, 1974). So TXB₂ concentration indicates the degree of platelet activation and aggregation. The level of TXB₂ is about 2.45 μ g/ml after thrombin-induced aggregation of human platelets (Samuelsson, 1976). It can be easily measured through a TXB₂ enzymeimmunoassay (EIA) system (Biotrak, 1994) with a sensitivity of 3.6 pg/ml.

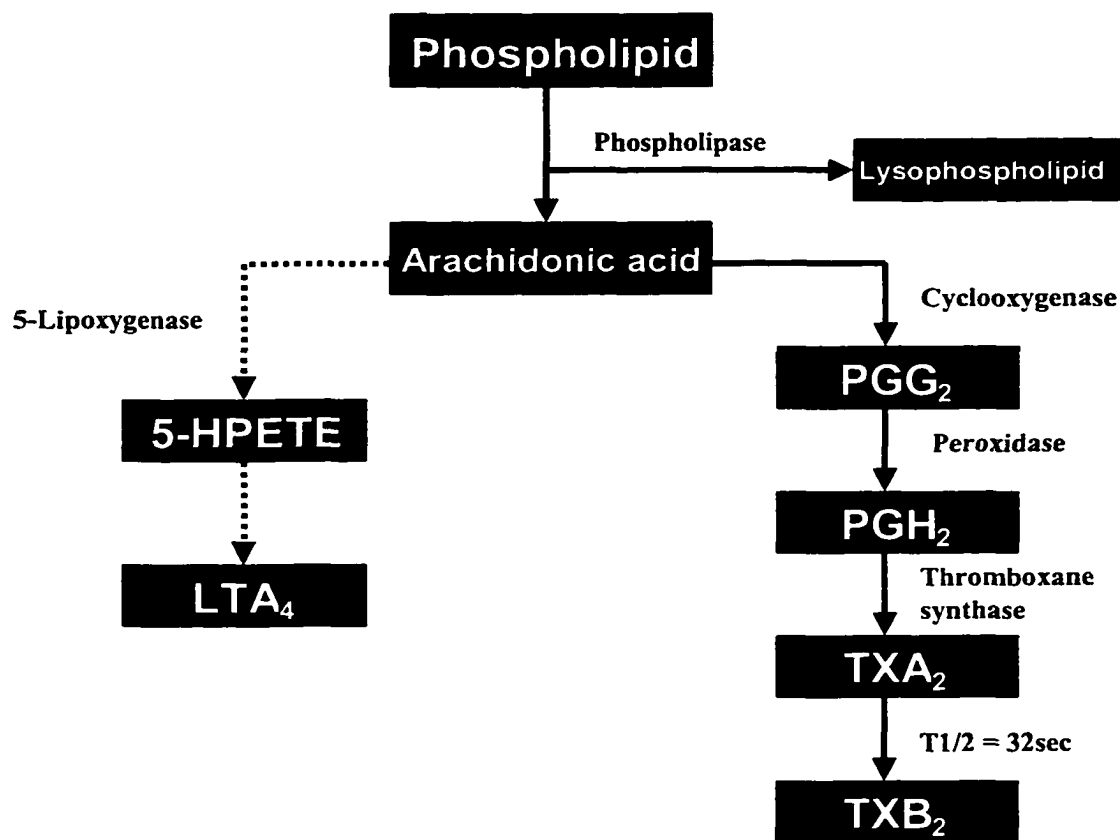


Figure 1.3 The pathway of thromboxane B₂

1.2.4 Shear Stress Plays Important Roles in Platelet Activation and Adhesion

The mechanism involved in platelet activation, aggregation, and adhesion is complicated, and shear stress is an important mechanical factor in many aspects. Morphological, biochemical, and functional changes of human platelets were found at high shear stress (Brown, 1975). Shear stresses of 50 dynes/cm² and higher trigger platelet activation, cause the release of granule contents into the suspending medium, and elicit platelet aggregation (Dewitz, 1978; Moritz, 1988; Belval, 1984; Ikeda, 1991; Huang, 1993).

The magnitude of shear stress in a cylindrical tube is proportional to blood flow viscosity, and inversely proportional to the third power of the blood internal radius. The relationship is expressed by the solution for Poiseuille flow:

$$\tau = \frac{4\mu Q}{\pi R^3},$$

where τ is shear stress, μ is dynamic viscosity, Q is flow rate, and R is the radius of the vessel. This equation assumes fully developed flow and ignores effects found in the arterial system such as curvature, branching and tapering.

Measurements using different modalities show that shear stress ranges from 1 to 6 dynes/cm² in the venous system and between 10 and 70 dynes/cm² in the arterial vascular vessels (Malek, 1999). The range of wall shear stress magnitude is shown in Figure 1.4.

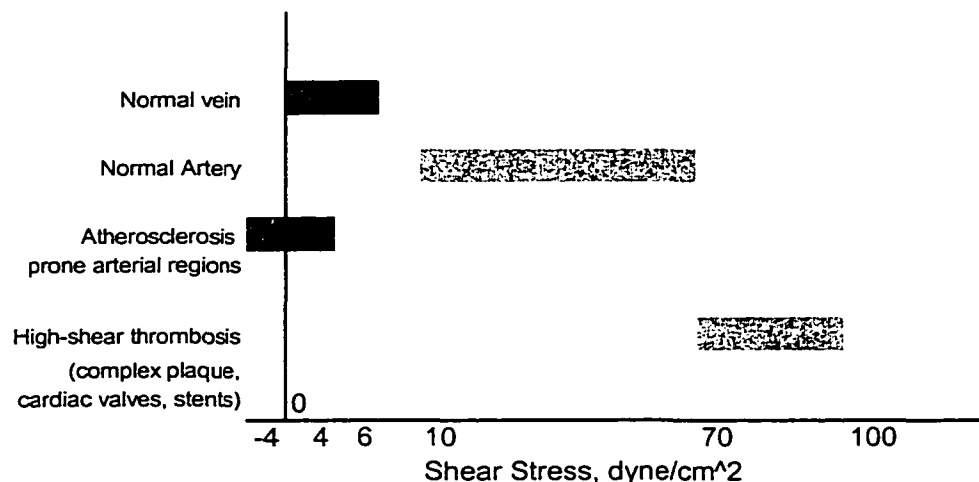


Figure 1.4 Range of wall shear stress magnitude (modified from Malek, 1999)

The biochemical environment can be changed due to abnormal fluid mechanical conditions. In areas of vessel stenosis, in arterioles, or in the microcirculation, the effects of vWF are more important at high shear rates (Baumgartner, 1980; Turitto, 1983;

Turitto, 1985). It was suggested that shear stress-induced binding of vWF multimers to platelet GPIb, causes an increase of $[Ca^{2+}]$ and platelet aggregation, both of them potentiated by vWF binding to the platelet GPIIb-IIIa complex (Chow, 1992). The reactivity of the exposed materials and the local shear rate, defined by the blood flow and the luminal cross section, can regulate platelet deposition to injured vascular wall (Badimon, 1986).

Shear stress can bring platelets close to the wall through convection and enhanced diffusion (Aarts, 1988). With the laser-Doppler technique, Aarts *et al.* (1988) found red blood cells were in the center of blood flow, while platelets were concentrated near the wall. This high concentration at the wall increased with higher average tube hematocrit and wall shear rates. The authors suggested that platelet transport might be enhanced by a shear rate-dependent rotary motion. In a stenosis model, deposition onto the wall depended on the wall shear stress distribution along the stenosis, increasing in areas of flow recirculation and reattachment (Bluestein, 1997).

1.2.5 Nitric Oxide Released from Endothelial Cells

Nitric oxide (NO), a free radical, is an important messenger in the biological system. NO has crucial roles in vasodilation (Palmer, 1987), inhibition of platelet aggregation (Mellion, 1981; Salvemini, 1989), intercellular communication in the central nervous system (CNS) (Garthwaite, 1988), neurotransmission in peripheral nervous system (PNS), atherosclerosis formation (Bruckdorfer, 1990), osteoclastic inhibition (MacIntyre *et al.*, 1991), and many other physiological functions (Lowenstein, 1994).

NO could be produced by all kinds of cells (Moncada, 1991). NO is produced from L-Arginine by nitric oxide synthase (NOS) in the physiological system (Murad, 1999). Three isoforms of mammalian NOS have been identified in the past studies. Neuronal NOS (nNOS or NOS-1) was first characterized from rat cerebellum (Bredt, 1990). Inducible NOS (iNOS or NOS-2) was purified from mice macrophages (Stuehr, 1991) and endothelial NOS (eNOS or NOS-3) was found in bovine aortic endothelial cells (Forstermann, 1991).

It was found that humans and other mammals maintain a finite steady state concentration of nitric oxide in the circulation (Freeman, 1978). But a decrease in the bioavailability of NO is a characteristic feature in those patients with coronary artery disease (Zeicher, 1996).

NO can inhibit platelet aggregation via activation of intraplatelet soluble guanylate cyclase, increases cyclic GMP (cGMP) (Mellion, 1981, Lieberman, 1991). Fibrinogen binding to platelets is also inhibited by NO (Mendelsohn, 1990). Platelets can adhere to a damaged endothelial layer, collagen, and other surfaces, while NO can reduce (Sneddon, 1988) and inhibit (Radomski, 1987) platelet adhesion to vascular endothelial cells. Substances released from α granules and dense granule secretion (Broekman, 1991; Lieberman, 1991) can be inhibited. Michelson *et al.* (1996) reported that 1) the increased cGMP level by NO can negatively regulate the platelet surface expression of P-selectin, CD63, and the GIIb/IIIa complex but not the platelet surface expression of GPIb-IX complex and 2) hemoglobin within erythrocytes inhibit the effects of NO on platelet surface glycoproteins.

1.3 The Layer-by-Layer Self-Assembly Technique

1.3.1 Introduction

Iler (Iler, 1966) was the pioneer who developed the principle of alternate adsorption for film formation of charged colloidal particles and proteins. Later, layer-by-layer (LbL) self-assembly by means of alternate adsorption of linear polycations and polyanions was introduced (Decher, 1991, 1997, 1993, 1994a; Lvov, 1993d; Lvov, 1993a; Lvov, 1993c; Lvov, 1993b). The assembly procedure is presented in Figure 5. A positively charged surface is first coated with polyanions followed by polycations. The outermost layer is negatively charged nanoparticles. The assembly steps can be repeated for further deposition of polyelectrolytes or nanoparticles. Naturally, polyions have to be used at pH levels that provide a high degree of ionization.

It is important to have the resaturation of polyion adsorption, resulting in the alternation of the terminal charge after every subsequent layer deposition, which implies that there is no principle restriction to the choice of polyelectrolytes. There is the possibility of designing ultrathin ordered films in the range of 5 to 1000 nm, with a precision better than 1 nm and a definite knowledge of their molecular composition. This technique has been applied successfully to many water-soluble polyions (including conductive polyions, polysaccharides, polypeptides, DNA and polynucleotides) (Lvov, 1994a, 1994b; Mao, 1993; Decher, 1994b; Hong, 1993; Schmitt, 1993; Korneev, 1995, Leasche, 1998; Cheung, 1994; Yoo, 1998), dyes (Yoo, 1996; Ariga, 1997) and proteins (Lvov, 1994c &, 2000; Brynda, 2000). Additionally, viruses (Lvov, 1994a), ceramics

(Kleinfeld, 1994), and charged nanoparticles (Kotov, 1995; Schmitt, 1997; Lvov, 1997; Lvov, 1998a) have been used in LbL assembly.

Protein / polyion multilayer assembly allows proteins to be organized in layers and to build up such layers following "molecular architecture" plans (Lvov, 2000). The method has been extended to build up multiprotein films, i.e. alternate monolayers of proteins in predetermined orders. It is important to use alternating linear or branched polyion layers for the successful assembly of protein multilayers. Flexible linear polyions penetrate between protein globules and act as electrostatic glue. The concept of "electrostatic polyion glue," which keeps together neighboring arrays of proteins, is central to this approach.

A standard approach for film preparation is as following: (1) An aqueous solution of polyion and protein at concentration of 0.1 - 1 mg/mL is adjusted in pH such that the two components are oppositely charged. For proteins, we shifted the solution pH on 1-2 units from their isoelectric point to provide 20-60 elemental charge units for a globule. (2) A substrate is selected that carries a surface charge (e.g., plates or polymer filters covered by a layer of cationic poly (ethylenimine) (PEI) which may be readily attached to many surfaces). (3) The substrate is alternately immersed in polyion and protein solutions for 20 min with 1 min intermediate water rinsing. The pH of the rinse solution is selected to keep the polyions ionized. (4) The sample is usually dried in a stream of nitrogen, although drying may disturb the assembly process, and is not necessary for the procedure. The polyion predominately used in the assembly: polycations - poly(ethylenimine) (PEI), poly(dimethyldiallylammonium chloride) (PDDA), poly(allylamine) (PAH), poly(lysine), chitosan; polyanions - poly(styrenesulfonate) (PSS), poly(vinylsulfate), poly(acrylic

acid), heparin, dextran sulfate, sodium alginate, and DNA. Polypeptides and polysaccharides are essential in forming biocompatible nanofilms.

X-ray reflectivity measurements of polyion films adsorbed from aqueous solutions show patterns with profound intensity oscillations. From the periodicity of these oscillations (Kiessig fringes), the thickness of a single polyion layer can be calculated as the total film thickness (Decher, 1997; Lvov, 1993d) and knowing the number of the adsorption steps. Growth steps of 1.1 - 2.0 nm per bilayer are typical for linear polyanion /polycation assemblies, while the thickness of each monolayer often equals one half of this value (Lvov, 1993d; Lvov, 1993a; Lvov, 1993c; Lvov, 1993b; Decher, 1993; Decher, 1994a; Lvov, 1994a; Lvov, 1994b). These values correspond to a polyion cross-section and show that in one cycle of excessive adsorption approximately one monolayer covers the substrate. Polyion films are insoluble in water and in many organic solvents and are stable to at least 200°C (Lvov, 1993a; Lvov, 1994b).

The outermost layer of a film dominates the film surface property (Yoo, 1996). The contact angle of a coated film was different from the substrate after surface modification (Yoo, 1998; Ai, 2002c; Ai, 2002d; Ai, 2002e). A hydrophobic surface can be changed to hydrophilic by applying different films on it. PEI, PSS, Gelatin, Poly-D-lysine, and collagen nanofilms decrease the contact angle on silicone rubber. These materials were used to assemble ultrathin films on silicone for cell adhesion and growth. The thickness of each individual layer and the total film thickness can be adjusted precisely by changing the ionic strength of the solution from which the polyions are adsorbed (11). Neutron reflectivity analysis of the films composed of alternate layers of poly(styrenesulfonate) (PSS) and hydrogen containing polyallylamine (PAH) has proved

that polyanion / polycation films possess a uniform thickness and a multilayer structure. The interfaces between layers in polyion films are not sharp but exhibit partial interpenetration (30 % of their thickness) between neighboring polymeric layers (Decher, 1997; Schmitt, 1993; Korneev, 1995; Leasche, 1998). A distinct spatial component separation may be achieved between the first and the third or fourth neighboring polyion layers (Decher, 1997).

LbL assembly is a fundamental approach for designing organized films that contain different protein monolayers in precise locations. The production of ordered protein / polyion multilayers is an easy and general process, which may be applied to any water-soluble protein providing a surface charge. The technique lends itself to several biomedical applications. First, biosensors can be fabricated by using different proteins with a predetermined order that would produce sequential enzymatic reactions. Second, bio/nanoreactors can be made by deposition of enzyme/polyion multilayers onto nano-carriers. Third, biocompatible films can be adsorbed onto medical devices, where the surface properties (e.g., wetting, hardness and lubricating ability) may be adjusted by deposition of polyion films. Fourth, biological cells can be encapsulated to block unwanted recognitions. Fifth, drug delivery carriers can be made with controlled release and targeting functions.

1.3.2 Biocompatible Ultrathin Films

Biocompatible films are composed of multilayer assemblies of natural polyions, such as DNA, polynucleotides, and polysaccharides (e.g., heparin, chondroitine, and chitosan). DNA and polynucleotides (polyuridylic and polyadenylic acids) can be readily

assembled in alternation with polycations (PEI, PAH, polylysine) (Lvov, 1993a; Sukhorukov, 1996). Polysaccharides with oppositely charged polyions can be assembled on a surface to provide biocompatibilities. Cationic chitosan has been assembled with anionic PSS at pH 4 (Lvov, 1998b). An albumin / heparin multilayer assembly for biocompatible coatings was developed by Brynda (2000).

Polyions can also be assembled on biological surfaces. The technique overcomes a fundamental obstacle preventing the use of colloidal materials on biosurfaces: self-assembly onto a proteinaceous surface is hindered by the heterogeneity of the chemical groups on such surfaces. LbL polyion assembly covers heterogeneous surfaces and makes them inert in biological liquids. The assembly of a (poly(lysine) / alginate) multilayer on a gelatin surface resulted in a 200-fold drop of the adsorption of human fibroblast cells, as compared with the untreated surface (Elbert, 1999). This approach would allow treatment of a limited area of tissue via multiple rinsing steps with polyelectrolyte solutions, thus generating a thin coating on tissue surfaces, and providing inherent biocompatibility and degradability.

Biocompatible nanofilms formed on silicone rubber can provide a hydrophilic surface (Ai, 2002c; Ai, 2002e; Ai, 2002d). Poly-D-lysine, gelatin, collagen, fibronectin, and laminin were used in assembly of films. Layer thickness varied from 1 nm to 4 nm as monitored from QCM studies. The total film thickness was determined from the layer numbers and the material composition. Films coated on silicone were hydrophilic compared with unmodified silicone rubber, as verified from contact angle measurements. Endothelial cells, nerve cells, and hepatocytes attached and grew on the films.

Biocompatible films were patterned on a polydimethylsiloxane (PDMS) substrate through micrcontact printing (Ai, 2002f). Patterning of micro/nanospheres was achieved with the layer-by-layer self-assembly technique. Lines patterned from 4.5- μm microsphere and 45-nm nanosphere micropattern matched with the 60 μm microchannels from the PDMS stamp. The process differs from other methods for patterning self-assembled monolayers in that metal thin film coatings and alkanethiol solution were not required. PDMS substrates were unmodified before stamping. Polycation poly(ethylenimine) and polyanion poly(styrenesulfonate) were used as ink solution to form an ultrathin film on PDMS stamp through electrostatic LbL self-assembly. The multilayer film of (PEI/PSS)₃/PEI was assembled with a thickness of 12 nm. Then negatively charged 4.5- μm microspheres or 45-nm fluorescence nanospheres were adsorbed on the precursor film through the electrostatic interaction. Finally, microspheres or nanospheres were patterned on the PDMS substrate through contact printing. Positively charged poly-D-lysine was later adsorbed on negatively charged microspheres to form patterned biocompatible films. Bovine coronary arterial endothelial cells were attached on poly-D-lysine/microsphere patterns.

Biocompatible films assembled on microchannels increased cell adhesion and growth on the sidewalls of channels (Li, 2002). Using photolithography, ICP dry etching and softlithography, 100 μm channels were fabricated in PDMS. Gelatin nanofilms were coated on the channels through LbL self-assembly. Smooth muscle cells were cultured on PDMS flat surface as a control. Improved cell adhesion was observed on channels coated with gelatin multilayers. Most cells grew along the channel sidewall. There was a

significant difference in the alignment angle between the smooth muscle cells growing on the flat surface and 100 μm channel ($P < 0.05$).

Multilayer films which contain ordered layers of protein species were assembled by means of alternate electrostatic adsorption mostly with positively charged PEI, PAH, PDDA, chitosan or with negatively charged PSS, DNA and heparin (Lvov, 1995; Kong, 1999; Kong, 1994; Lvov, 1996; Hodak, 1997; Caruso, 1997; Caruso, 1998a; He, 1998; Kong, 1998; Onda, 1999). The pH of the protein solutions was set apart from the isoelectric point so that proteins were sufficiently charged under the experimental conditions. Water-soluble proteins, including, cytochrome c and P450, lysozyme, histone type YIII-S, myoglobin (Mb), pepsin, horseradish peroxidase (POD), hemoglobin, glucoamylase (GA), concanavalin A (Con A), albumin, glucose oxidase (GOx) (Kong, 1999; Hodak, 1997;), catalase, invertase, diaphorase (Kong, 1999; Lvov, 1996), Bacteriorhodopsin (He, 1998), immunoglobulin IgG (Caruso, 1997; Caruso, 1998a) were used at a concentration of 0.1 ~ 2 mg/mL or ca. 10^{-5} M. The surface structure of the solid support can affect the stability of proteins, and thus, precursor films of alternate PEI/PSS were used as standard surfaces.

All the proteins undergo the alternate adsorption with organic polyions for unlimited numbers of cycles. The mass increment at each step was reproducible. It is noteworthy that the protein's adsorption steps correlate with their molecular weights. Protein layer thicknesses as estimated from X-ray reflectivity, or scanning electron microscopy and molecular dimensions of proteins show good correspondence, suggesting a relatively uniform monolayer formation.

Increased biological activity and enhanced stability of polyions/proteins were found in the films. Assembled proteins are in most cases not denatured (Kong, 1999; Kong, 1994; Caruso, 1997; Kong, 1998). Proteins immobilized in multilayers with strong polyions such as PSS, PEI, and PDDA were insoluble in buffer for a pH range between 3 and 10. Protein multilayers with weak polyions were partially soluble in solutions with a pH close to the isoelectric point of one of the components (Brynda, 2000; Onda, 1999). Moreover, in some cases layer-by-layer immobilization with linear or branched polyions enhanced the enzymatic stability. The immobilization of proteins in multilayers preserves them from microbial attack. For example, the glucose oxidase/PEI multilayer was kept for three months in a refrigerator at 5° C and preserved 90% of its initial enzymatic activity. Furthermore, glucose oxidase (GOx) in the multilayer with PEI was active up to 60° C, as compared with the 50° C GOx activity limit in solution (Onda, 1999). For the antigen-antibody reaction in IgG / PSS multilayers, the activity increased up to 5 IgG layers (Caruso, 1997). The compactness or openness of protein multilayers may be regulated. Glucose oxidase, myoglobin and albumin multilayer films were compact, but IgG/PSS multilayers had an open structure with areas as large as 100 nm diameter unfilled in the upper layers of the film (Caruso, 1998a).

1.3.3 Encapsulation of Micro/Nanotemplates

In the discussion above, polyelectrolytes, enzymes and nanoparticles were assembled on a plane surface. The assembly process elaborated for a solid support may be transferred for an assembly onto micro/nanotemplates such as porous carriers (Pommersheim, 1994) or onto the surface of charged particles with diameters of 0.5 - 5

microns (Caruso, 1998b; Caruso, 1999). The assembly of organized polyion shells on latex is promising for creation of complex catalytic particles. An assembly of organized protein shells on latex was recently demonstrated (Caruso, 1999). By alternate treatment with poly(ethylenimine) (PEI) and polyacrylic acid (PAA) solutions at pH 6.5, the multilayer shell of (PEI/PAA)₈ was formed onto 500- μ m diameter acidic phosphatase / alginate beads (Pommersheim, 1994).

Controlled releases of dye (Antipov, 2001) and drug microcrystals were achieved through nanoencapsulation (Qiu, 2001; Ai, 2002b; Ai, 2002g) with polyelectrolytes such as PAH, PDDA, PSS, polysaccharides and polypeptides. Dye or drug release at different pH environments was slowed after encapsulation and controlled through the shell thickness. The permeability of PAH/PSS multilayers of the thickness of 20 nm for fluorescein dye microparticles was about 10^{-9} m/s (Antipov, 2001). Charged polyions and polypeptides were alternatively deposited on furosemide microcrystals through LbL assembly (Ai, 2002b; Ai, 2002g; Ai, 2002e). The sequential deposition on the surfaces of furosemide particles of PDDA and PSS was followed by adsorption of polypeptides. The release of furosemide from the coated particles was measured in aqueous solutions of pH 1.4 and pH 7.4. At both pH values, the release of furosemide from the encapsulated particles was slowed (10-300 times longer) as compared with unencapsulated furosemide. The thickness of the encapsulating membrane was ca. 115 nm for six bilayers of PSS/gelatin. The results provide a method to achieve prolonged drug release through self-assembly of nano-materials on drug microcrystals.

Cells could also be used as microtemplates for fabrication of nano-shells. Platelets were coated with 78-nm silica nanoparticles, 45-nm fluorescent nanospheres, or bovine

immunoglobulin G (IgG) through LbL assembly by alternate adsorption with oppositely charged linear polyions (Ai, 2001a; Ai, 2002h; Ai, 2002a). Sequential deposition on platelet surfaces of cationic PDDA and anionic PSS was followed by adsorption of nanoparticles or immunoglobulins. Nano-organized shells of platelets were demonstrated by TEM and fluorescence microscope images. Bovine IgG was assembled on platelets, as verified with anti-bovine IgG-FITC labeling. Localized targeting of anti-IgG shelled platelets was also demonstrated. An ability to coat blood cells with nano-organized shells can have applications in cardiovascular research and targeted drug delivery.

Bio/nanoreactors were fabricated by coating enzyme multilayers on nanosized latex (Lvov, 2001a; Fang, 2002b; Fang, 2002a). Organized multilayers of nanoparticles (9-, 20-, 45-nm diameter silica or 12-nm magnetite) and glucose oxidase (GOx) were assembled in alternation with oppositely charged polyelectrolytes on 420-nm latex particles. Stepwise growth of the multilayer films on latex was confirmed by microelectrophoresis and transmission electron microscopy. The inclusion of silica layers on latex yields a higher surface area, resulting in greater GOx adsorption and thereby increasing the catalytic activity of the bio-reactor. The bioactivity was proportional to the core surface area and also to the number of GOx layers in the shells. Also the presence of magnetic nanoparticles allows self-stirring of the nanoreactors with rotating magnetic field and enhances its productivity.

Nano-sized hollow shells were fabricated by dissolving cores encapsulated in multilayers of polyelectrolytes (Caruso, 1998b). Shells were used as enzyme carriers (Lvov, 2001b). Stable hollow polyelectrolyte capsules were produced by means of the LbL assembling of PAH, and PSS, on melamine formaldehyde microcores followed by

the core decomposition at low pH. These capsules are impermeable for urease in water and become permeable in a water/ethanol mixture. The capsules were loaded with urease in water/ethanol mixture and then resuspended in water. The urease molecules are kept in the capsule, whereas the small urea molecules rapidly diffuse through the capsule wall providing a substrate for the biocatalytic reaction.

In the enzyme crystal templating procedure, protein crystals (10- μm diameter catalase or 0.2- μm diameter α -chymotrypsin) were treated sequentially with poly(styrenesulfonate) (PSS) and poly(allylamine) (PAH) or chitosan to form 5-8 layer coverage (Caruso, 2000; Sukhorukov, 2000). The proteins were encapsulated in polyion shells which are penetrable by small molecules (such as ions and low molecular weight substrates), but which prevent protein leakage. By changing a solvent pH, nanocrystals were dissolved that resulted in the formation of spherical capsules containing a high concentration (50 – 70 wt %) enzyme solution. Enzyme activity was retained in these microcapsules, and the enzyme was stabilized against microbe attacks (Caruso, 2000).

1.4 Hypothesis and Specific Aims

1.4.1 Hypothesis

Nano-encapsulated platelets express lower activation and adhesion response induced by high shear stress.

1.4.2 Study Objectives

A human coronary artery stenosis model will be built to test the hypothesis. Endothelial cells will be seeded onto the inner surface of the model to simulate a

physiological environment for the study of platelet activation. Fixed and live platelets will be coated with polyions, nanoparticles, and antibodies for assembly test. Live platelets coated with an outermost layer of heparin will be used in all flow studies. Platelet activation and adhesion after encapsulation will be compared with unmodified platelets. Overall platelet activation will be determined by TXB₂ assay. The amount of nitric oxide released from endothelial cells will be determined from fluorescence nitric oxide sensor. A cell viability/cytotoxicity fluorescence sensor will be used to label platelets in order to measure the degree of platelet adhesion on collagen.

Specific experiments are as following:

Flat silicone rubber substrates and the inner surface of silicone model will be coated with different nanofilms.

Fixed platelets will be encapsulated with polyions, nanoparticles, or antibodies. Live platelets will be encapsulated with polyions and an outermost layer of heparin. Cell viability/cytotoxicity will be determined from a specific fluorescence sensor.

Laminar flow at a Reynolds number of 436 will be imposed on the model. High shear stress will be generated by a 90% area reduction stenosis, and the degree of platelet activation will be determined from TXB₂ concentration after flow as a function of the maximum shear stress at the stenosis.

The nitric oxide released from endothelial cells at different locations will be measured through a fluorescence nitric oxide sensor.

Models coated with a collagen nanofilm will be used to test platelet adhesion in the flow experiment. Encapsulated and unmodified platelets will be labeled with a cell

viability/cytotoxicity fluorescence sensor. The degree of platelet adhesion is determined from the fluorescence intensity difference before and after the flow experiment.

CHAPTER 2

MATERIALS AND METHODS

2.1 Introduction

Activation and adhesion of modified and unmodified platelets were studied under flow conditions. Platelet solution was perfused through a 90% area reduction stenosis coated with either collagen or endothelial cells. The 90% area reduction was selected to provide a high shear stress, and the cosine shape was chosen because fluid dynamic data were already available for this geometry.

Platelets were separated from the whole bovine blood by centrifugation. Layer-by-layer self-assembly was used to modify the surface properties of the platelet. Platelet viability and cytotoxicity after encapsulation were measured by using fluorescence Live/Dead sensor. Overall platelet activation through the stenosis model was determined by a Thromboxane B2 assay. Platelets were tagged with a fluorescent marker so that adhesion onto the collagen-coated model could be measured from fluorescence intensity change before and after each flow experiment. A fluorescence nitric oxide sensor was used to quantify the nitric oxide released from endothelial cells in response to shear stress.

2.2 Coronary Artery Stenosis Silicone Model

2.2.1 Model Geometry

The flow model with an axisymmetric stenosis was designed to simulate the stenosis coronary artery. The model had a diameter of 6.35 mm with the stenosis diameter of 2.12 mm. The detailed geometry of the stenosis model is shown in Figure 2.1. A 3-D view of the model core is shown in Figure. 2.2.

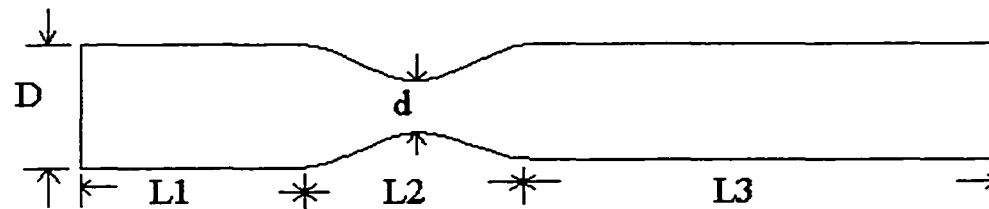


Figure 2.1 The core of the stenosis model

Where $D = 6.35$ mm; $d = 2.12$ mm; $L1 = 63.50$ mm; $L2 = 19.05$ mm; $L3 = 165.10$

mm

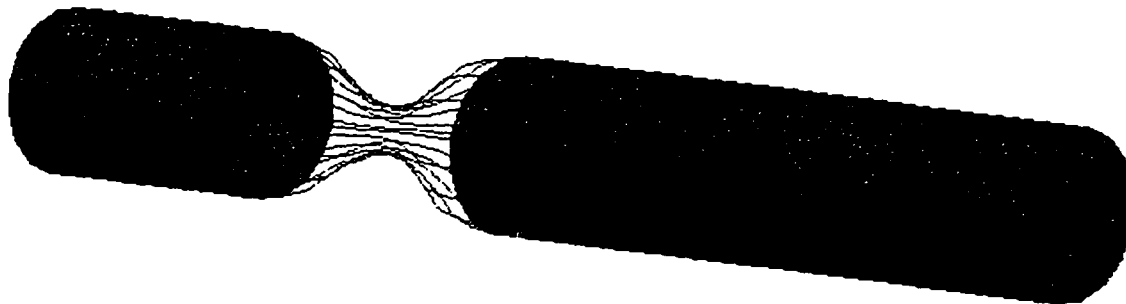


Figure 2.2 The 3-D view of the stenosis model

The stenosis of the model is cosine shaped with a 90% area reduction. The length of stenosis is nine times of the diameter of the minimum stenosis diameter (d). The shape is described by:

$$\frac{r_s}{R} = 1 - \frac{1 - \sqrt{A}}{2} \cdot \left(1 + \cos\left(\frac{2\pi}{3} \cdot \frac{z}{D}\right) \right) \quad -1.5 < \frac{z}{D} < 1.5$$

where

r_s : the radius of the stenosis

R : the radius of the non-stenosis area

Z : the axial position from the greatest stenosis severity (zero value at the stenosis center)

D : the diameter of the non-stenosis tube

A : the area of the stenosis diameter ($A = 0.1$)

2.2.2 Casting the Coronary Artery Stenosis Model

The Aluminum (Alloy 7075 Aluminum, McMaster) model core was fabricated by using an Optimum™ Ultra Precision Machining System. The flow model was constructed by molding Sylgard 184 polymer (Dow Corning) around the core in a Plexiglas box (Figure. 2.3a). To prepare the liquid silicone for casting, siloxane oligomers and siloxane cross-linkers were mixed in a ratio of 10:1 by weight. Any air bubbles in silicone were removed with a vacuum pump. The mixed silicone liquid was then carefully poured into the Plexiglas box. The silicone model cured to a solid state after three days at room temperature (25°C), after which the model was removed from the

Plexiglas box (Figure. 2.3b, c). Finally, the aluminum core was gently removed and the cured silicone model was thoroughly rinsed with water.

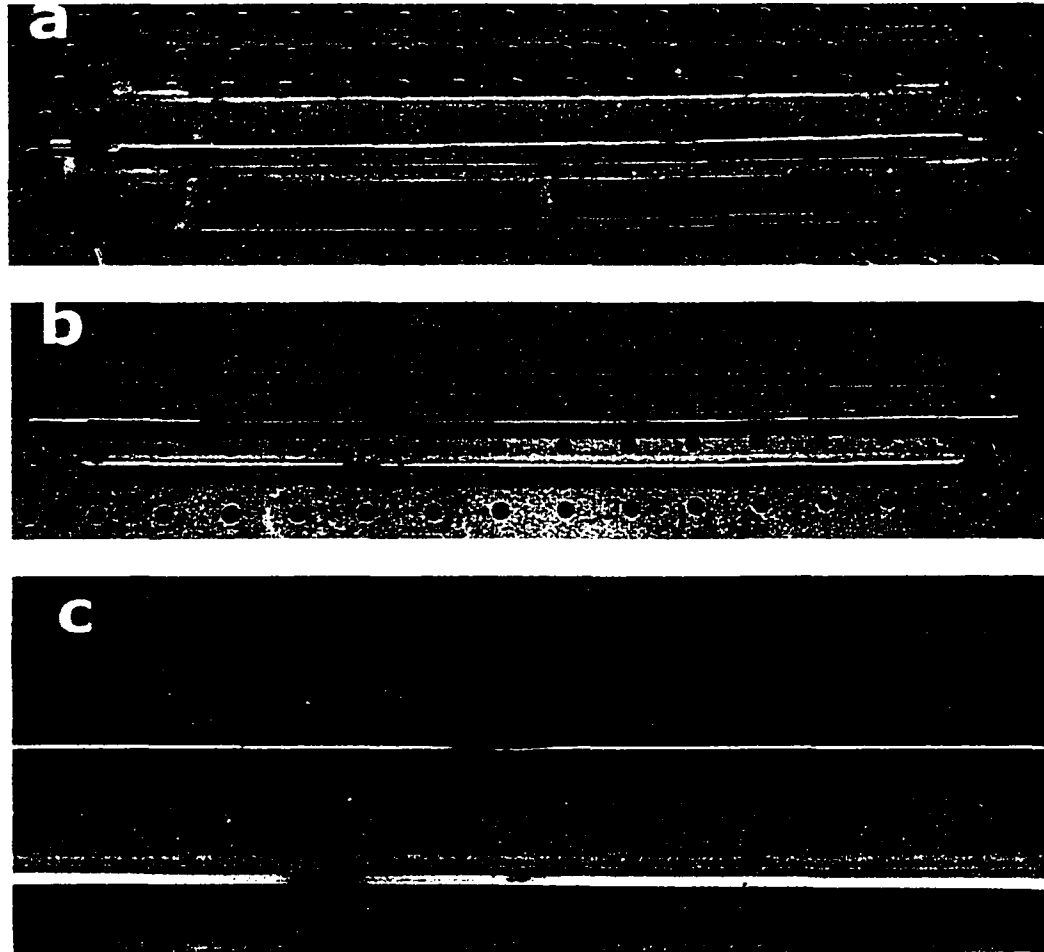


Figure 2.3 The stenosis model of coronary artery

(a) Aluminum core in the casting box. (b) Core and cast model removed from the casting box. (c) Close up of b. The circular holes on the support platform are spaced 1 inch apart.

2.3 Silicone Surface Modification through Micro/ Nano-Film Coating

2.3.1 Gelatin-Glutaraldehyde Crosslinking on a Flat Silicone Rubber Substrate

2.3.1.1 Silicone Rubber Substrate. A silicone (Sylgard 184, Dow Corning) rubber film was coated on the bottom of a 35 × 10 mm cell culture dish (Becton Dickinson). Liquid silicone was prepared by the same process used for the flow model material. A sample of 0.5g of freshly mixed liquid silicone was then added to each 35 × 10 mm culture dish. The final solid substrate was formed after three days at room temperature.

2.3.1.2 Gelatin Crosslinking Methods. Two methods were used in the crosslinking of gelatin films on silicone rubber substrates. In the first method (Fig 2.4), gelatin powder Type B of bovine skin (Gloom 225, Sigma) and glutaraldehyde (GA) (Aldrich) were mixed before coating. The ratio of gelatin:GA is preferably from 256:1 to 64:1. To avoid hydrolysis and loss of gel strength, gelatin solution was made freshly before the coating procedure. In this study, three proportions of 256:1, 128:1 and 64:1 were used. A gelatin concentration of 5% was achieved in every final mixed solution. GA concentrations were 0.02%, 0.04%, and 0.08% in the different coating solutions. The silicone-coated 35 × 10 mm culture dishes with silicone coatings were pre-wetted with 100% ethanol, and then washed twice with deionized water. The newly mixed solution was applied to the silicone for 20 minutes at 27°C. The gelatin solution was poured from the dish and washed three times with deionized water. A 1% Glycine (Sigma) solution was added, incubated for 30 min, and then washed 3 times with deionized water. Finally, the surface was washed once with culture medium. A gelatin film formed after 5 hours in the flow hood.

The second method (Method II) is illustrated in Fig. 2.1. The silicone surface was pre-wet with 100% ethanol, and washed twice with deionized water. A 5% gelatin solution was then added into culture dish, and allowed to sit for 40 min at 27°C, after which the gelatin was poured from the dish. A 2.5 % glutaraldehyde solution was added and incubated for 20 min. The glutaraldehyde was then discarded and the dish washed 3 times with deionized water. A 1% Glycine solution was then added, incubated for 30 min, and washed 3 times with deionized water. Culture medium was used to wash the dish once as a final treatment. The gelatin film was ready to use after another 5 hours.

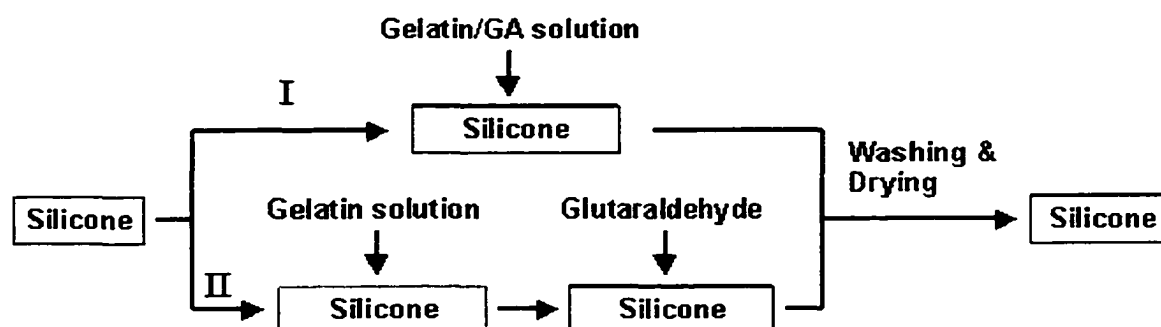


Figure 2.4 Two methods of gelatin/GA crosslinking on a silicone rubber substrate

2.3.1.3 Gelatin Film Thickness. To determine the thickness of gelatin/GA crosslinking film coated on silicone rubber, Petri dishes were weighed on a scale before and after the coating procedure. The gelatin/GA film thickness was calculated by using the measured weight difference.

2.3.1.4 Cell Culture. Clonetics® Endothelial Cell Basal Medium 500 ml (CC-3121) was obtained from Cambrex Corp. Clonetics® Endothelial Cell Growth Medium (CC-4133, Cambrex) contained 0.5 ml human epidermal growth factor, 0.5 ml hydrocortisone, 0.5 ml 1000X Gentamicin sulfate - Amphotericin-B, 10 ml Fetal bovine serum (FBS), and 2 ml Bovine Brain Extract (3 mg/ml protein content). The final media was prepared by gently mixing CC-3121 and CC-4133 together before using. Bovine coronary arterial endothelial cells (BCAEC) were obtained from a fresh bovine heart and used after the second passage. BCAEC were obtained from a fresh bovine heart and used after the second passage. The bovine coronary artery was rinsed three times with phosphate buffered saline (PBS) to remove blood, then 0.25% collagenase solution was injected into the artery and incubated for 30 minutes at 37°C in a CO₂ incubator. Collagenase solution was then centrifuged at 1000 rpm to collect cells. Cell pellets were dispersed in the media. Cells were cultured in a CO₂ incubator (Sanyo Scientific) under 95% air/5% CO₂ at 37°C in a humidified atmosphere. Cells were ready for use once enough had accumulated. The seeding density was about 7.48×10^4 cells/cm² on the modified and unmodified silicone rubber surfaces.

2.3.1.5 Measurement of Contact Angle. To better understand the surface energy of a modified silicone surface, contact angles were measured through the Sessile Drop method. Measurements were taken when gelatin/GA crosslinked films formed after 24 hours. Deionized water drops were used in the measurement. For each surface, ten measurements were collected.

2.3.1.6 Viscosity Study. To understand the gelatin-GA crosslinking process, the viscosities of gelatin-GA mixtures were dynamically measured at different time intervals.

Gelatin and GA were mixed before the measurements. Because the exact amount of GA involved in method II was unknown, all samples used here were from method I. The crosslinking occurred at room temperature (27°C). Before the measurements, the samples were pre-heated in a water bath (Model TC-500, Brookfield) to 37°C. Viscosity was measured on a digital viscometer (Model DV-II+ Version 3.2, Brookfield).

2.3.2 Coating Biocompatible Nanofilm on a Flat Silicone Rubber Substrate

Cationic poly(ethyleneimine) (PEI, MW 25,000, Aldrich) and anionic sodium poly(styrenesulfonate) (PSS, MW 70,000, Aldrich) were selected for the LbL assembly. To provide a physiological pH during the coating procedure, all preparation work was performed in 0.01M PBS solution at pH 7.4. Polypeptide such as poly-D-lysine (PDL) and gelatin type B were got from Sigma. Vitrogen[®] Collagen type I was obtained from Cohesion Technologies, Inc. Solutions of 3 mg/mL PSS, 2 mg/mL PEI, 1 mg/mL PDL, 1mg/ml collagen, and 1 mg/mL gelatin were prepared in pH 7.4 PBS.

The CellTracker Green BODIFY (C-2102, Molecular Probes) is a probe that freely passes through the cell membranes, but once inside the cell, it undergoes a glutathione S-transferase-mediated reaction, producing a cell-impermeant reaction product. Since glutathione levels in most cells are high (up to 10 mM) and glutathione transferase is ubiquitous, this CellTracker reagent should provide an excellent means for long-term studies of cell viability and cytotoxicity. The reagent can be loaded into cells by simply adding the CellTracker probe to the culture medium and then briefly washing with fresh medium before analysis.

2.3.2.1 Coating PEI/PSS Multilayers on PDMS. Three different films were coated on silicone rubber for cell adhesion and growth. All films required a base that consisted of several layers of PEI/PSS. These strongly charged polyelectrolytes PEI and PSS were coated on the substrate through LbL self-assembly (Fig 2.5, method 1). The silicone substrates in the cell culture dishes were pre-wet with 75% ethanol, then rinsed with deionized water twice. The surface was dried with nitrogen-gas. The first layer was coated with 1mg/ml PSS solution for 30 minutes. Nitrogen gas drying and PBS washing were performed before the second PEI coating. Further coatings were 15 minutes for every layer with drying and PBS washing. The procedure was continued until the required number of layers was reached. When cells were seeded directly onto PEI, 11 total layers were formed. When cells were seeded directly onto PSS, 12 total layers were formed.

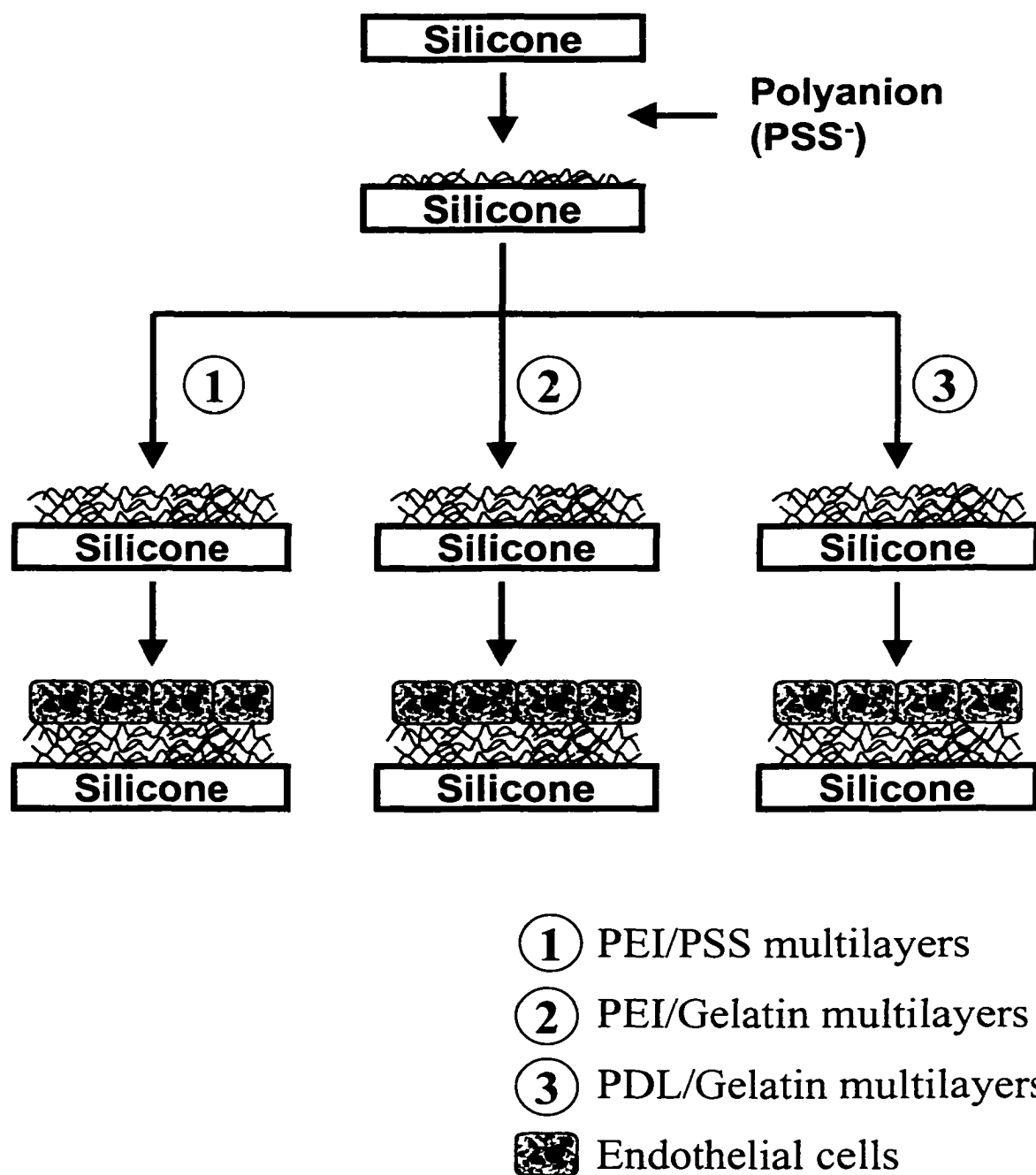


Figure 2.5 Coating PEI/PSS film on silicone rubber substrate

2.3.2.2 Coating PEI/Gelatin Multilayers on Silicone Rubber. The procedure of coating biocompatible nanofilm on a flat silicone rubber substrate is briefly described in Figure 2.5 (method 2). A precursor film of (PSS/PEI)₂ + PSS was assembled by the

procedure outlined in the previous section. Multilayers of (PEI/Gelatin)₅ were then coated on the precursor layer through the electrostatic LbL self-assembly. The coating method was similar to the precursor layers, but a longer incubation time (30 minutes) for gelatin was required. A film with the architecture of (PSS/PEI)₂ + PSS + (PEI/Gelatin)₅ was formed on the silicone rubber substrate through LbL self-assembly.

2.3.2.3 Coating PDL/Gelatin Multilayers on Silicone Rubber. The procedure of coating biocompatible nanofilm on a flat silicone rubber substrate is briefly described in Figure 2.5 (method 2). A precursor film of (PSS/PEI)₂ + PSS was assembled by the procedure already described. Then multilayers of (PDL/Gelatin)₅ were coated on the precursor layer through the electrostatic LbL self-assembly. Again, 30 minutes of coating was required for the gelatin was required. The final film architecture was (PSS/PEI)₂ + PSS + (PDL/Gelatin)₅.

2.3.2.4 Coating PSS/Collagen Multilayers on Silicone Rubber. The procedure of coating biocompatible nanofilm on a flat silicone rubber substrate is briefly described in Figure 2.6. A precursor film of (PSS/PEI)₂ was deposited on the silicone rubber by the previously described coating procedures. The collagen used here was type I (Vitrogen, Cohesion Technologies, Inc). A solution of 1 mg/ml collagen was used in the assembly procedure. Multilayers of (PSS/Collagen)₅ were coated on the precursor layer through the electrostatic LbL self-assembly, allowing 30 minutes for each collagen layer. The final film architecture was (PSS/PEI)₂ + (PSS/Collagen)₅.

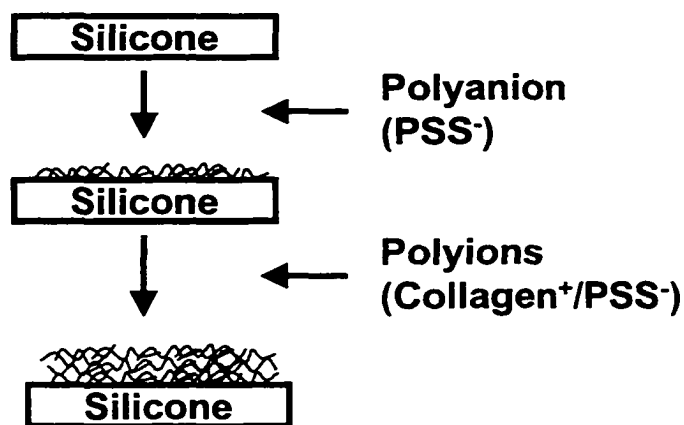


Figure 2.6 Coating PSS/Collagen film on PDMS substrate

2.3.2.5 Measurement of Contact Angle. To better understand the surface energy of a modified silicone surface, contact angles were measured through the Sessile Drop method. Measurements were taken after every layer was coated and dried. Deionized water drops were used in the measurement.

2.3.2.6 Monitoring the Thickness of A Nanofilm. To monitor polyion layer formation on silicone rubber at pH 7.4, the coating procedure was elaborated on 9-MHz quartz crystal microbalance (QCM, USI-System Inc, Japan) electrodes. The QCM frequency shift (ΔF) caused by the stepwise adsorption process was measured. The mass and thickness of each assembled layer was derived from ΔF . For these calculations, the Sauerbrey equation (Sauerbrey 1959) was used with the scaling method of Lvov (Lvov 1995).

2.3.3 Coating a Collagen Nanofilm onto the Inner Surface of a Silicone Model

Platelet adhesion on collagen substrate was carried out in the coronary artery stenosis silicone model. Collagen/polyion film was coated on the inner surface of a

stenosis model through LbL self-assembly (Fig 2.7). The silicone model was first rinsed with deionized water twice. Then one ending of the model was sealed with a stopper. 3mg/ml PSS solution was gradually added into the model and incubated for 30 minutes. PSS solution was discarded after coating and rinsed three times with deionized water. Gentle nitrogen gas drying was performed to remove the remained water inside the model. Coating the second layer of PEI was similar to the first layer. Washing and drying was necessary before the third layer coating. A precursor film of (PSS/PEI)₂ was assembled on the inner surface of the silicone model after repeating the previous coating procedures. Then multilayers of (PSS/Collagen)₅ were coated on the precursor layer through the electrostatic LbL self-assembly. The coating method was similar to the precursor layers, but forming a complete collagen layer required a 30-minute exposure to the collagen. The final film architecture was (PSS/PEI)₂ + (PSS/Collagen)₅ was formed on the inner surface of a silicone model. The model was sterilized with 10 X Gentamicin solution (Sigma) and was dried with nitrogen gas before use.

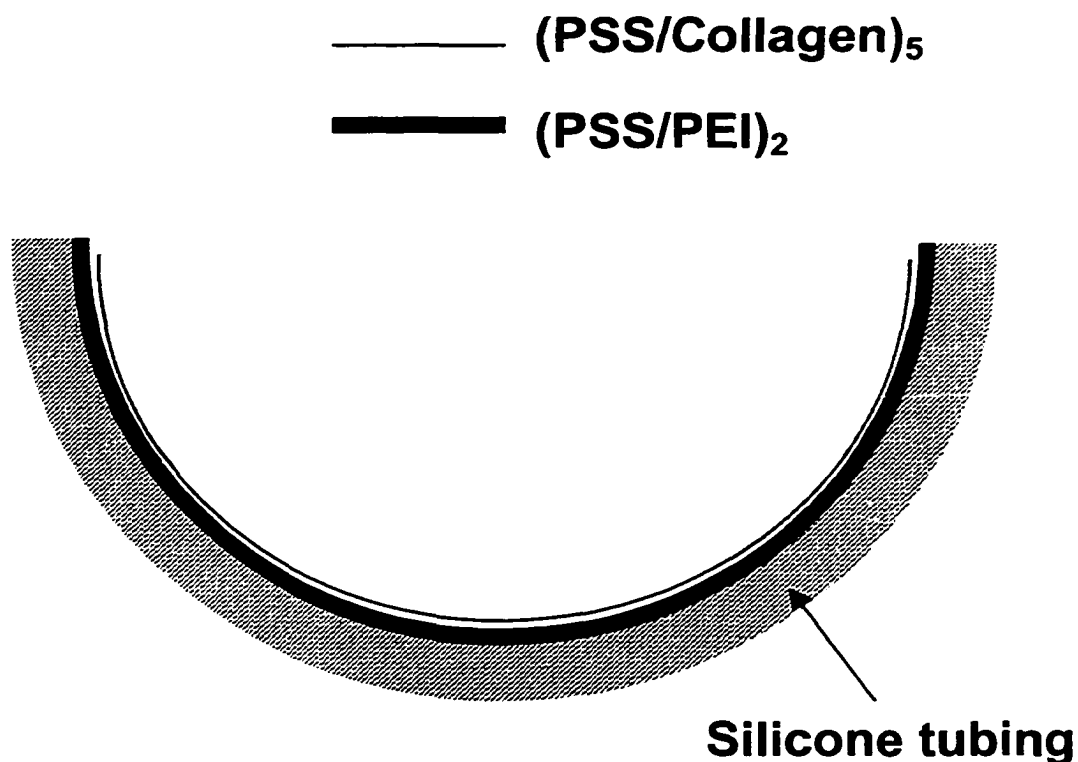


Figure 2.7 Cross-sectional view of a collagen nanofilm coated on the inner surface of a silicone model.

2.3.4 Seeding Endothelial Cells onto the Gelatin Nanofilm Coated on the Silicone Rubber Substrate

2.3.4.1 Cell Adhesion and Growth on PEI/gelatin Nanofilm. A PEI/Gelatin film was coated on the silicone rubber through LbL self-assembly as described before (Figure 2.8). Endothelial cells were seeded on the nanofilm to test the film biocompatibility. The precursor layer of (PSS/PEI)₃ + PSS was first coated on the silicone rubber substrate. A (PEI/gelatin)₅ multilayer was further assembled on the precursor layer to form the nanofilm. Cells were seeded onto the nanofilm-covered silicone rubber substrate with a density of 3.6×10^5 cells/cm².

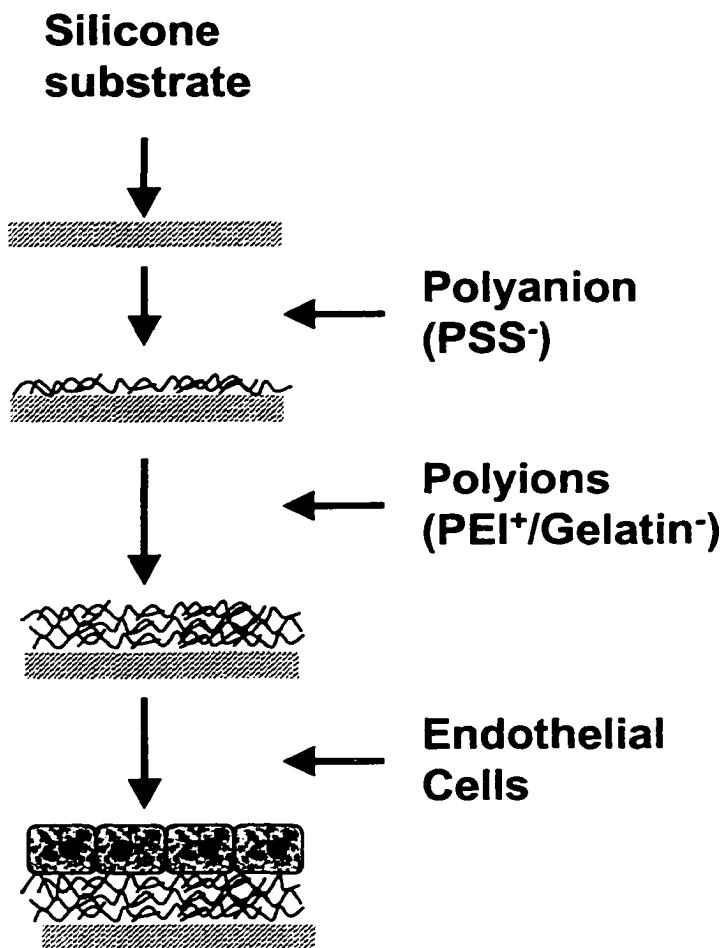


Figure 2.8 Seeding endothelial cells on PEI/Gelatin nanofilm coated on silicone rubber substrate

2.3.4.2 Cell Adhesion and Growth on PDL/gelatin Nanofilm. The film composed of (PDL/gelatin) multilayers was coated on the PDMS substrate and endothelial cell seeding was performed.

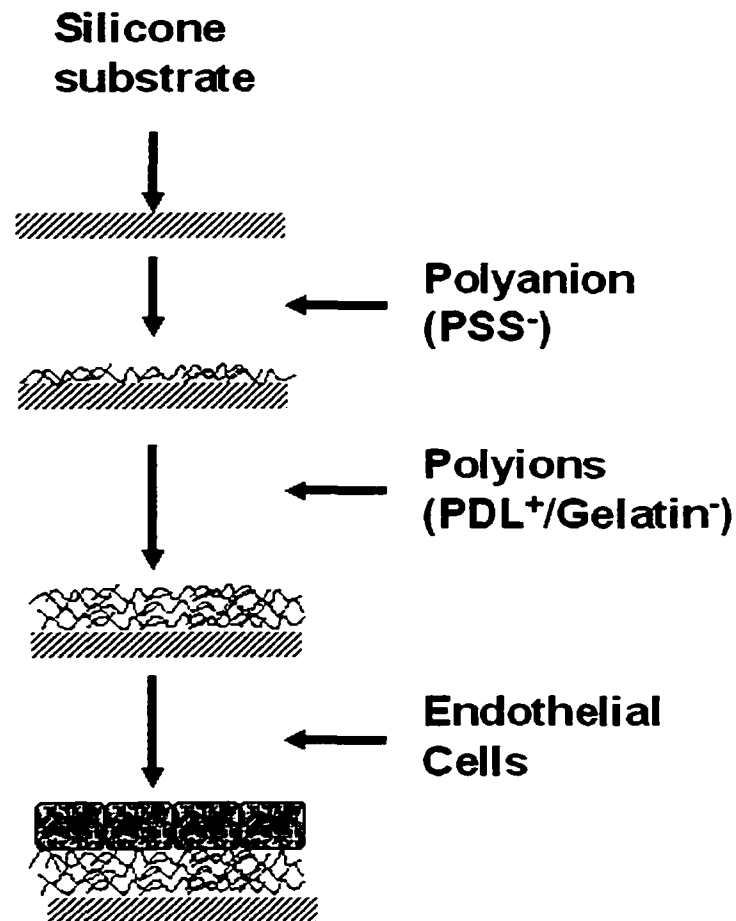


Figure 2.9 Seeding endothelial cells on PDL/Gelatin nanofilm coated on silicone rubber substrate

2.3.5 Seeding Endothelial Cells on the Inner Surface of Silicone Model

The inner surface of a silicone model was modified for endothelial cells adhesion and growth. An ultrathin film composed of PDL/Gelatin multilayers was coated on the inner surface of a stenosis model through LbL self-assembly (Figure 2.10). The silicone model was first rinsed with deionized water twice. Then one end of the model was sealed with a stopper. A 3 mg/ml PSS solution was gradually added into the model and incubated for 30 minutes. The PSS solution was discarded after coating and rinsed three

times with deionized water. Nitrogen-gas drying was performed to remove the remaining water inside the model. Then a polycation layer of PEI was assembled on the PSS layer. Washing and drying was necessary between assembling every two layers. A precursor film of $(\text{PSS}/\text{PEI})_2 + \text{PSS}$ was assembled on the inner surface of the silicone model after repeating the previous coating procedures. Then multilayers of $(\text{PDL}/\text{Gelatin})_5$ were further coated on the precursor layer through the electrostatic LbL self-assembly. The final film architecture was $(\text{PSS}/\text{PEI})_2 + \text{PSS} + (\text{PDL}/\text{Gelatin})_5$. The model was sterilized with 10 X Gentamicin solution and dried with nitrogen gas before using.

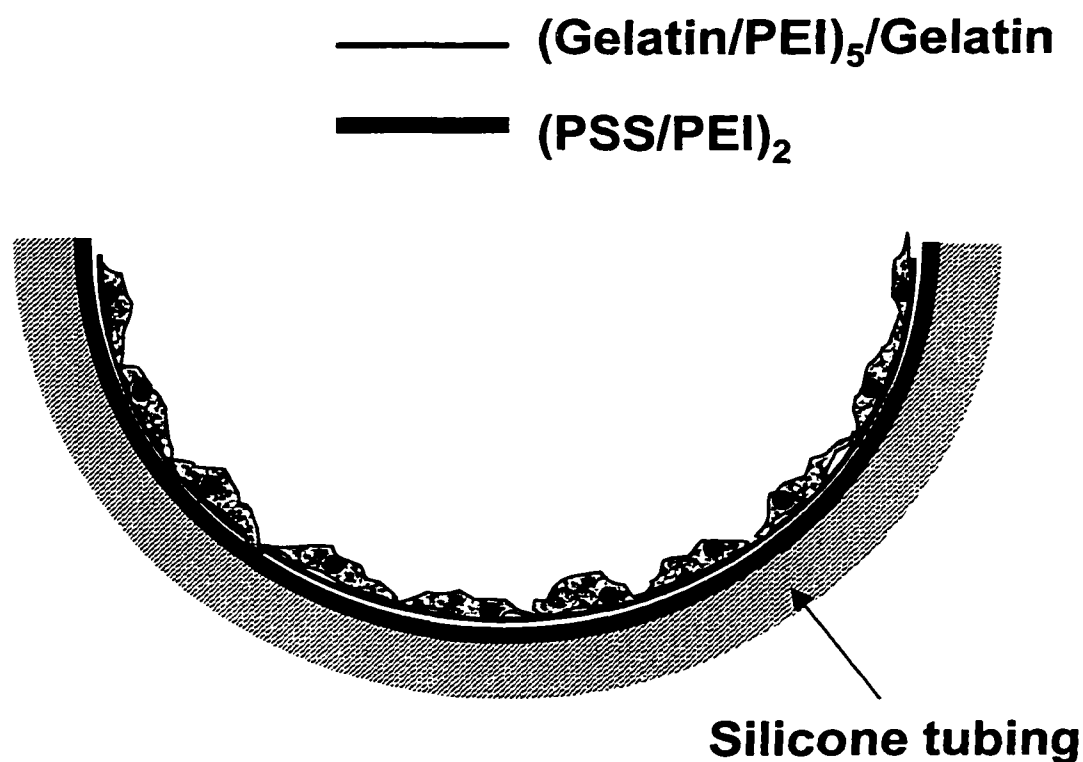


Figure 2.10 The cross-section view of a silicone model with inner surface coverage of endothelial cells

Before cell seeding, the model was rinsed with cell culture media once. Endothelial cells with a seeding density of 4.2×10^5 cells/cm² were incubated in the

model in a CO₂ cell culture incubator. The model was turned manually from one side to another every hour after seeding. After eight hours of seeding, a flow system with media supply was hooked up with the model (Figure 2.11). The system is composed of a silicone model, a variable speed pump (Fisher Scientific, Model NO. 13-876-2), and a bottle of culture media. Silicone tubing was used to connect all parts of the system. Cell adhesion on the inner surface of the model is more stable after pre-treated with low shear stress flow (Dardik, 1999). The seeded model was treated for 24 hours with 1 dyne/cm² shear stress before running the platelet solution.

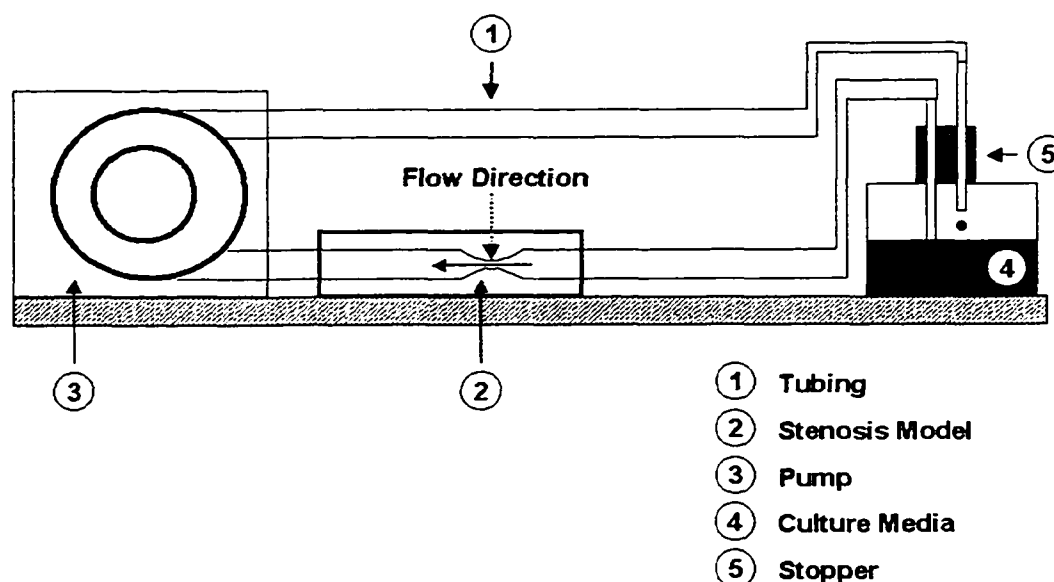


Figure 2.11 Culture endothelial cells in a flow system

2.4 Nano-Encapsulation of Platelets

2.4.1 Nano-Encapsulation of Fixed Platelets

2.4.1.1 Reagents and Materials. Cationic poly(dimethyldiallylammonium chloride) (PDDA, MW 200,000, Aldrich) and anionic sodium poly(styrenesulfonate)

(PSS, MW 70,000, Aldrich) were selected for the LbL assembly. To provide a physiological environment during the coating procedure, all preparation work was performed in 0.01 M PBS solution at pH 7.4. Silica nanoparticles of 78-nm diameter (Nissan Chemical Industries, Japan) and yellow-green fluorescence nanospheres (FN) of 45-nm diameter (Polysciences, Inc) were used for the assembly. PSS, silica and FN are negatively charged, while PDDA is positively charged at pH 7.4. Solutions of 3 mg/mL PSS, 2 mg/mL PDDA, 10 mg/mL silica, and 2.5 mg/mL FN were prepared in pH 7.4 PBS. Solutions of 0.5 mg/mL bovine IgG (Sigma) and 0.2 mg/mL anti-bovine IgG-FITC (Sigma) were used.

2.4.1.2 Platelets. Platelets were purified from fresh bovine blood. Platelet rich plasma (PRP) was obtained through centrifugation (Eppendorf 5804R centrifuge) at 250 g for 20 minutes at 22°C. Immediate fixation of PRP in 1% paraformaldehyde solution was carried out for two hours. Platelets were further purified by centrifugation at 500 g for 5 minutes and dispersed in phosphate buffered saline (PBS). The final platelet concentration was ca. 2×10^9 /mL.

2.4.1.3 Instrumentation. An Eppendorf 5804R centrifuge was used for the shell assembly. A quartz crystal microbalance, transmission electron microscope (TEM, Philips-CM10, Netherlands) and fluorescent microscope (Nikon, Eclipse, 2000) were used for structural analysis of the nano-ensembles.

2.4.1.4 Platelets Nano-Assembly. It is important to apply linear polycation/polyanion layers on microtemplates before assembly of proteins and nanoparticles. Flexible linear polyions cover the cell surface and act as “electrostatic glue” which holds oppositely charged nanoparticles or antibodies. A platelet surface is

negatively charged because most platelet surface glycoproteins have isoelectric points lower than 7.4 (McGregor, 1980). Figure 2.12 shows three methods of an assembly to functionalize platelet shells. In route (A), the outermost layers of FN/PDDA/FN were assembled by alternation of negatively charged fluorescent latex with positively charged PDDA. In route (B), a Silica/PDDA/Silica shell was deposited. For both methods, an additional outermost layer of PDDA was assembled as a protection layer (to prevent loss of silica or fluorescent nanoparticles). In route (C), an immunoglobulin bilayer of composition (PSS/IgG)₂ was assembled.

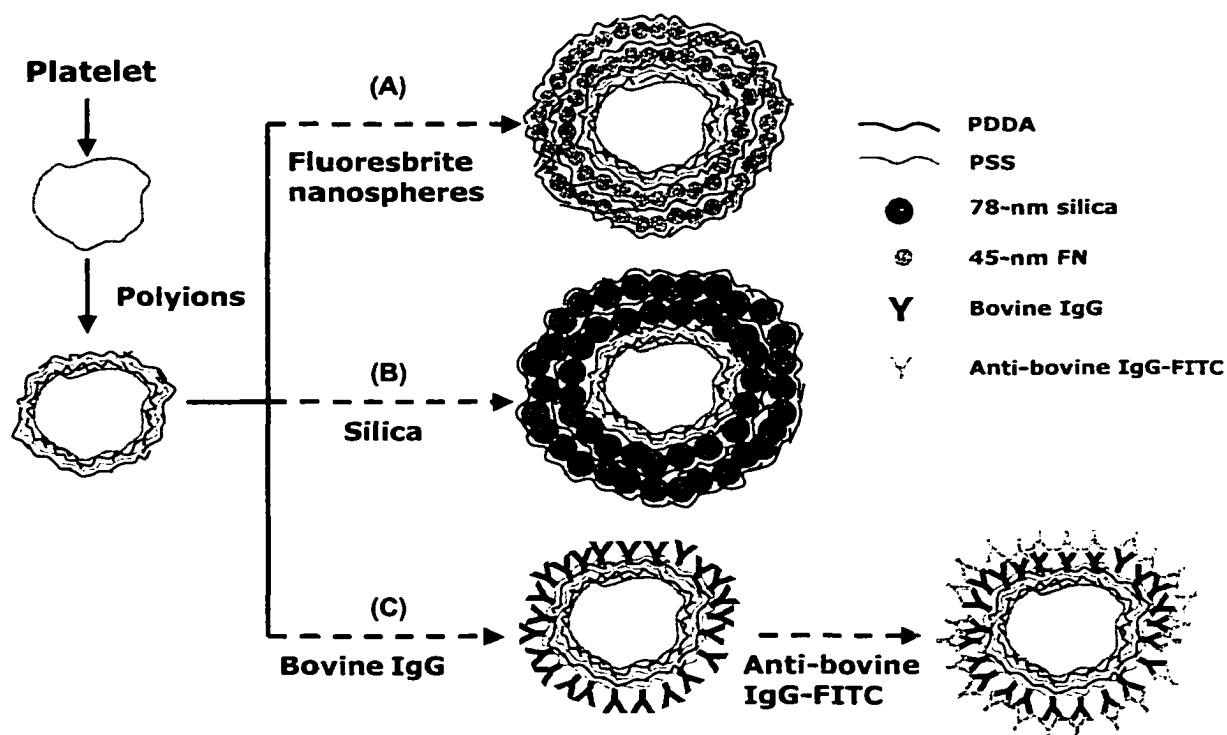


Figure 2.12 Scheme of three methods of an assembly to functionalize platelet shells

Next, bovine IgG was deposited through LbL self-assembly at a specific area in the silicone tubing, and the other parts of the tube remained uncovered with IgG (Figure. 2.13). One tenth of the length (8 mm) of protein-deposition-resistant silicone medical

tubing was selectively coated with bovine IgG on the inner surface. A solution of platelets shelled with anti-bovine IgG-FITC was then passed through the tubing 20 times. Afterwards, the tubing was rinsed, dried, and studied under a fluorescence microscope.

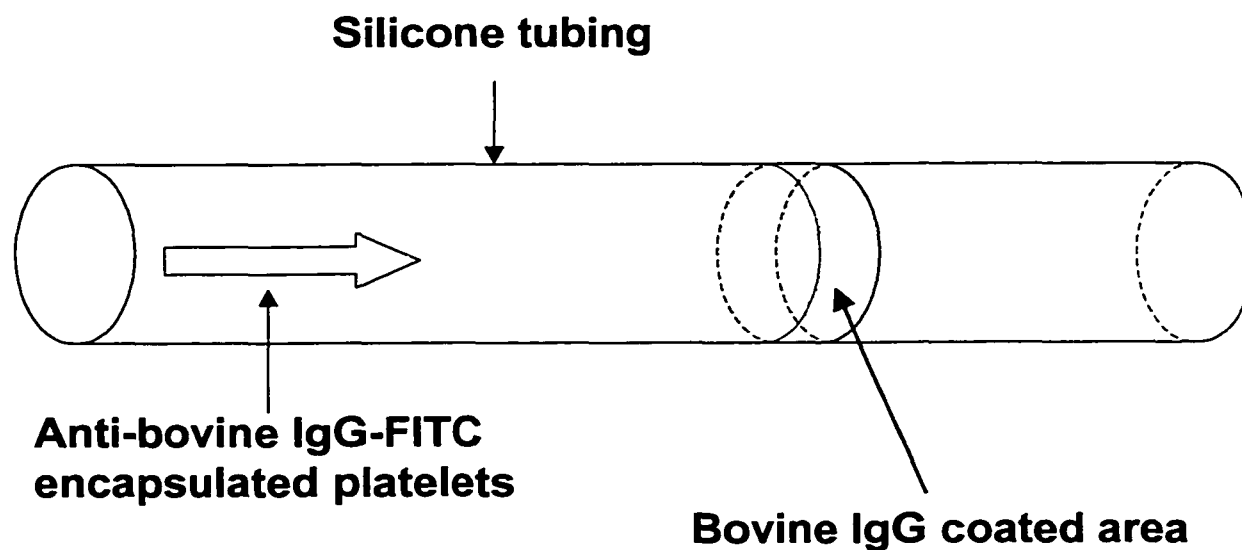


Figure 2.13 Anti-bovine IgG-FITC encapsulated platelets targeting to the IgG coated area

Positively charged PDDA was first deposited on the platelets. Adsorption was allowed to proceed for 20 minutes to ensure complete coverage. Platelets were separated from the PDDA solution by centrifugation at 550 g for 5 minutes. After three washing cycles, a layer of PSS was assembled. The adsorption procedure was similar to that used for the PDDA layer. A PDDA/PSS/PDDA multilayer was assembled on platelets as a precursor before deposition of nanoparticles or IgG.

To monitor polyion and nanoparticle layer formation on platelets at pH 7.4, the coating procedure was elaborated on 9-MHz QCM electrodes. The QCM frequency shift (ΔF) caused by the stepwise adsorption process was measured and used to calculate mass

and thickness of the layers deposited at every assembly step. For these calculations, the Sauerbrey equation was used (Sauerbrey, 1959) and scaling was performed (Lvov, 1995).

2.4.2 Nano-Encapsulation of Live Platelets

In contrast to the previous approach, platelets were also assembled with nano-shells while alive. Two layers were assembled on live platelets (Figure. 2.14). Platelets were first exposed with positively charged polyanion PDDA for 5 minutes and then washed. Then polysaccharide heparin was assembled as the outermost layer. Adsorption of a PDDA/heparin multilayer on QCM electrodes was used as an indirect measure of shell formation on platelets.

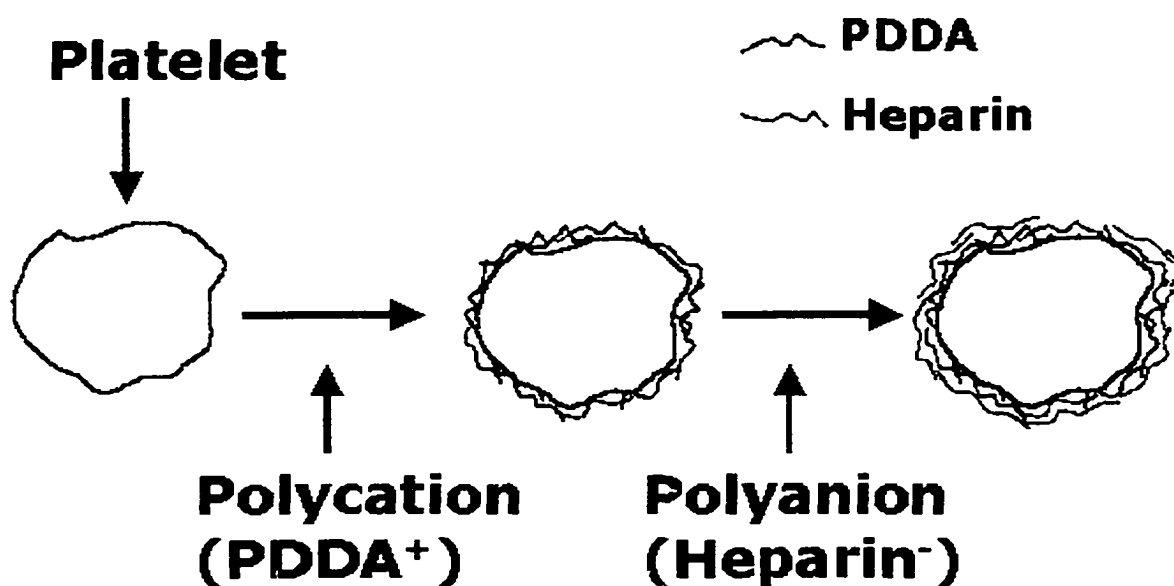


Figure 2.14 Live platelets assembly

2.4.2.1 Platelet Live/Dead Viability and Cytotoxicity Analysis. The LIVE/DEAD[®] Viability/Cytotoxicity Assay Kit (Molecular Probes, L-3224) provides a two-color fluorescence cell viability assay that is based on the simultaneous determination of live

and dead cells with two probes that measure two recognized parameters of cell viability- intracellular esterase activity and plasma membrane integrity. It has been shown that calcein AM and ethidium homodimer (EthD-1) are optimal dyes for this application (Papadopoulos, 1994). This method is generally faster, cheaper, safer and a more sensitive indicator of cytotoxic events than alternative methods. The assay has been used to quantify apoptotic cell death (Jacobsen, 1996) and cell-mediated cytotoxicity (Papadopoulos, 1994). The amount of live and dead/damaged cells were counted by using a fluorometer.

2.4.2.2 Labeling Procedure. The following procedure is used to label the cells for live/dead analysis:

1. Remove the LIVE/DEAD reagent stock solutions from the freezer and allow them to warm to room temperature.
2. Add 20 μL of the 2 mM EthD-1 stock solution (Component B) to 10 mL of sterile PBS, vortexing to ensure thorough mixing. This procedure creates an approximately 4 μM EthD-1 solution.
3. Combine the reagents by transferring 5 μL of the supplied 4 mM calcein AM stock solution (Component A) to the 10 mL EthD-1 solution. Vortex the resulting solution to ensure thorough mixing. The final solution contains approximately 2 μM calcein AM and 4 μM EthD-1.
4. Redisperse the encapsulated platelets in the final working solution and incubate for 30 minutes at room temperature.
5. Following incubation, add 20 μL of the platelet solution on a clean microscope slide.

6. For quantitative assay, add 1 ml of 10 times diluted platelet solution into the fluorometer cell and record the reading at corresponding wavelengths. The excitation wavelength for live platelets labeled with Calcein is 494 nm. The emission wavelength is 517 nm. For dead platelets labeled with EthD-1, the excitation wavelength is 528 nm, and the emission wavelength is 617 nm.

2.5 Model Setup

The setup of the model in a flow system is shown in Figure 2.15. The syringe is driven by a self-made syringe pump. The syringe pump is composed of a speed control box, a motor (SLO-SYN Synchronous/Stepping Motors, Superior Electronic, Part No. M062-LF-402F), an Adjustable DC power supply (PSA-305, Samlex Electric Company Ltd), and a Triple output DC power supply (E3630A, Hewlett Packard). Nalgene 50 Silicone Tubing (Nalge Company, Model NO. 8060-0060) was used in connecting the model and the syringe. A 60 ml syringe (Becton Dickinson) was used to inject the platelet solution into the model. The syringe can be pushed forward or backward by the stepper motor according to the control settings. The Reynolds number of coronary artery blood flow is calculated by using the following equation:

$$Re = \frac{4\rho Q}{\pi D\mu},$$

where

Q: Flow rate

ρ : Density of fluid

D: Diameter of the blood vessel or silicone model

μ : Viscosity of fluid

Here, we used the following numbers for related parameters as a simulation of human coronary artery blood flow. For a typical coronary artery, the flow rate of coronary artery blood flow, density of blood, diameter of coronary artery, and viscosity of blood are $4 \text{ cm}^3/\text{sec}$, 1.05 g/cm^3 , 0.35 cm , and $0.035 \text{ g/s}^{-1}\text{cm}^{-1}$ respectively. The corresponding Reynolds number of the coronary artery flow is 436. The same Reynolds number was kept in our silicone coronary artery stenosis model. The platelet solution has a viscosity of $0.01 \text{ g/s}^{-1}\text{cm}^{-1}$ and a density of 1.01 g/cm^3 . The diameter of non-stenosed section of the model is 0.635 cm . The corresponding flow rate in the silicone flow model is $2.15 \text{ cm}^3/\text{sec}$, and the velocity of inlet flow is 6.78 cm/sec .

Platelet solution was injected into the model by the syringe, and a hemostat (3) was used to stop the flow into the side branch direction. The hemostat was released when the fluid was returned to the syringe so that the solution would not pass backwards through the model. The platelet solution was then re-injected into the model by the syringe under the same flow condition. In all, 20 injections were performed. The experiment was carried out inside a sterile flow hood. The stenosis model, tubing, and the syringe were all sterilized by 10 X Gentamicin solution before the onset of flow.

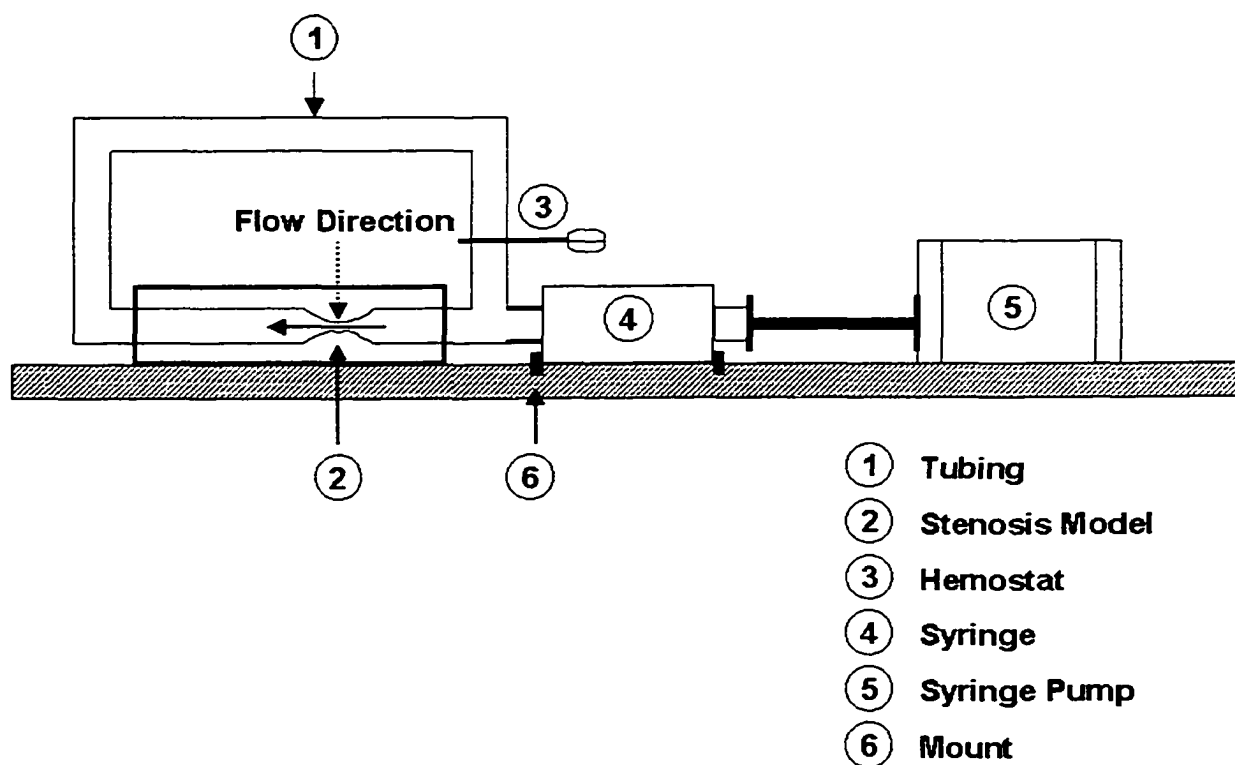


Figure 2.15 The setup of a stenosis model in a flow system

2.6 Thromboxane B₂ Measurement through ELISA

Samples of platelet solution were obtained after the flow experiment for measurement of thromboxane B₂ concentration. An Enzyme-Linked Immunosorbent Assay (ELISA) was performed to determine the amount of TXB₂ released from platelets.

2.6.1 Contents of the Assay System

The assay system contained the following:

Microtitre plate. Plate contains 12 X 8 well strips coated with donkey anti-rabbit IgG.

Thromboxane B₂ peroxidase conjugate. Thromboxane B₂-horseradish peroxidase, lyophilized.

Thromboxane B2 standard. Thromboxane B2 2.56 ng, lyophilized.

Antiserum. Rabbit anti-thromboxane B2, lyophilized.

TMB substrate. Enzyme substrate containing 3,3', 5,5'-tetramethylbenzidine (TMB)/hydrogen peroxide in dimethylformamide.

Assay buffer concentrate. Assay buffer concentrate, 5 ml. On dilution this bottle contains 0.1 M phosphate buffer, pH 7.5 containing 0.9% NaCl and 0.1% bovine serum albumin and preservative.

Wash buffer concentrate. Wash buffer concentrate of 12.5 ml. On dilution the reagent contains 0.01 M phosphate buffer, pH 7.5 containing 0.05% TweenTM20.

The detailed assay protocol is described in Figure 2.16.

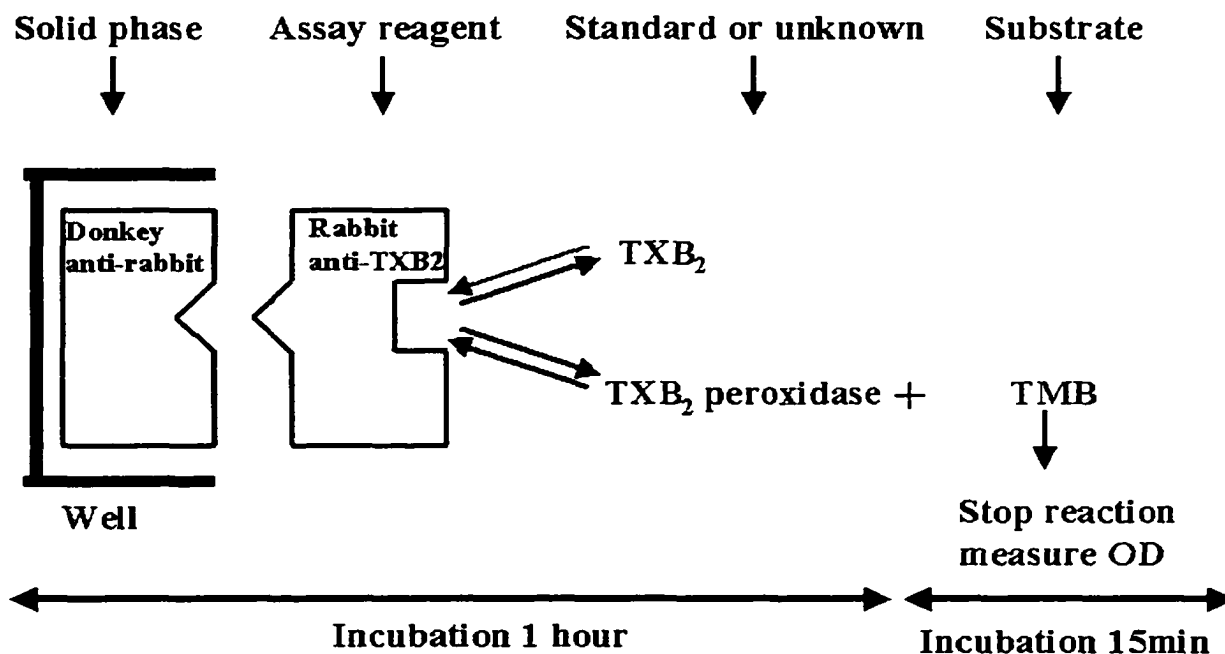


Figure 2.16 TXB₂ measurement through ELISA (modified from BIOTRAK, 1994)

A 1 ml sample of concentrated platelets was added into a centrifuge tube (tube I), mixed with 2 ml acetone, and shaken for 2 min. The mixture was then centrifuged at 4°C

(12,000 g, 3 min). The supernant was transferred to a second tube (tube II), and 2 ml hexane was added. This tube was shaken for 2 min and centrifuged at 4°C for 5 min at 12,000 g. The upper hexane layer was discarded and the pH of the lower layer was adjusted to 3.0 ~ 4.0 with 1M citric acid. After addition of 2 ml chloroform, the tube was shaken for 2 min, and centrifuged at 4°C for 5 min at 12,000 g. The lower chloroform layer contained the extracted TXB₂. The super layer was collected into a third tube (tube III) and extracted again with 2 ml chloroform. The super layer of tube III was discarded. The extracts from tube II and III were dried under nitrogen or vacuum.

2.6.2 Enzymeimmunoassay Procedure

2.6.2.1 Reagent Preparation. All reagents must be allowed to equilibrate to room temperatures before use.

Assay Buffer. Transfer the previous extracts to a 50 ml graduated cylinder by repeated washing with distilled water. Adjust the final volume to 50 ml with distilled water and mix thoroughly.

Standard. Carefully add 2.0 ml diluted assay buffer add replace the stopper. Mix the contents of the bottle until completely dissolved.

Thromboxane B₂ peroxidase conjugate. Add 6.0 ml diluted assay buffer and replace the stopper. Mix the contents of the bottle until completely dissolved. The solution will contain thromboxane B₂-horseradish peoxidase in phosphate buffer containing 0.9% sodium chloride, 0.1% bovine serum albumin and preservative.

Antiserum. Add 6 ml diluted assay buffer and replace the stopper. Gently mix the contents of the bottle until a complete solution is obtained. The solution will contain anti-

thromboxane B₂ serum in phosphate buffer containing 0.9% sodium chloride, 0.1% bovine serum albumin and preservative.

2.6.2.2 Preparation of Working Standards. Eight different working standard concentrations were prepared from 0.5 pg to 64pg. Label 7 centrifuge tubes 0.5pg, 1pg, 2pg, 4pg, 8pg, 16pg, and 32 pg. Pipette 500 μ l assay buffer into all tubes. Pipette 500 μ l of the stock standard (1.28 ng/ml) into the 32 pg tube and mix thoroughly. Transfer 500 μ l from the 32 pg tube to the 16 pg tube and mix thoroughly. Repeat this doubling dilution successively with the remaining tubes. Aliquots of 50 μ l from each serial dilution together with the stock solution will give rise to 8 standard levels of TXB₂ ranging from 0.5 to 64 pg per well.

2.6.2.3 Assay Protocol. The detailed assay protocol is summarized in the following table. Five mixtures are prepared, a substrate blank, a test for nonspecific binding, a zero standard, thromboxane B₂ standards, and the test samples. To prepare each sample, the reagent listed on the left hand column of the table is mixed in the indicated amount and order.

Table 2.1 Thromboxane B₂ Enzymeimmunoassay Protocol (volume unit: μ l)

Reagent	Assay Mixture				
	Substrate blank	Non-specific binding (N)	Zero standard (B ₀)	Standards	Samples
Buffer	--	100	50	--	--
Standard	--	--	--	50	--
Sample	--	--	--	--	50
Antiserum	--	--	50	50	50
Conjugate*	--	50	50	50	50

Table 2.1 continued.

Cover the plate, and incubate at room temperature (15°C) for 1 hour while shaking. Aspirate and wash all wells four times with 400 µl wash buffer. Immediately dispense 150 µl TMB substrate into all wells.					
TMB substrate	150	150	150	150	150
Cover the plate and mix on a microtitre plate shaker for exactly 15 minutes.					
1 M Sulphuric acid**	100	100	100	100	100
Shake to mix contents and determine optical density at 450 nm within 30 minutes.					

*: Thromboxane B2 peroxidase conjugate

** : 1M sulphuric acid was used to stop the reaction

2.6.2.4 Calculation of Results. The percent bound for each standard and sample was calculated by using the following equation.

$$\frac{B}{B_0} \% = \frac{(\text{Sample_or_standard_OD} - \text{NOD})}{B_0\text{OD} - \text{NOD}} \cdot 100$$

where

OD: optical density

NOD: optical density of non-specific binding

B0OD: optical density of the zero standard

2.7 Platelet Adhesion Test

Sample platelet solution before and after the flow experiment was collected for platelet adhesion analysis. Before running through the stenosis model, encapsulated and unmodified platelets were labeled with LIVE/DEAD ® Viability/Cytotoxicity Assay Kit.

Then fluorescence intensity of both samples was measured. After the flow experiment, samples were collected and again measured the fluorescence intensity. In every measurement, 494-nm excitation was used, and the component at 517 nm in the emission spectrum was measured.

2.8 Nitric Oxide Fluorescence Sensor

Nitric oxide from endothelial cells was measured with a fluorescence sensor DAF-FM diacetate (Molecular Probes, D-23842). The compounds, developed by Kojima and collaborators (Kojima, 1998), are essentially nonfluorescent until they react with NO to form a fluorescent benzotriazole (Figure 2.16). DAF-FM diacetate is cell-permeant and passively diffuses across cellular membranes. When inside cells, it is de-acetylated by intracellular esterases to become DAF-FM. The fluorescence quantum yield of DAF-FM is ~ 0.005 , but after reacting with nitric oxide, it increases about 160-fold, to ~ 0.81 (Kojima, 1999). The excitation and emission wavelengths of DAF-FM are 495 nm and 515 nm, respectively. The spectra of the NO adduct of DAF-FM are independent of pH above pH 5.5 (Kojima, 1999). Also, the NO adduct of DAF-FM is photostable for image capture. Finally, DAF-FM is highly sensitive for NO with a detection limit of 3 nM.

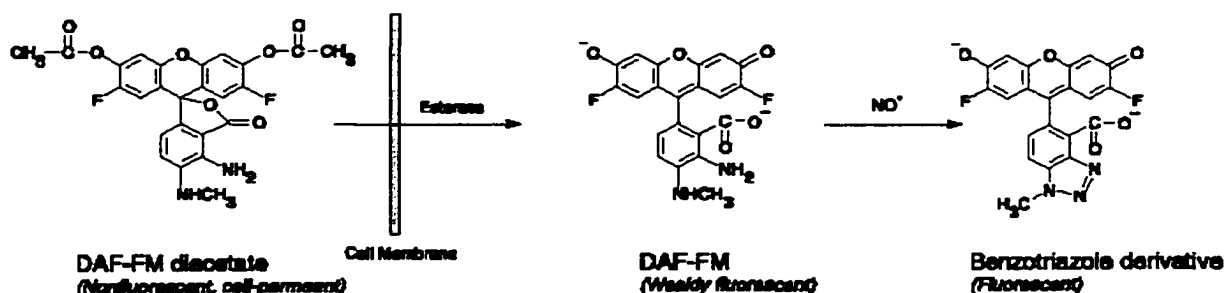


Figure 2.17 Reaction scheme for the detection of nitric oxide (NO) by DAF-FM and DAF-FM diacetate

A 5 mM stock solution of DAF-FM diacetate (D-23842, 1 mg) with a molecular weight of 496.42 was prepared in 0.4 ml anhydrous DMSO. Then 20 μ l aliquots were added in a centrifuge tube and stored at -20°C . The final working solution was 5 μ M as diluted 1000 times in PBS from the stock solution.

The silicone model coated with endothelial cells was first incubated with working DAF-FM diacetate solution for 30 minutes. Then the solution was discarded, and the platelet solution was driven through the model by the syringe pump. Finally, the model was rinsed with PBS, and cut into five parts (Figure. 2.17). Endothelial cells were peeled off from the model by using trypsin solution. Cells were collected by centrifuge at 1000 rpm and redispersed in a 0.5 ml PBS solution. The number of cells was counted by using a hemacytometer. A total of 10^6 cells from every sample was used for analysis. Endothelial cells cultured in Petri dish without DAF-FM diacetate incubation were used as a negative control. All samples were analyzed by flow cytometry. The number of cells was counted by using a hemacytometer (C.A. Hausser & Son). Finally, the intensity of fluorescence signal was calculated based on the number of cells per region.

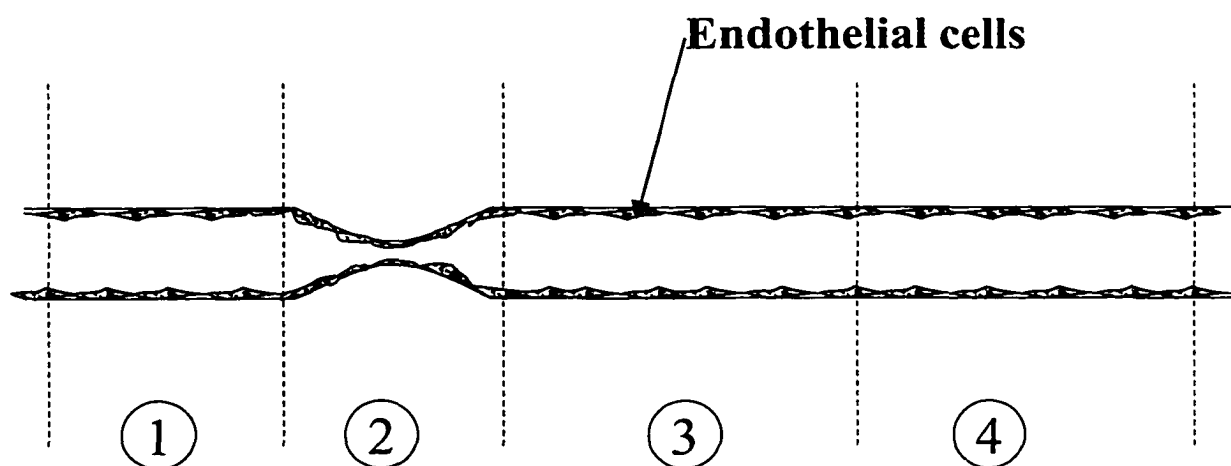


Figure 2.18 Regions of endothelial cells used for NO release measurement

2.9 Data Analysis

In the platelet targeting experiment, a MatLab image-processing program was used to analyze the area of targeted platelets. In every platelet activation and adhesion experiment, unmodified and encapsulated platelets were from the same blood source. The paired T test ($\alpha = 0.05$) was used to analyze thromboxane B₂ level and platelet adhesion results.

CHAPTER 3

RESULTS

3.1 Silicone Surface Modification for Endothelial Cell Adhesion and Growth

3.1.1 Gelatin-Glutaraldehyde Crosslinking on Silicone Rubber for Cell Adhesion and Growth

3.1.1.1 Gelatin Film Thickness. The approximate gelatin film thickness was calculated from the amount of gelatin/GA crosslinked on silicone rubber substrates, the bottom area of a Petri dish, and the density of gelatin. The thickness of a gelatin film was in the range of 110 ~ 160 μm . The detailed film thickness is listed in Table 3.1.

Table 3.1 The Thickness of Gelatin/GA Crosslinked Films

	Methods	Thickness (μm)
METHOD I	Gelatin:GA = 64:1	138.5 \pm 15.3
	Gelatin:GA = 128:1	132.2 \pm 24.1
	Gelatin:GA = 256:1	135.0 \pm 17.4
METHOD II	5% Gelatin, 2.5% GA	143.0 \pm 27.6

The gelatin/GA (Gelatin:GA = 64:1) crosslinking resulted in a film thickness of $138.5 \pm 15.3 \mu\text{m}$ on silicone rubber. The film thickness was $132.2 \pm 24.1 \mu\text{m}$ and $135.0 \pm 17.4 \mu\text{m}$ for gelatin:GA = 128:1 and gelatin:GA = 256:1 respectively. There was no significant difference among three groups, so the amount of gelatin remaining onto silicone rubber substrates was dependent on different GA concentrations. In method II, the gelatin film thickness was $143.0 \pm 27.6 \mu\text{m}$, and there was no statistically significant difference from method I.

3.1.1.2 Contact Angle. The surface properties of unmodified silicone rubber and gelatin-coated silicone rubber were characterized through contact angle measurements. Usually a lower contact angle represents a hydrophilic surface. Membranes formed on silicone rubber through gelatin/GA crosslinking displayed significantly lowered contact angles ($p < 0.01$). The unmodified silicone rubber surface was hydrophobic with a contact angle of $107 \pm 1.1^\circ$ (Figure 3.1). In the first method, the contact angles of gelatin modified surfaces were $84 \pm 1.1^\circ$, $77.2 \pm 1.6^\circ$, and $75.1 \pm 1.9^\circ$ for gelatin:GA of 256:1, 128:1, and 64:1, respectively. Crosslinking of gelatin:GA = 64:1 on silicone rubber has the lowest contact angle and is thus the most hydrophilic of the three surfaces modified by method I. The contact angle measured on method II gelatin/GA crosslinking modified surface was $73.3 \pm 1.1^\circ$. It is hydrophilic but no significant difference was found when compared with method I gelatin:GA = 64:1. All these modified surfaces are significantly hydrophilic in comparison to unmodified silicone ($p < 0.01$).

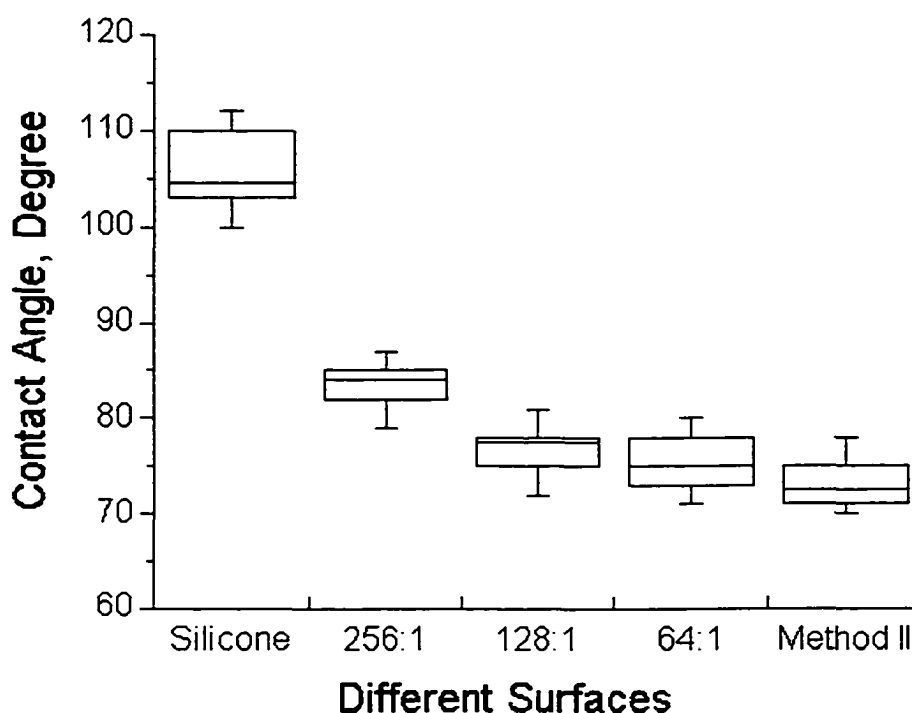


Figure 3.1 Contact angles of different surfaces. The contact angle on the unmodified silicone rubber is $107 \pm 1.1^\circ$

All modified surfaces are hydrophilic. In method I, the contact angles of gelatin modified surfaces were $84 \pm 1.1^\circ$, $77.2 \pm 1.6^\circ$, and $75.1 \pm 1.9^\circ$ for gelatin:GA of 256:1, 128:1, and 64:1, respectively. The contact angle on method II modified silicone rubber is $73.3 \pm 1.1^\circ$.

3.1.1.3 Viscosity Study. Gelatin/GA crosslinking was observed as the liquid solution solidified during the gelation procedure. Viscosity of gelatin/GA mixtures was used as a measure of crosslinking (Figure 3.2). In the shortest amount of time (45 minutes), gelatin:GA = 64:1 solution turned to a solid gel status. For 0.08% GA concentration (gelatin:GA = 64:1), viscosity was recorded every five minutes for a total period of 45 minutes. The initial viscosity was 4.56 mPa·s and 17.5 mPa·s at 30 minutes. The viscosity increased exponentially to 190.4 mPa·s at 35 minutes. Finally, it reached 513 mPa·s at 45 minutes. Readings could not be taken at 50 minutes since the mixture had already gelled. The gelatin:GA = 128:1 did not gel as quickly as the 64:1 solution

and was not in a complete solid state after 5 hours. The viscosity increased slowly with time. The final viscosity was 71.8 mPa·s. So 0.04% GA concentration in crosslinking was in a less degree compared with 0.08% GA concentration. The viscosity of 0.02% GA (gelatin:GA = 256:1) varied slightly after 5 hours. The initial viscosity was 4.1 mPa·s and the final viscosity was 6.8 mPa·s. The solution was still in a liquid status. The viscosity of the method II solution was not measured here because it was not known how much GA reacted with gelatin. Viscosity of 5% gelatin solution was measured as a comparison to those crosslinked solutions. The viscosity was stable around 2 mPa·s during 5 hours of measurement.

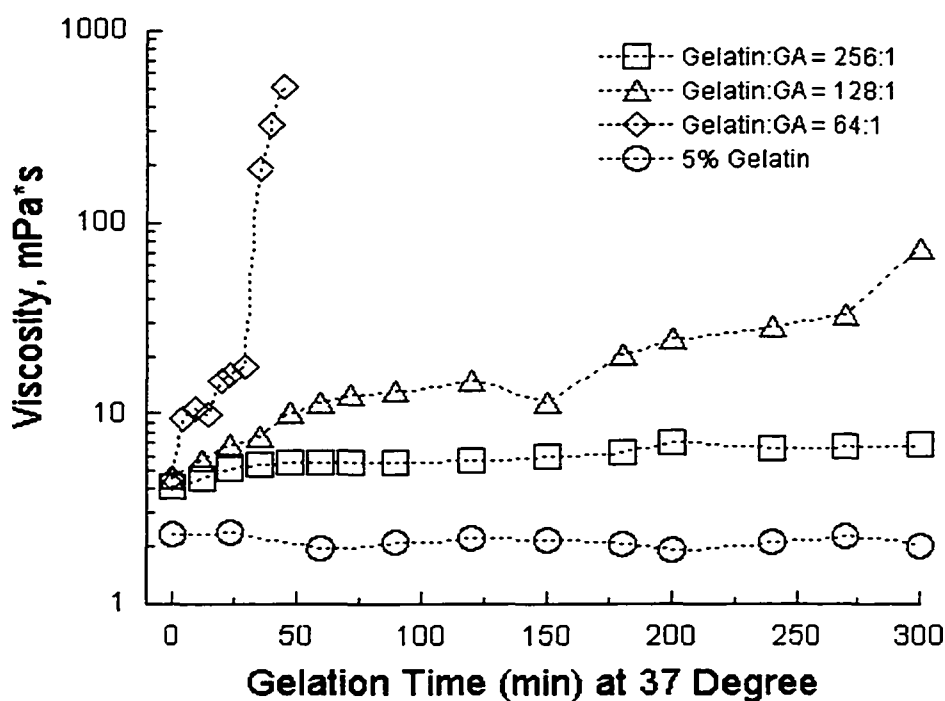


Figure 3.2 Viscosity measurements of different gelatin solutions

3.1.1.4 Endothelial Cell Adhesion and Growth. Endothelial cell attachment and growth were observed at 4 hours, 12 hours, 24 hours, 48 hours and 72 hours after seeding. Here, photos taken at 72 hours are shown for comparison among different silicone rubber surface modifications. The initial seeding density is 7.48×10^4 cells/cm². After 72 hours of seeding, the cell density was about $1.09 \pm 0.26 \times 10^5$ cells/cm², $1.00 \pm 0.23 \times 10^5$ cells/cm² and $5.13 \pm 0.12 \times 10^4$ cells/cm² for method I with GA concentration of 0.08%, 0.04% and 0.02%, respectively. On the modified surface provided by method II, the cell density was about $8.82 \pm 0.08 \times 10^4$ cells/cm². Some cell adhesion was found on silicone rubber.

At 4 hours after seeding, cells were partially attached to the modified and unmodified surfaces. At 12 hours, cells on modified surfaces were all well attached and growing, while most of the cells on silicone surface were detached and clumped together. At 24 hours, cells on all gelatin-modified surfaces were growing well. Minimal cell attachment on silicone was observed. After 48 hours, no cell attachment was observed on unmodified silicone rubber, and some cell fragments were seen in the media. While all cells were attached onto the modified surfaces.

At 72 hours (3 days) after seeding, cells were growing well on the method I (GA concentrations of 0.04% and 0.08%) modified surface (Figure 3.3a & b) and the method II modified surface (Figure 3.4). Cells attached on the above surfaces were in round or oval shapes usually indicating good adhesion and growth. On the method I (GA: 0.02%) modified silicone surface, cells were differentiated after 72 hours (Figure 3.3c) indicating bad adhesion. Almost no cell adhesion was found on the unmodified silicone surface (Figure 3.5).

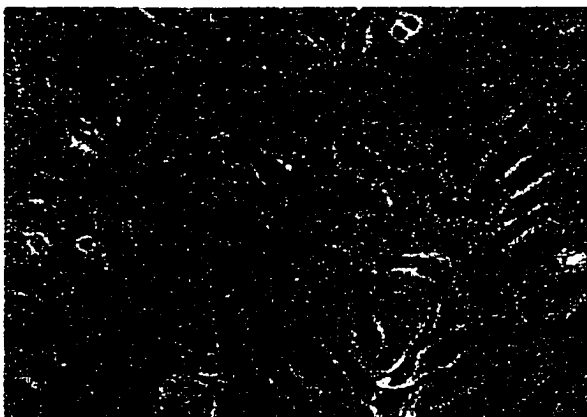


Figure 3.3a Cells attached on method I (GA: 0.08%) modified surface at 72 hours
Cells were well attached on the gelatin/GA modified silicone rubber substrate
(Magnification: $\times 200$).



Figure 3.3b Cells attached on method I (GA: 0.04%) modified surface at 72 hours
Endothelial cells covered most areas and in a subconfluent state (Magnification: $\times 200$).

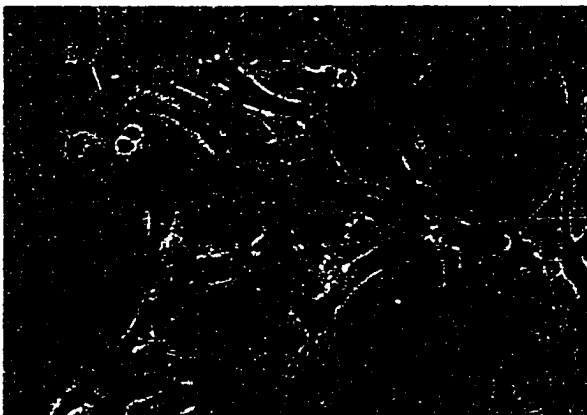


Figure 3.3c Cells attached on method I (GA: 0.02%) modified surface at 72 hours
Cells were attached to the modified surface (Magnification: $\times 200$) but the adhesion was
not satisfied in comparison to Figure 3a & b.

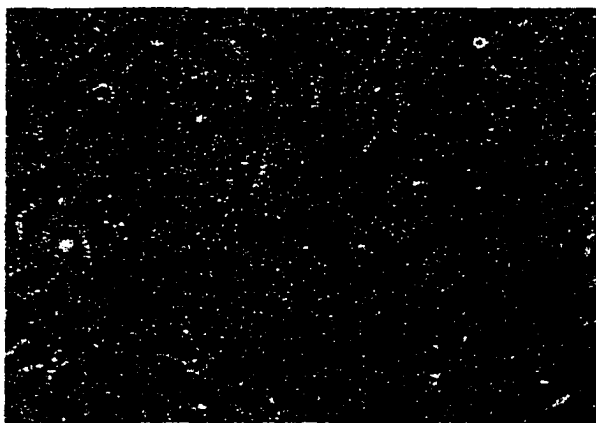


Figure 3.4 Cells attached on method II modified surface at 72 hours
Cell adhesion was nice hours (Magnification: $\times 200$) and similar to method I (GA: 0.08%) modified silicone rubber (Figure 3.3a).



Figure 3.5 Cells attached on silicone rubber surface at 72 hours
Few cells were attached on silicone rubber and other cells were floating in the media (Magnification: $\times 200$).

3.1.2 Coating a Biocompatible Nanofilm on Silicone Rubber

3.1.2.1 Contact Angle Measurements. Contact angle measurements were made for the PEI/PSS multilayers. The mean contact angles on PEI and PSS surfaces were 76° and 83° respectively. The contact angle measured on the silicone rubber surface was 108° .

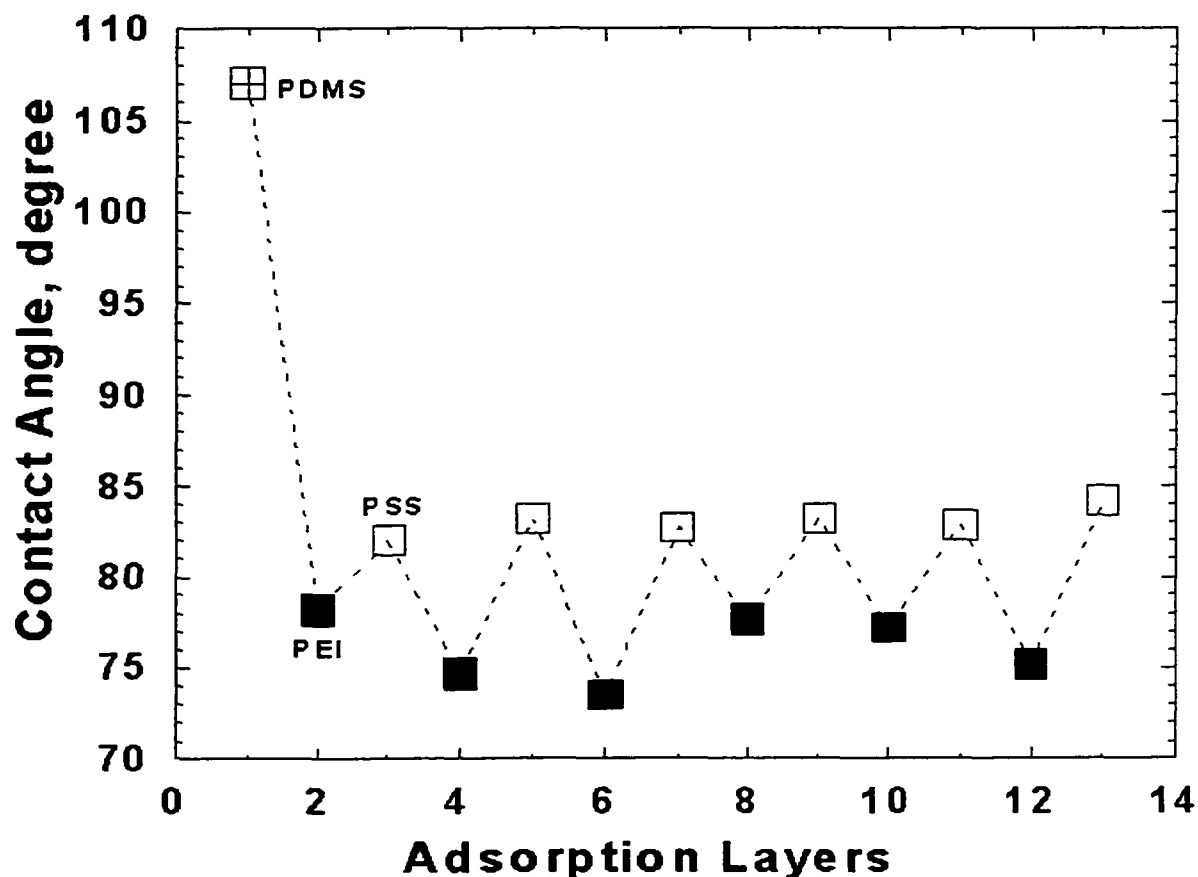


Figure 3.6 Contact angle measurements vs adsorption layers

Nanofilms coated on silicone rubber substrate with the outermost layer of poly-D-lysine, gelatin, collagen, fibronectin, laminin, hyaluronic acid, or heparin are hydrophilic (Ai, 2002e). Here, contact angle changes with the film composition of (PEI/PSS)₂ + (PEI/Gelatin)₅ are shown in Figure 3.6. Every polymer layer was characterized by a unique contact angle. Unmodified silicone was hydrophobic with a contact angle of 107°. The mean contact angles on PEI and PSS are similar to those in Figure 3.5 The averaged contact angle of the gelatin layer was about 55°, which indicated a significantly hydrophilic surface in comparison to unmodified silicone rubber.

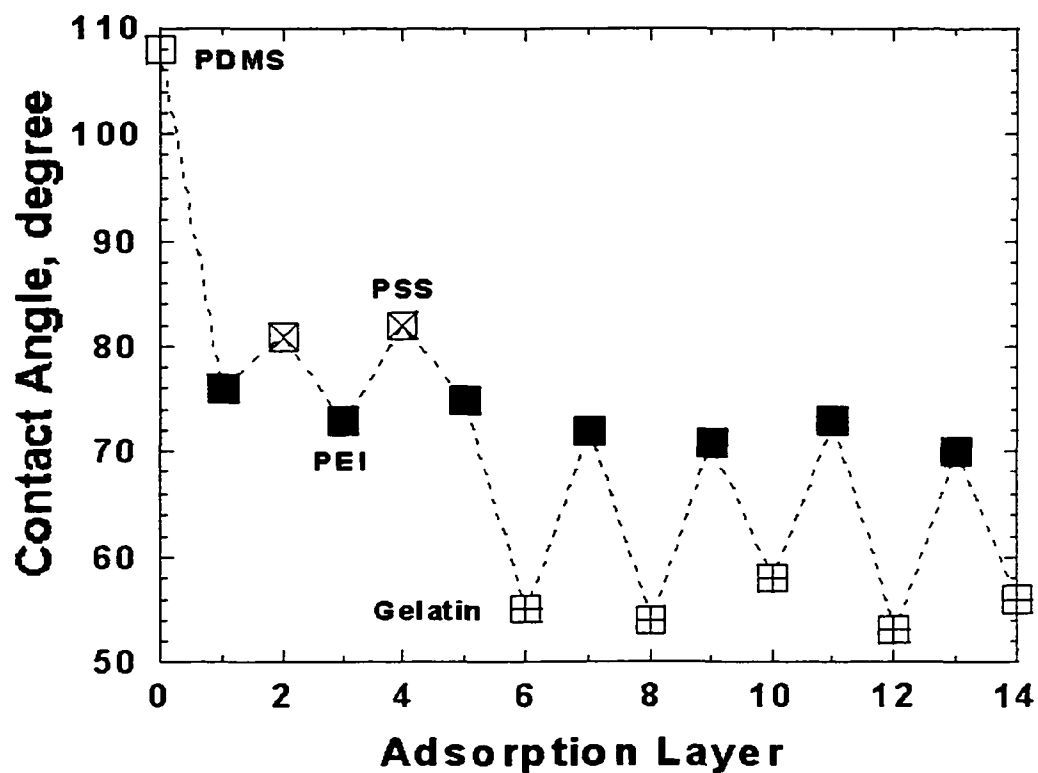


Figure 3.7 Contact angle measurements during the coating procedure

3.1.2.2 Nanofilm Thickness. Film growth on PDMS was indirectly estimated through coating multilayers on quartz crystal microbalance (QCM) electrodes. QCM frequency shifts were proportional to the amount of mass adsorbed on the electrodes. The thickness of a single layer ranged from 0.5 nm to 4 nm. The added mass and the coating thickness (ΔL) can be calculated from the frequency shift (ΔF) according to the Sauerbrey equation combined with a special scaling (Sauerbrey, 1959; Lvov, 1995). For the instrument used in this study, the calibration is ΔL (nm) = 0.017 ΔF (Hz).

The frequency shift vs adsorption layers of (PEI/PSS)₆ is shown in Figure 3.7. The film thickness was about 30 nm. Linear film thickness growth was noticed with the number of layers increased. The averaged layer thickness of PEI was 2.4 nm, similar to a PSS layer.

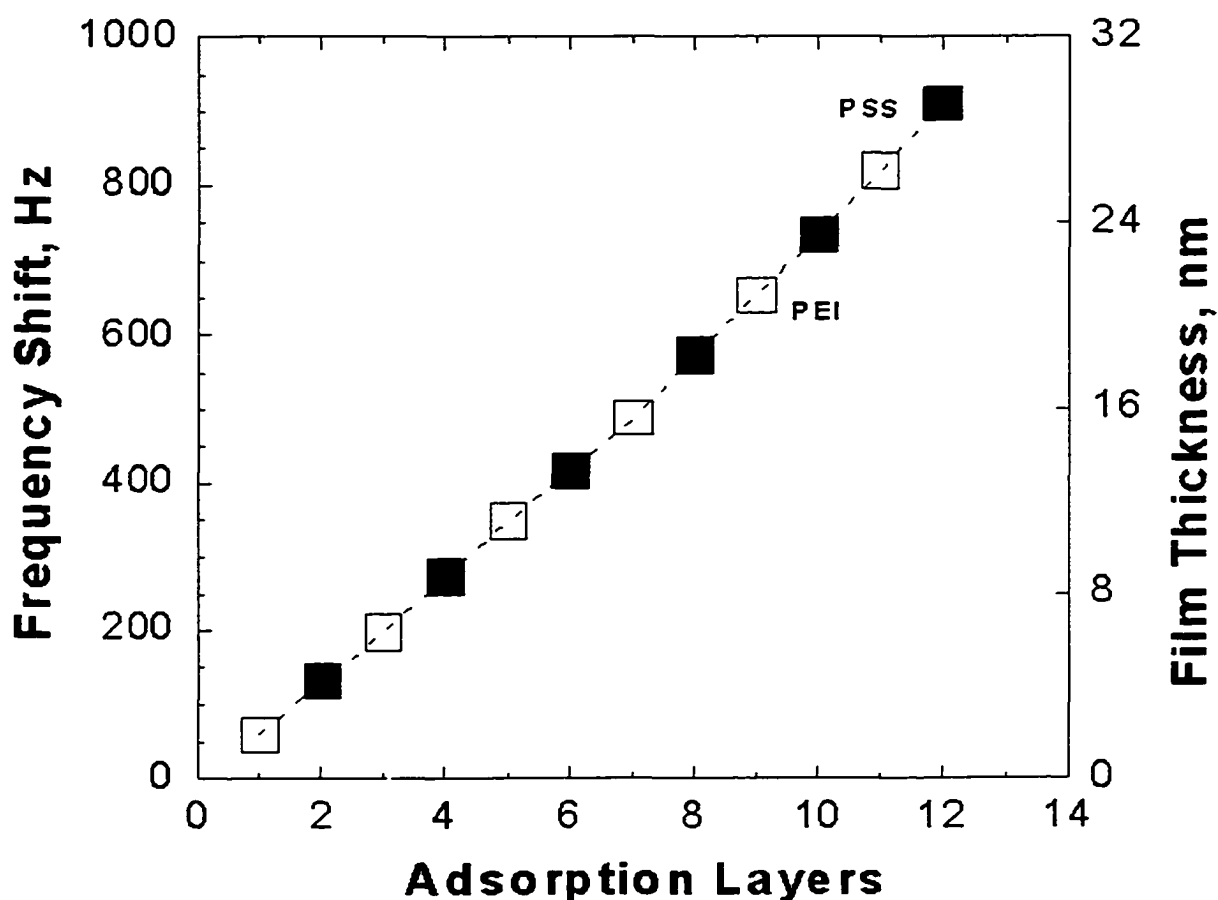


Figure 3.8 (PEI/PSS)₆ film growth vs frequency shift

The film with the composition of (PEI/PSS)₃ + (PEI/gelatin)₅ thickness vs the adsorption layer is shown in Figure 3.8. The precursor layer of (PEI/PSS)₃ was first adsorbed on the QCM electrode with a frequency shift of 460 Hz corresponding to a thickness of 14.5 nm. The first gelatin layer has a thickness of 1.5 nm. But the following PSS layer has a negative frequency shift of 20 Hz. Every gelatin layer was adsorbed on the electrode alternatively with a polycation layer of PEI. A PEI layer with a negative frequency shift indicating a previous adsorbed gelatin layer was partially removed by the strongly charged polycation PEI. Here, every PEI layer has a negative frequency

following a gelatin layer. The averaged frequency shift of a PEI layer was -25 Hz. A total of five gelatin layers were adsorbed and the averaged layer thickness was of 1.4 nm.

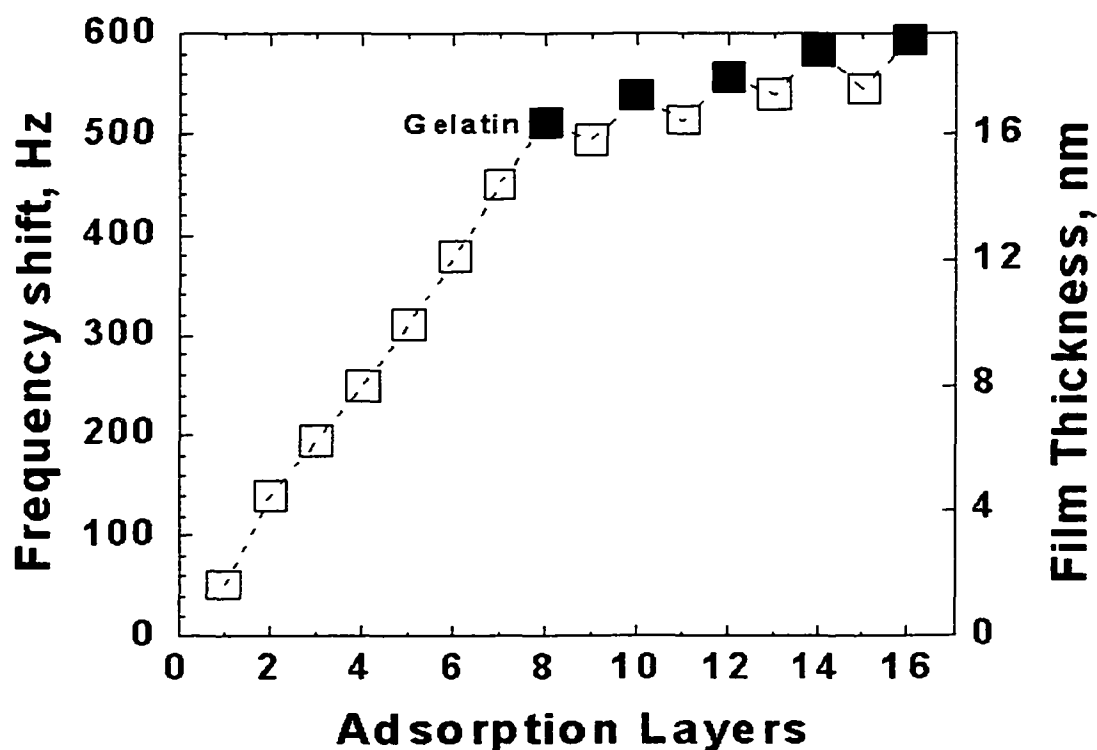


Figure 3.9 PEI/gelatin film thickness vs adsorption layers

Multilayers of PDL/gelatin were assembled on the QCM electrode (Figure. 3.9). Here, a positively charged polypeptide PDL was used instead of the polycation PEI in film formation. The averaged gelatin layer thickness was 2 nm compared with 1.4 nm formed in (PEI/gelatin) multilayers. No gelatin layer removal was observed in the assembling process. The alternative adsorption with PDL resulted in linear film growth vs adsorption layers. The thickness of the PDL layer increased as more layers were

coated. The averaged layer thickness of PDL was 2.2 nm. Thus, PDL/gelatin multilayers with predictable gelatin layer thickness could be built and no partial removal.

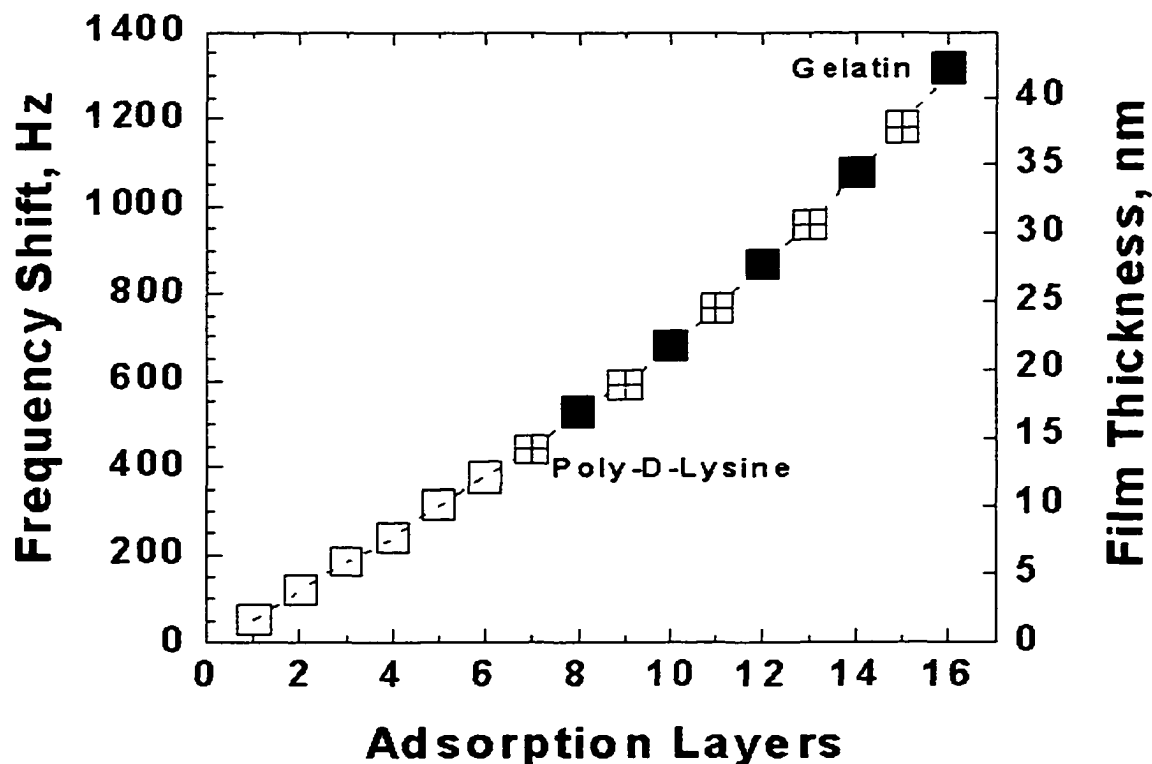


Figure 3.10 PDL/gelatin film frequency shift/thickness vs adsorption layers

3.1.2.3 Endothelial Cell Adhesion and Growth on Gelatin Nanofilm. In addition to seeding endothelial cells on the gelatin nanofilms, other cells such as nerves cells, smooth muscles, and hepatocytes were successfully seeded on polypeptide nanofilms (Ai, 2002e).

PEI/PSS multilayers with different outermost layers were tested for cell adhesion and growth. Cells could not adhere on the $(\text{PSS/PEI})_6$ film with the PEI as the outermost layer three days after seeding. In contrast, most cells attached onto the film composed of $(\text{PSS/PEI})_5 + \text{PSS}$ with the outermost layer of PSS. The reason was not clear; it may rely

on a higher cytotoxicity caused by polycation PEI. Or the surface charge of endothelial cells may have been positive which helped cell adhesion on negatively charged PSS layer. However, even the film with PSS as the outermost layer could not maintain the cells for more than one week. Neither of these polyion layers was biocompatible for cell adhesion and growth. In another experiment, a polyion film with the outermost layer of PDDA was tested, but no cell adhesion was observed after 3 days of seeding.

The film of $(\text{PSS/PEI})_3 + \text{PSS} + (\text{PEI/gelatin})_5$ was also coated on a silicone rubber substrate for cell adhesion and growth. Most cells were well adhered on the film after 24 hours of seeding, and cell adhesion remained stable 2 weeks after seeding.

Finally, the film with the polypeptide layers $(\text{PDL/gelatin})_5$ was deposited on silicone rubber for cell adhesion and growth test. Endothelial cell attachment and growth were observed at 4 hours, 24 hours, 72 hours, one week, and one month after seeding. The initial seeding density was 1.13×10^5 cells/cm². After one week of seeding, the cell density reached to 1.35×10^5 cells/cm². As mentioned before, no cell adhesion was found on an unmodified silicone rubber substrate after 3 days of seeding.

Partial cell adhesion to the PDL/Gelatin nanofilm was observed after 4 hours of seeding. At 24 hours, cells were well attached on PDL/gelatin multilayers. Cells labeled with Cell Tracker (Molecular Probes) continued to grow on the modified silicone rubber substrate one week after seeding (Figure 3.11). Endothelial cells were well attached on the nanofilms even after one month.



Figure 3.11 Bovine coronary artery endothelial cells attached on a $(\text{PEI}/\text{PSS})_2 + (\text{PDL}/\text{gelatin})_5$ nanofilm

3.2 Nano-Encapsulation of Platelets

3.2.1 Nano-Encapsulation of Fixed Platelets

3.2.1.1 Elaboration of the Polyion / Nanoparticle / Immunoglobulin Assembly on a Plane Surface. For routes (A) and (B), the film thickness is shown for each adsorption cycle in Figure 12 (A). Film thickness was calculated from QCM frequency shifts. A film thickness of polyions varied with ionic strength of the solutions. It was reasonable to have a 2-nm bilayer thickness for PDDA/PSS deposited at 0.137 M NaCl in PBS. Assembly steps for 78-nm silica or 45-nm FN nanoparticles were easily detected because the film thickness sharply increased. The increases in measured thickness were close to the diameters of nanoparticles used.

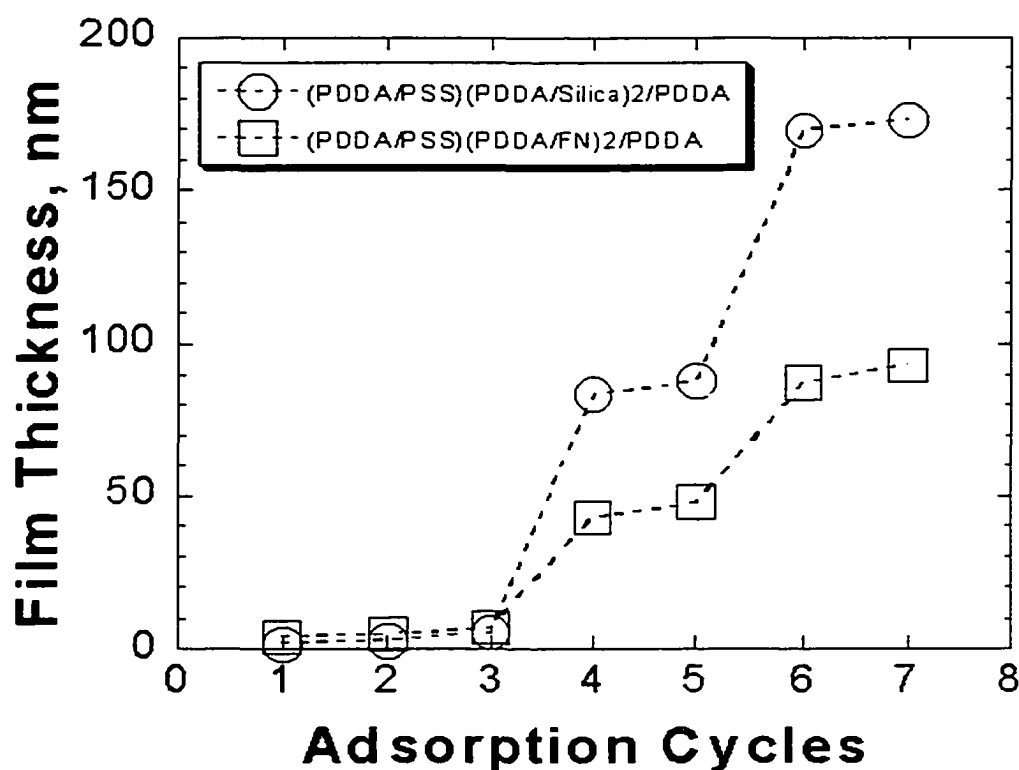


Figure 3.12 Film thickness of each assembly layer for (PDDA/PSS)(PDDA/Silica)₂/PDDA and (PDDA/PSS)(PDDA/FN)₂/PDDA

The first three layers are 5 to 7 nm thick. The (PDDA/Silica) layers are 78 to 82 nm thick, corresponding to the diameter of the silica particles. The (PDDA/FN) layers are 36-40 nm thick, corresponding again to particle diameter.

Assembly of (PSS/IgG)₅ and (PSS/anti-IgG)₅ multilayers are shown in Figure. 13(B). Each point represents an IgG or anti-IgG adsorption layer. The pre-layer sequence was PDDA/PSS/PDDA, and additional layers of (PSS/IgG)₅ or (PSS/anti-IgG)₅ were added later. The averaged frequency shift of every IgG layer was 89 Hz. As calculated, IgG adsorption density during 30 min on QCM electrodes was 3.7 mg/m². To demonstrate the specific binding ability of assembled IgG, the resonator (with outermost IgG) was dipped in a solution of anti-IgG-FITC for 30 min. The bound anti-IgG-FITC

layer coverage was 5.6 mg/m^2 . Thus, IgG in the multilayer is specifically recognized by anti-IgG. On another electrode, multilayers of $(\text{PSS}/\text{anti-IgG})_5$ were assembled. The outermost anti IgG layer remained biologically active. The adsorption density of the bound IgG layer is 7.2 mg/m^2 , almost twice the thickness of 3.7 mg/m^2 found for the $(\text{PSS}/\text{IgG})_5$ layers. Thus, more IgG was absorbed onto anti-IgG than IgG bound to PSS layer. The biological specific binding between antigens and antibodies thus appears to be stronger than electrostatic binding.

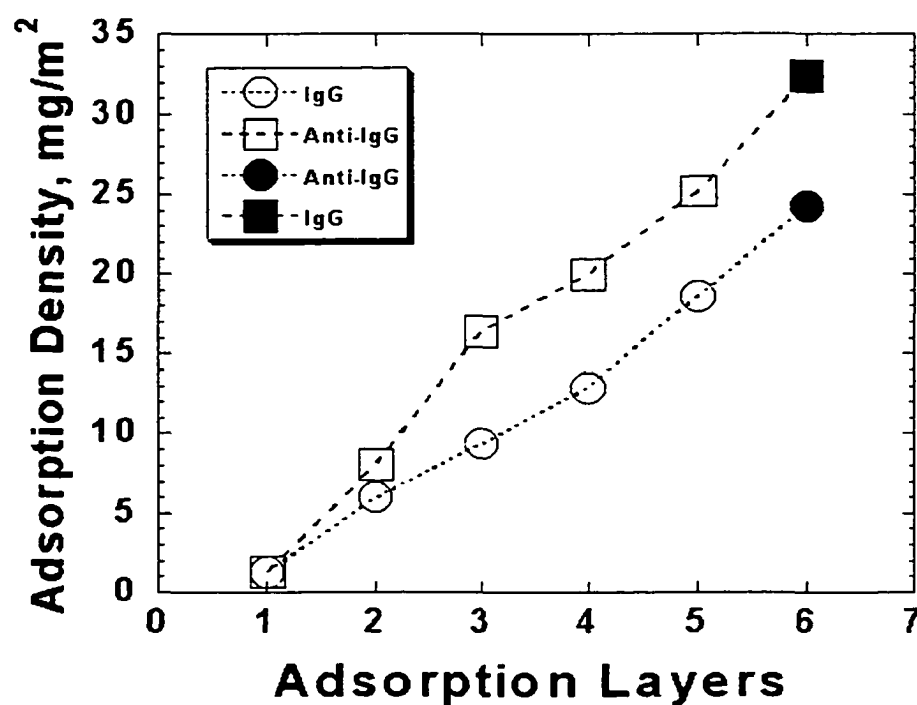


Figure 3.13 Adsorption density of each assembly layer for IgG and anti IgG coatings For $(\text{PSS}/\text{IgG})_5/\text{anti IgG}$, every IgG layer has an average density of 3.7 mg/m^2 , and the final anti IgG layer has a density of 5.6 mg/m^2 and the final IgG layer has a density of 7.2 mg/m^2 .

Usually the isoelectric point (PI) of IgG was near pH 7. The exact PI value of bovine IgG was not known here. The charge of IgG could be weakly negative or positive

at pH 7.4. Whereas the procedure is not limited to polyanion PSS, polycation PDDA was used to assemble IgG in a separate experiment. The averaged film thickness of each IgG layer was about 2.1 mg/m^2 (Figure 3.14). It was much smaller than the value of 3.7 mg/m^2 for IgG adsorbed on PSS layers. The reason is not clear. Assembly of IgG was at pH 7.4, which is slightly higher than its isoelectric point (Caruso, 1997). The orientation of IgG molecules on the film surface is not definite. An upright position would be helpful for binding of anti-IgG.

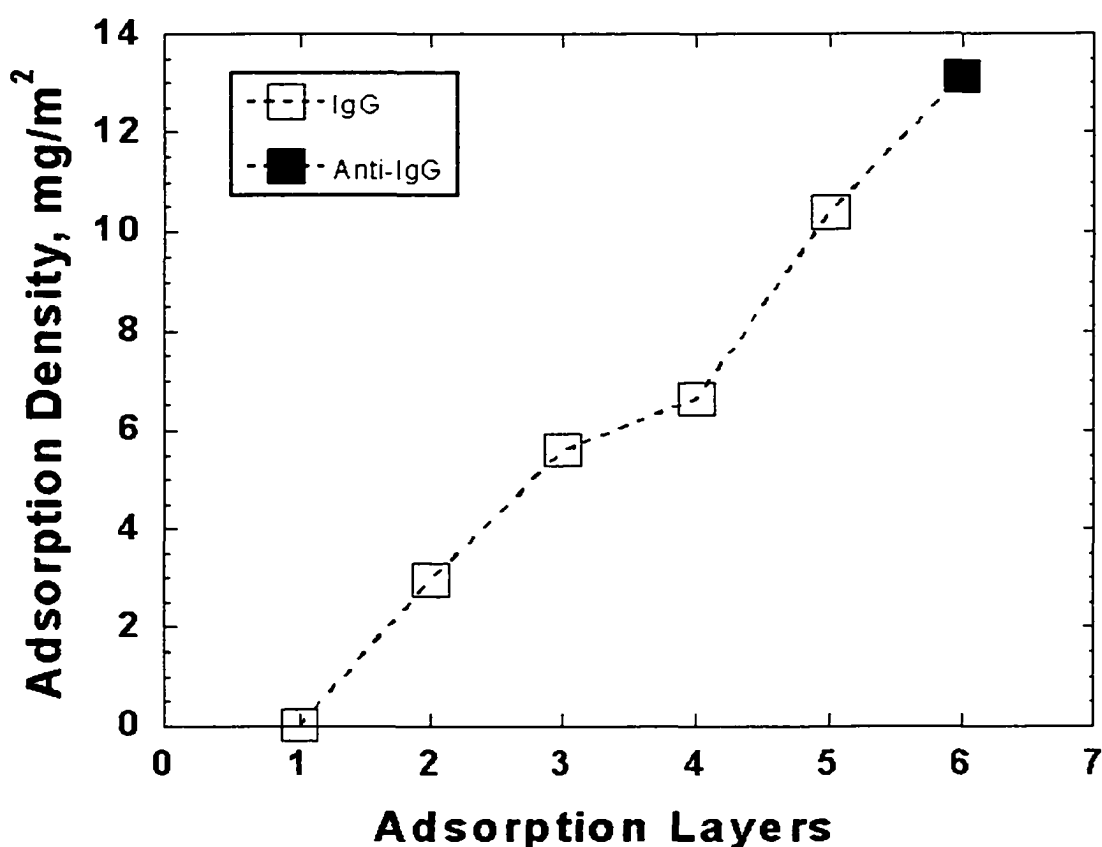


Figure 3.14 Assembly procedure of $(\text{PDDA}/\text{IgG})_5 + \text{Anti-IgG}$
 Adsorption density of each assembly layer for IgG and anti IgG coatings was shown in the assembly with PDDA. The averaged IgG adsorption density is 2.1 mg/m^2 . The final adsorbed anti-IgG layer has a density of 2.75 mg/m^2 .

3.2.1.2 Assembly of Polyion / Nanoparticle / Antibody Coating on Platelets.

Transmission electron microscopy (TEM, Philips CM10) and fluorescence microscopy (Nikon) were used to examine the results of silica nanoparticle and FN shell assembly on platelets respectively. A bovine platelet in the initial non-treated state is shown in Figure 3.15a the diameter of the platelet is 2.5 μm . In Figure 3.15b, four platelets coated with silica shells are presented. One of them (arrow) is presented in Figure 3.15c at higher magnification. The platelet (not the same one from Figure 3.15a) is covered with silica nanoparticles. The size of the platelet was retained after the silica encapsulation, but its shape was slightly disturbed.

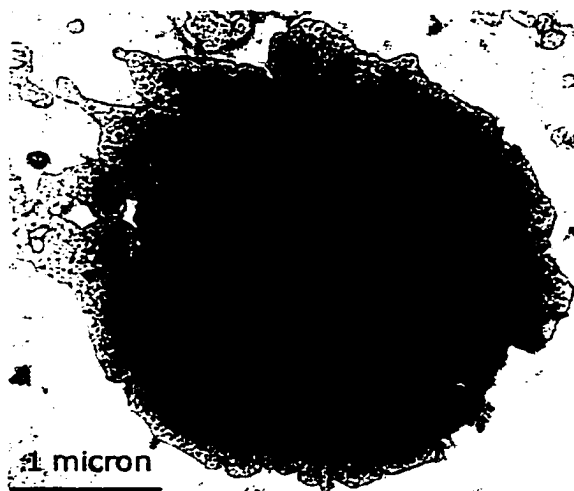


Figure 3.15a. A bovine platelet (TEM image $\times 21\text{K}$)
The platelet is intact (not a cross sectional view). The inner components could not be clearly viewed. The platelet membrane is clearly presented.

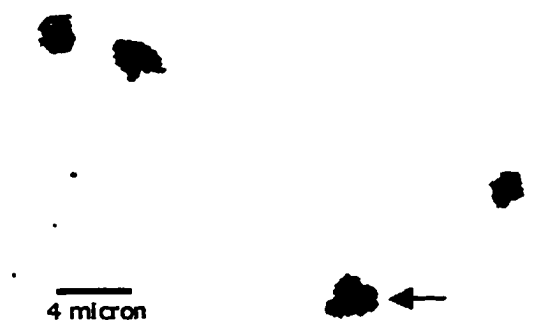


Figure 3.15b. Four platelets coated with 78 nm silica shell with composition PDDA/PSS/PDDA+(Silica/PDDD)₂ (TEM × 1.65K)

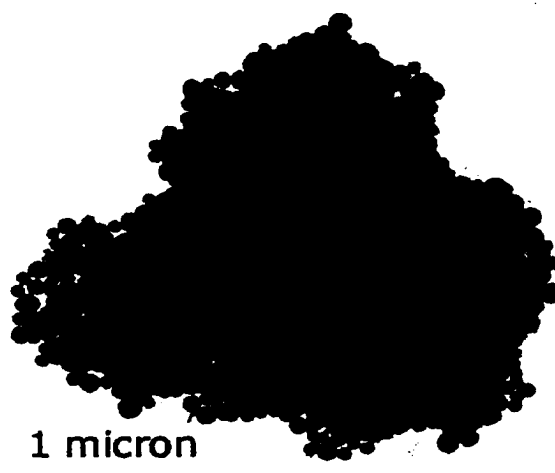


Figure 3.15c. A magnified image of a platelet (arrow) from (b) (TEM × 21K)
 The platelet ($D=2.8 \mu\text{m}$) is totally covered with 78-nm silica. The size of the platelet in (c) is close to that of the platelet in (a).

In another experiment, platelets were covered with fluorescent nanospheres following the construction plan PDDA/PSS/PDDA+(FN/PDDA)₂, Figure. 3.16 (a). These platelets have a yellow-green color under a fluorescence microscope due to FN coverage of the platelet surface, indicating full surface coverage with FN-nanoparticles.



Figure 3.16a Platelets coated with 45 nm fluorescence nanospheres
(Magnification: 1K) Both single platelet and clumped platelets were seen in the same field. Platelets were yellow-green in color and membranes were clearly seen.

Figure. 3.16b shows platelets assembled with an outermost layer of $(PSS/IgG)_2$ that were exposed to a solution of fluorescent anti-IgG-FITC. Before the antigen-antibody recognition, platelets were invisible under the fluorescent microscope, but after the specific recognition reaction the platelet membrane became visible. Thus, the IgG assembled on the platelet surface was specifically recognized and bound by anti-IgG-FITC, and immunoglobulin-covered platelets can be targeted to specific sites based on this interaction.



Figure 3.16b Platelets assembled with bovine IgG and labeled with anti-bovine IgG-FITC
(Magnification: 1.8K). Platelets were clearly viewed due to fluorescent FITC.

Next, bovine IgG was deposited through LbL self-assembly at a specific area in the silicone tubing, and the other parts of the tube remained uncovered with IgG. One tenth of the length (8 mm) of protein-deposition-resistant silicone medical tubing was selectively coated with bovine IgG on the inner surface. A solution of platelets shelled with anti-bovine IgG-FITC was then passed through the tubing 20 times. Afterwards, the tubing was rinsed, dried, and studied under a fluorescence microscope. Results are shown in Figure 3.17. The samples were taken from targeted (A) and non-targeted (B) areas. After analysis with MatLab image processing software, the fluorescence signal from the targeted areas was 154-times larger than that from non-targeted areas, indicating binding of platelets predominantly to the IgG labeled site. This experiment demonstrates the ability to target antibody-modified platelets to specific sites (expressing related antigens) in blood vessel.

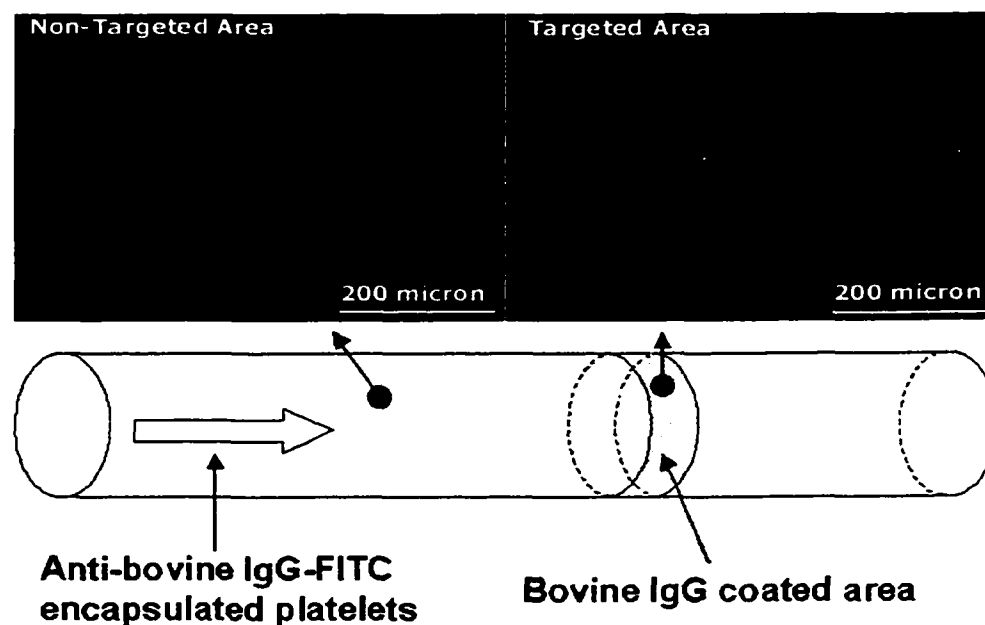


Figure 3.17 Anti-IgG shelled platelets targeted to an area based on anti-IgG-FITC recognition of IgG covered regions

Most of the IgG area was bound by modified platelets, and the fluorescence signal was obvious.

3.2.2 Nano-Encapsulation of Live Platelets

Live platelets were coated with polyelectrolytes of (PDDA/Heparin). Most cells were still alive after coating as determined from the labeling with Live/Dead Cytotoxicity Dye.

3.2.2.1 Elaboration of the Polyion / Heparin Assembly on the Plane Surface. To understand the PDDA/heparin assembly on live platelets, the adsorption steps were performed on QCM electrodes. The frequency shift vs adsorption layers were shown in Figure. 3.18. The film was composed of (PDDA/PSS)₂ + (PDDA/heparin)₇. The polysaccharide heparin was negatively charged and deposited alternatively with polycation PDDA. The heparin layer thickness increased with the number of layers assembled on the electrode. The averaged heparin layer thickness was 3 nm. No removal phenomenon of heparin was observed after the adsorption of strongly charged polycations PDDA.

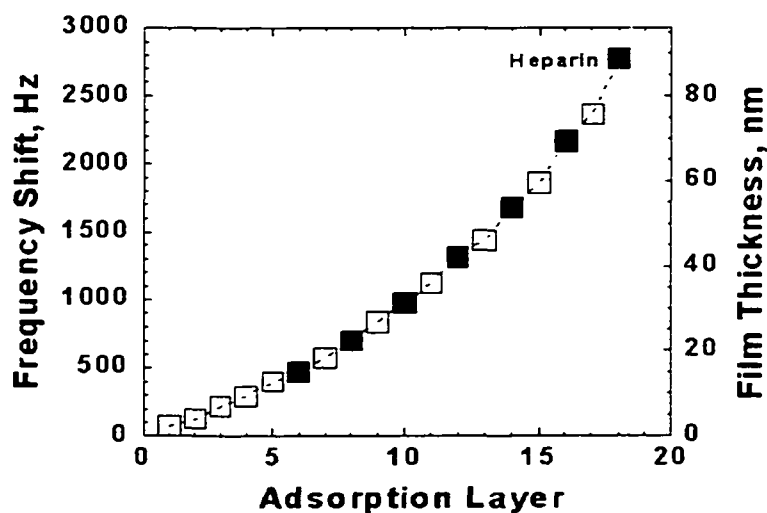


Figure 3.18 Frequency shift/film thickness vs adsorption layers of PDDA/heparin multilayers

The live platelets coated with (PDDA/heparin) were immediately labeled with the Live/Dead cell viability/cytotoxicity sensor. Live cells were green under the fluorescence microscope while dead or damaged cells were red. In our study, most platelets were green, as shown in Figure 3.19 and Figure 3.20. Initially, under the microscope, platelets were oval or round in shape (Figure 3.19). After 30 minutes, platelets changed from the normal disc shape to a compact sphere with long dendritic extensions (Figure. 3.20). Oval or round shaped platelets are likely to be in the resting state (inactivated), but platelets with long dendritic extensions are likely to be activated. This results indicated that platelets were not inactivated after encapsulated with polycation PDDA and polysaccharide heparin. Also, platelets were still responsive to external forces caused by the oil lens during the microscopy study. This means platelet function was preserved after encapsulation.



Figure 3.19 Platelets after encapsulation and labeled with LIVE/DEAD cell viability/cytotoxicity sensor under fluorescence microscope at 0 min

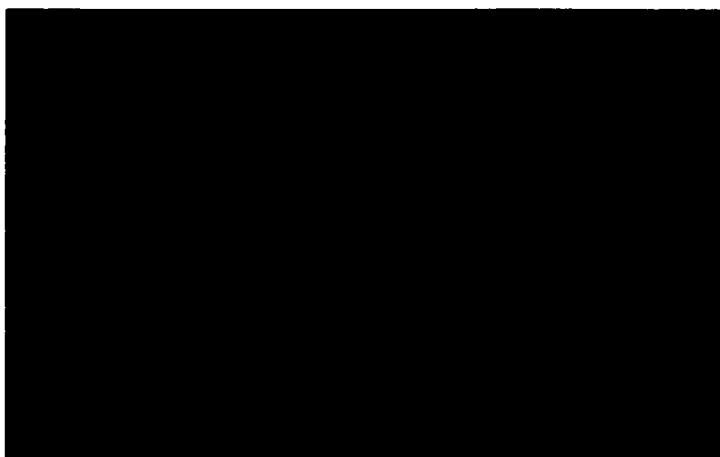


Figure 3.20 Platelets after encapsulation under fluorescence microscope at 30 min

Live/Dead cell viability/cytotoxicity sensor-labeled platelets were also studied with the aid of a fluorometer. Live and dead cells gave off fluorescence emissions at different wavelengths. In Figure 3.21, live platelets were excited at 494 nm and emitted fluorescence signal at 517 nm.

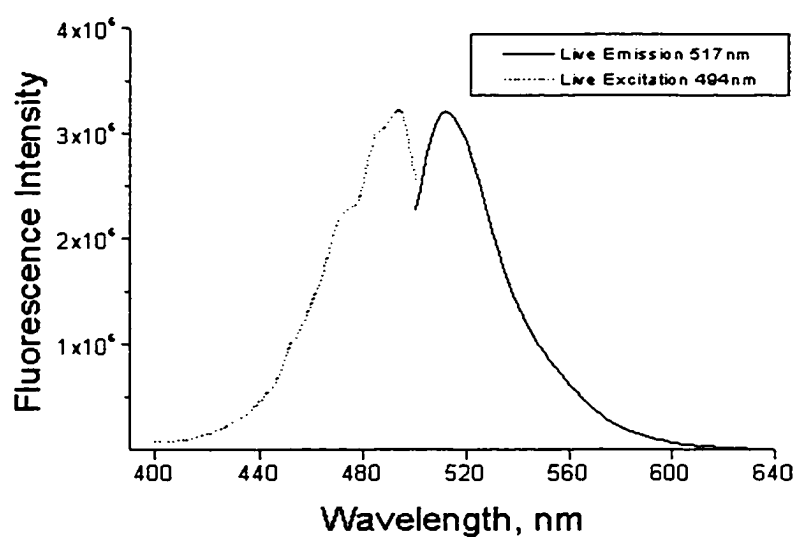


Figure 3.21 Live/dead platelet emission at different wavelengths

Dead platelets emitted fluorescence at 617 nm when excited at 528 nm (Figure. 3.22). The fluorescence intensity of live and dead platelets is summarized in Figure. 3.23. Live platelets have much stronger fluorescence intensity as compared with dead/damaged platelets. The emission fluorescence intensity of live platelets was about 3.2×10^6 , while that of dead platelets was 2271. The cell number ratio of live: dead cells is equal to 1409:1. This result indicates that most cells (99.93%) were alive and the encapsulation was non-cytotoxic.

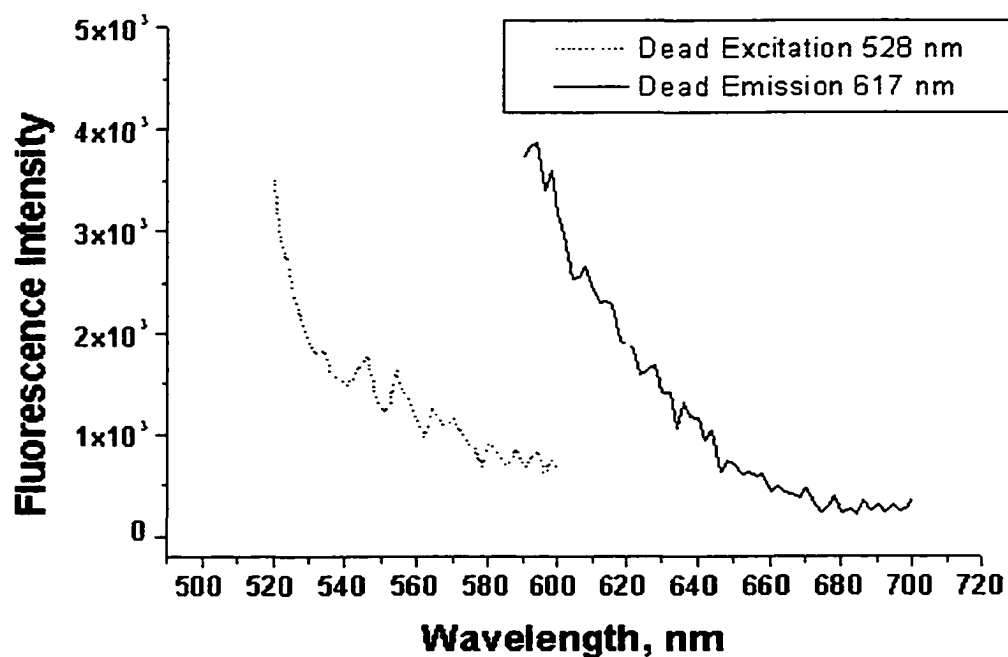


Figure 3.22 Fluorescence signal of dead platelets at 617 nm when excited at 528 nm

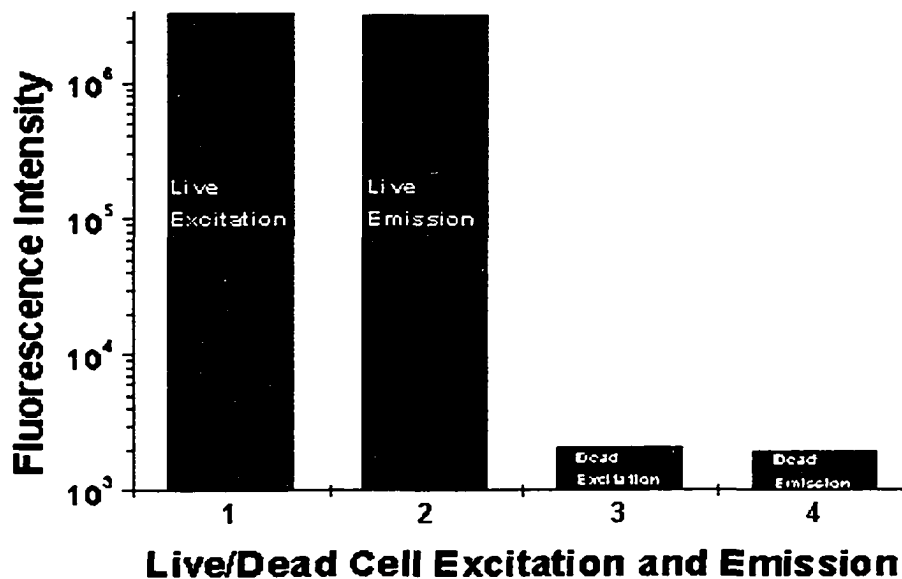


Figure 3.23 fluorescence intensity of live and dead platelets

3.3 Thromboxane B₂ Measurement through ELISA

The amount of thromboxane B₂ (TXB₂) released from uncoated and encapsulated platelets after flow through the endothelium-lined model was measured through ELISA. TXB₂ was calibrated from 0.5 to 64 pg with concentration varying from 7.7×10^{-4} to 9.8×10^{-2} pg/ μ l (Figure. 3.24). Sample concentration was estimated from the standard curve. The averaged TXB₂ level released from shelled platelets was 1.17 ± 0.22 ng/ml compared with 1.60 ± 0.09 ng/ml from non-shelled platelets (Figure. 3.25). After encapsulation, TXB₂ release from platelets was significantly decreased ($p < 0.01$).

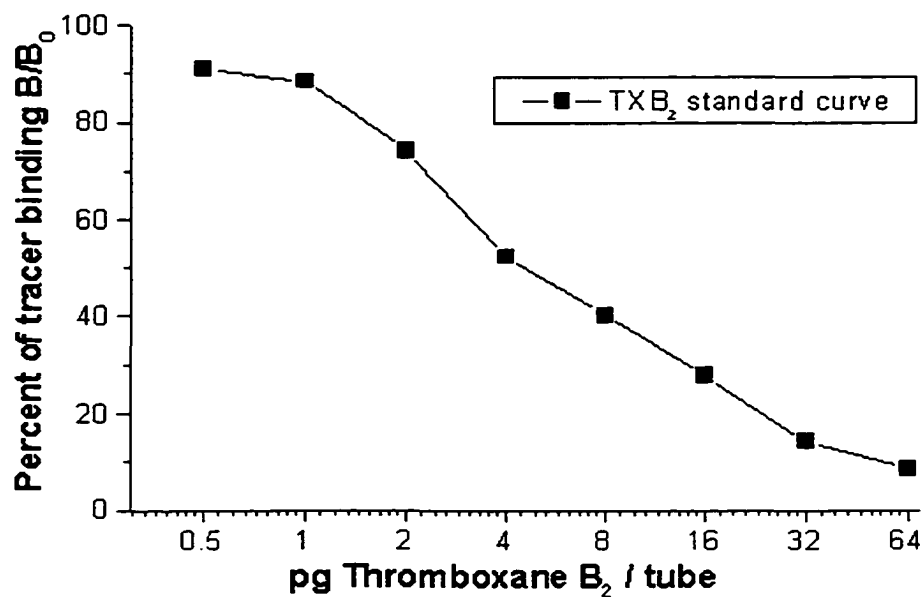


Figure 3.24 The Thromboxane B₂ standard curve

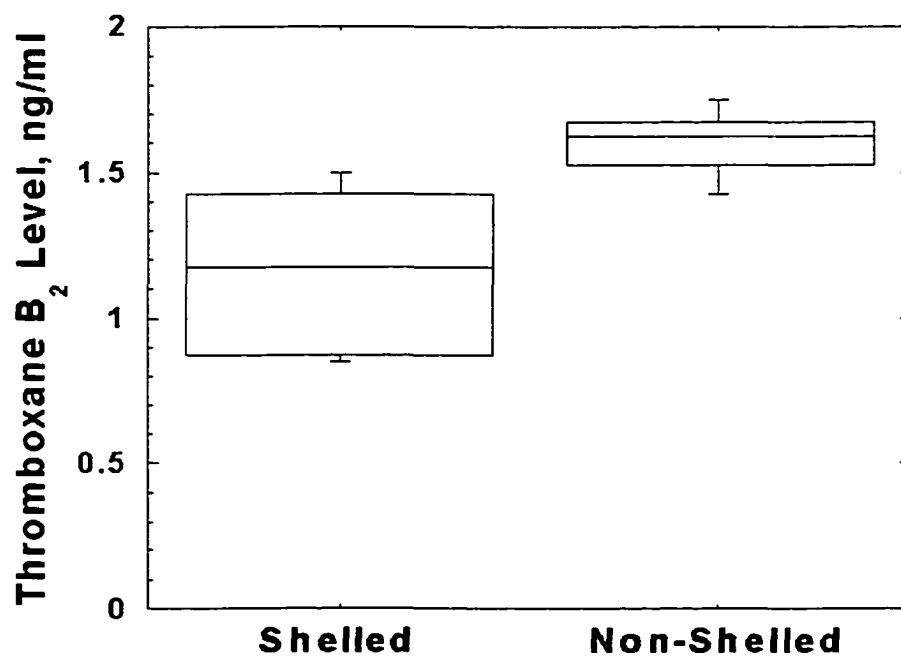


Figure 3.25 The level of TXB₂ released from shelled and non-shelled platelets

3.4 Platelet Adhesion Test in the Stenosis Model

The number of platelets before and after running through the collagen-coated silicone model was measured by fluorescence intensity counting. The fluorescence absorbance of Calcein used here was 517 nm (emission) for live platelets. The fluorescence absorbance of shelled and non-shelled platelets before and after running the model was recorded. Two groups were set for the experiment, the shelled platelets and the non-shelled platelets. Five samples were in each group, and data were paired. After running through the model, some platelets were adsorbed onto the coated collagen film on the inner surface of the silicone model, so the fluorescence intensity of platelets after running through the model was lower than the intensity before running the model. The difference of platelet fluorescence intensity divided by the intensity before running yields the percentage of platelet adhesion onto the collagen nanofilm. An example of the fluorescence intensity change of non-shelled platelets before and after running through the model is shown in Figure 3.26.

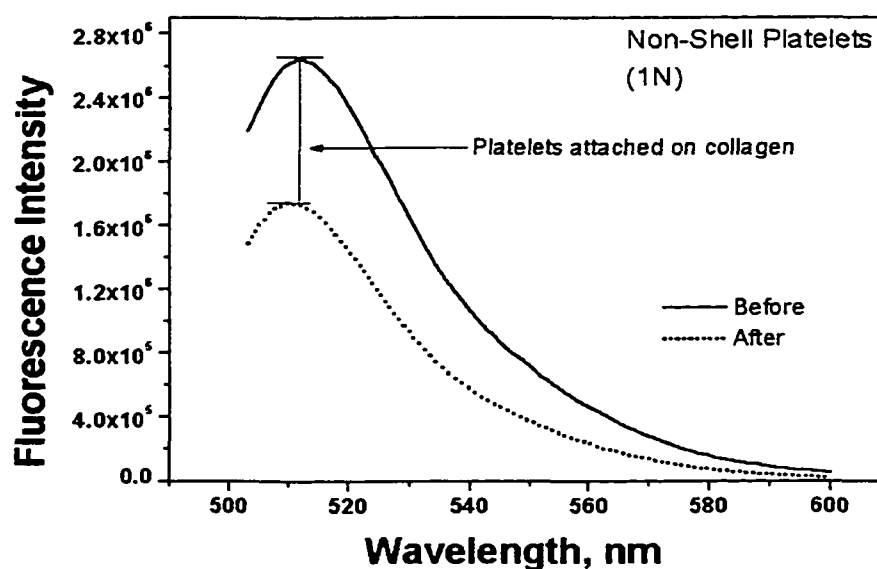


Figure 3.26 The fluorescence intensity of non-shelled platelets

PDDA/heparin encapsulated platelets showed less adhesion on collagen as compared with unmodified platelets ($p < 0.01$) (Figure. 3.27). Only 3.84% of shelled platelets were attached to the collagen film after running the fluid through the silicone model, whereas 36.84% of unmodified platelets were attached. Thus, PDDA/heparin encapsulation on platelets reduced the degree of platelet adhesion on collagen in the coronary artery stenosis model.

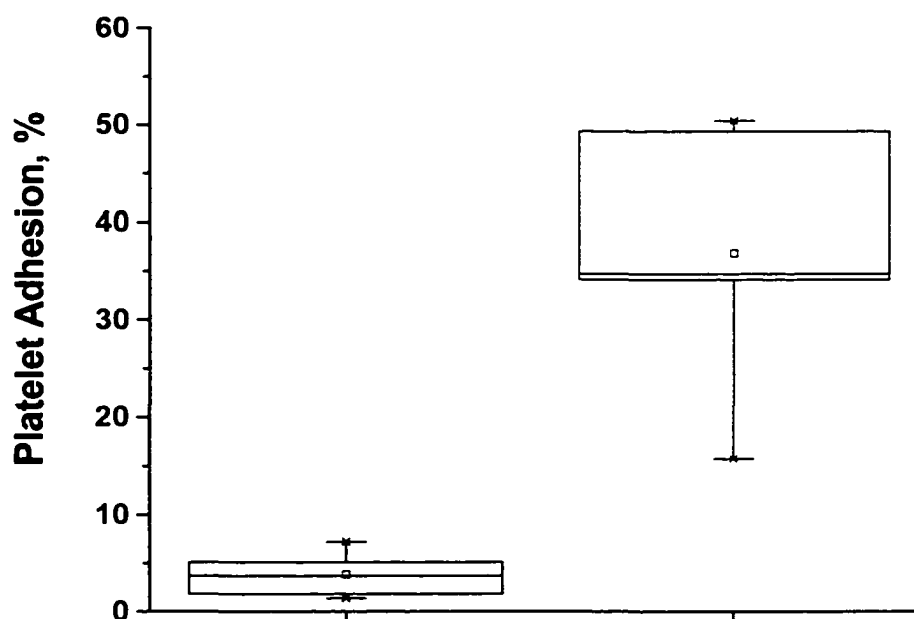


Figure 3.27 Percentage of shelled and non-shelled platelets adhesion to the collagen nanofilm

3.5 Nitric Oxide Release from the Endothelial Cells

A Nitric Oxide Fluorescence sensor was used to quantify the amount of NO release from the endothelial cells. Endothelial cells were collected from different parts of

the model for flow cytometry analysis. But the fluorescence sensor was not sensitive enough to measure the amount the nitric oxide released from endothelial cells under the flow condition ($Re = 436$). The negative control from cells without fluorescence labeling has a background signal of 2.94 (Figure. 3.28). The fluorescence intensity was 2.35, 2.12, 2.17, and 2.08 for region 1, 2, 3 and 4 respectively (Figure. 3.29). In Figure 3.29, the fluorescence intensity of NO was counted from region M1. Based on the amount of cells per region, the fluorescence intensity is replotted as shown in Figure. 3.30.

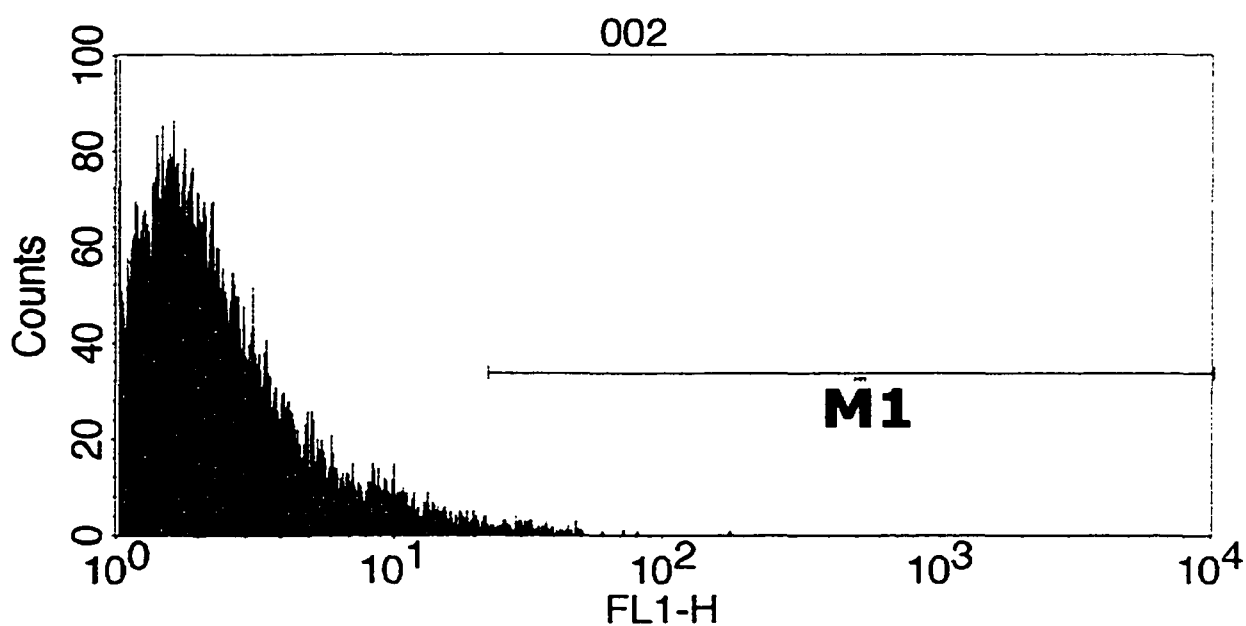


Figure 3.28 Fluorescence intensity of cells without DAF-FM diacetate labeling

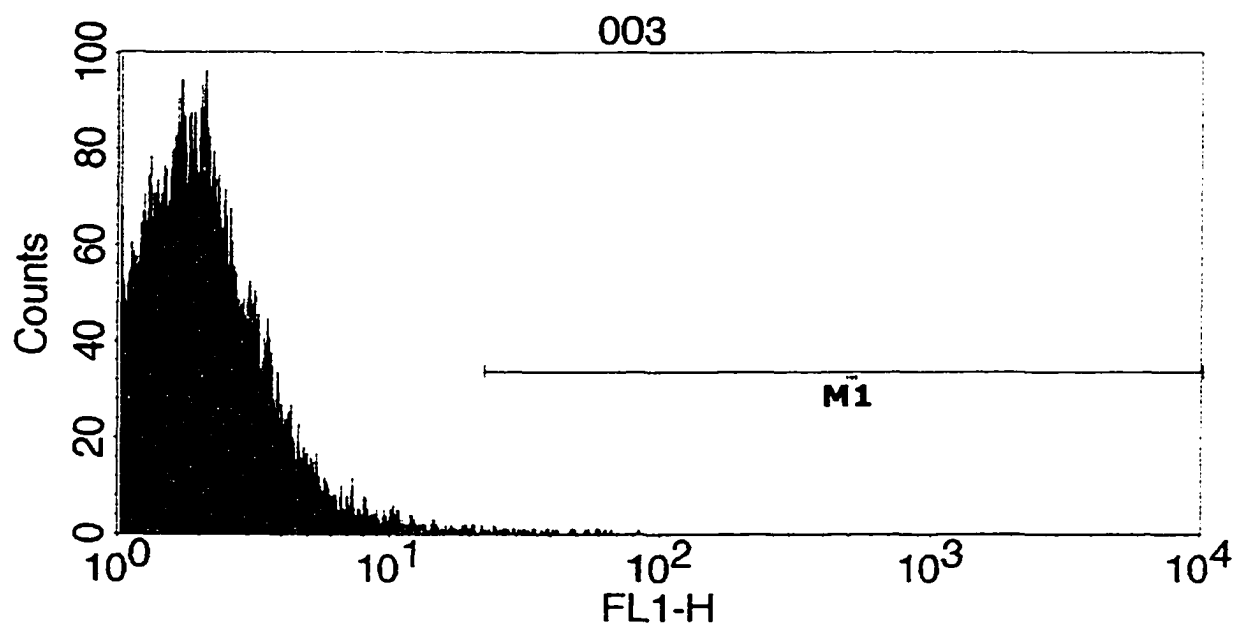


Figure 3.29a Fluorescence intensity of NO release at region 1

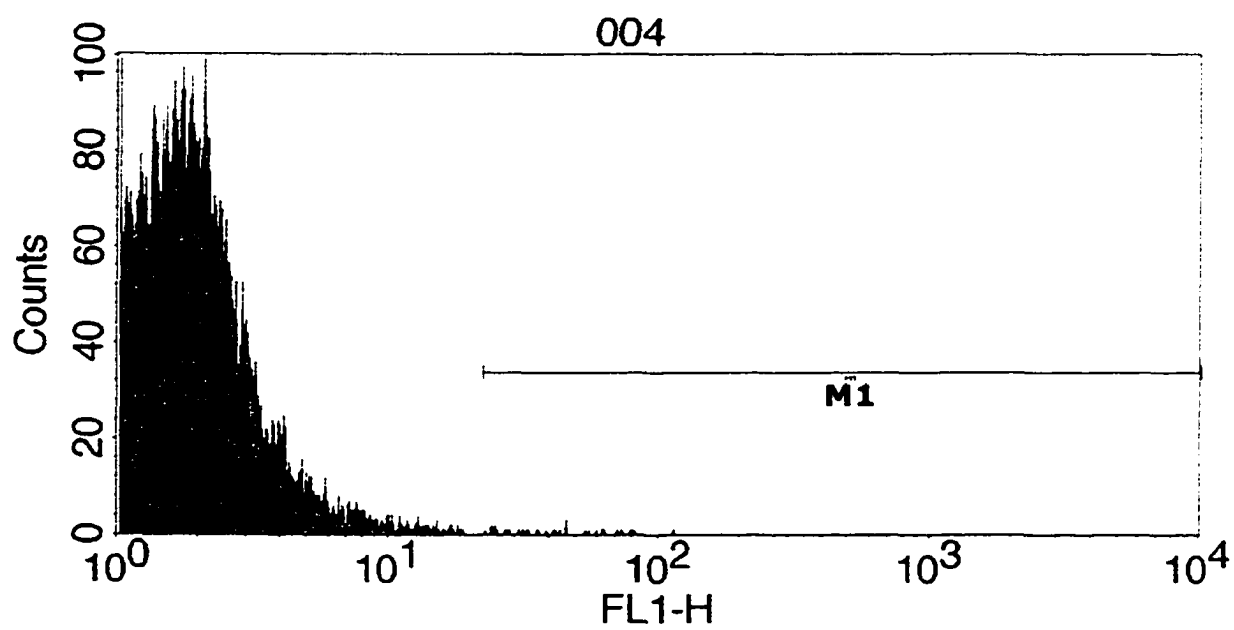


Figure 3.29b Fluorescence intensity of NO release at region 2

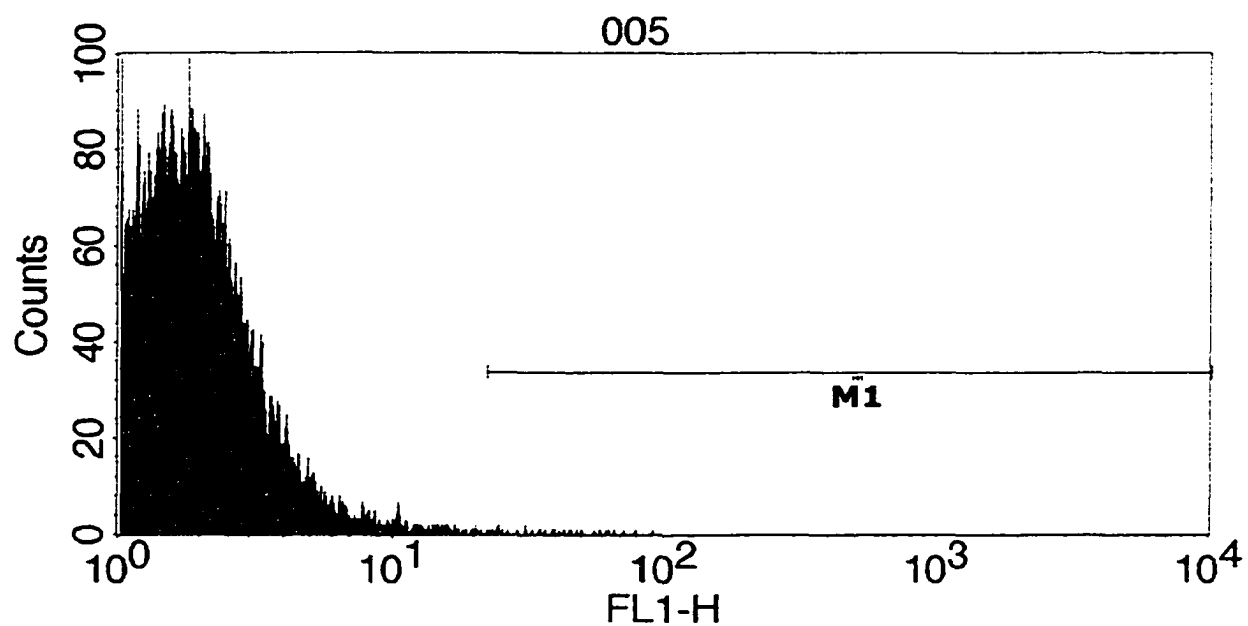


Figure 3.29c Fluorescence intensity of NO release at region 3

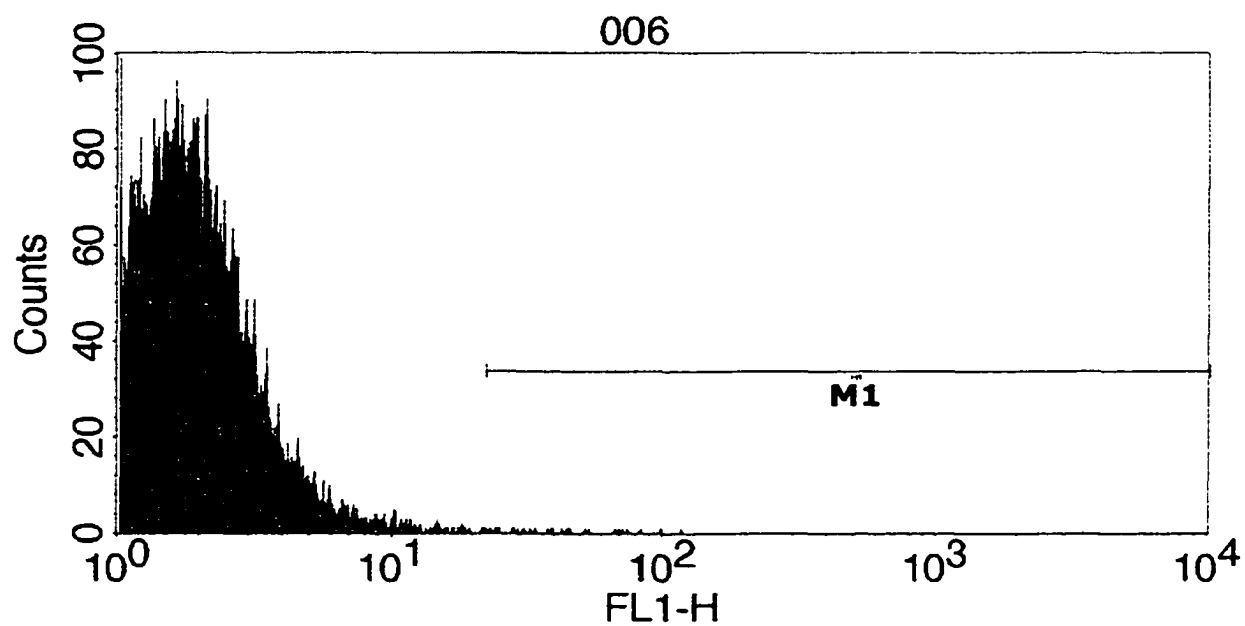


Figure 3.29d Fluorescence intensity of NO release at region 4

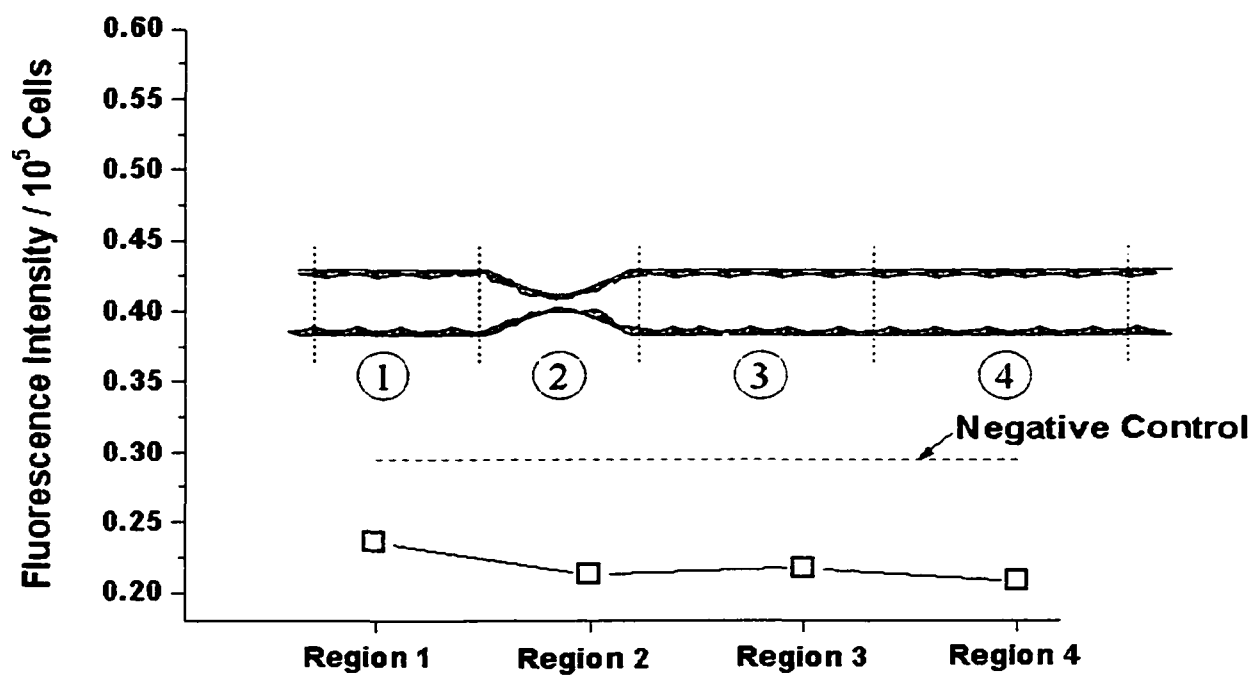


Figure 3.30 Fluorescence intensity of NO release at all regions

CHAPTER 4

DISCUSSION

4.1 Introduction

Polyion shells were assembled on the platelets to modify their functions under the high shear stress conditions caused by the stenosis. A coronary artery stenosis silicone model was built for nano-engineered platelet function analysis in this study. To simulate the physiological environment of a blood vessel, endothelial cells were seeded on the inner surface of the model. A micro/nano biocompatible film was coated on the inner surface of silicone model through layer-by-layer self-assembly. A poly-D-lysine/gelatin nanofilm was used to increase endothelial cell adhesion. Collagen coating on the inner surface of the model was used for platelet adhesion study. The architecture of a nanofilm is pre-determined and the thickness is predictable.

Encapsulation of platelets with polyions, nanoparticles, and antibodies brought a new method for cell surface modification. The coating was successful for both fixed and live platelets. Live platelets were still alive and functional after encapsulation. Polyions such as PDDA did not show obvious cytotoxicity to cells. The interaction between cells and coating materials was based on the electrostatic force in all polyions, except for the antibodies which relied on hydrophobic forces. Activation under shear stress was reduced

for the encapsulated platelets, as determined from the thromboxane B₂ measurement. Adhesion of shelled platelets to the collagen film was obviously lower than adhesion of unmodified platelets. Thus, a platelet's function can be changed by the nano-shell.

No obvious nitric oxide release was measured from endothelial cells seeded inside the model. The possibility may rely on the sensitivity of the fluorescence sensor or short time of flow treatment. Furthermore, a lack of L-arginine in the fluid may have prevented NO production. Although L-arginine was present in the culture medium during the culturing of the endothelial cells, the suspended platelet mixture used during the flow experiment did not have this essential amino acid.

4.2 Micro/Nanofilm Coated on a Silicone Substrate

A gelatin film with a thickness of 110 ~ 160 μm was coated on silicone rubber through crosslinking with glutaraldehyde. The film was hydrophilic and biocompatible for cell adhesion and growth. But glutaraldehyde was required, and it might be cytotoxic to cells.

Nanofilms of different architectures were coated on a PDMS substrate with an outermost layer of poly-D-lysine, gelatin, collagen, fibronectin, laminin, hyaluronic acid, or heparin (Ai, 2002e). In our study, PEI/PSS, PEI/gelatin, PSS/collagen or PDL/gelatin multilayers were assembled on silicone rubber as hydrophilic coatings. Different thin film monolayers have unique contact angles. An outermost layer dominates the surface property (Yoo, 1998). A gelatin monolayer has a smaller contact angle compared with a PEI or a PSS monolayer. So it is desired to use an outermost layer of gelatin in coating nanofilms on a silicone rubber substrate to increase the hydrophilicity.

PEI/PSS, and PDL/gelatin multilayers demonstrated linear film thickness growth in QCM studies. But a gelatin layer removal phenomenon was observed in constructing a film composed of PEI/gelatin multilayers. The reason is unclear. It is possible that the weakly charged gelatin layer was peeled off by strongly charge polycation PEI. After replacing PEI with the weakly charged polypeptide PDL, a linear PDL/gelatin film growth was observed. PEI/PSS multilayers also presented linear film growth without the removal phenomenon, but cells adhered to the film for only one week. A PDL/gelatin film is thus preferable for its biocompatibility. The thickness of a PDL/gelatin bilayer is about 4 nm and the total film thickness is pre-determined.

Endothelial cells adhered to hydrophilic films coated on a silicone rubber substrate. However, the film composed of a PEI/PSS multilayer was not stable enough to hold cells for more than one week. Cells could not adhere on the (PSS/PEI)₆ film with the outermost layer of PEI three days after seeding. Endothelial cells adhered on the film composed of (PSS/PEI)₅ + PSS with an outermost layer of PSS. A PEI layer might be cytotoxic to cells, or else the negative charge of the PSS layer was good for cell adhesion. Nonetheless, even the film with PSS as the outermost layer could not hold cells for more than one week. Neither a PEI nor a PSS layer was biocompatible for cell adhesion and growth. In another experiment, a polyion film with the outermost layer of PDDA was also tested but no cell adhesion was observed 3 days after seeding. Cell adhesion and growth were observed on PEI/gelatin, and PDL/gelatin multilayers up to one month. Cell-film interactions were monitored by using a Cell-Tracker fluorescence sensor. Most cells were alive on the nanofilms and no obvious cytotoxicity was observed. A PDL/gelatin film was used instead of a PEI/gelatin film coating on the inner surface of the silicone

model of coronary artery stenosis. Poly-D-lysine is a widely used biomaterial in cell culture, but the biocompatibility of PEI was not thoroughly understood even though it has been used in gene delivery (Baker, 1997; Gautam, 2000).

4.3 Nano-Encapsulation of Platelets

4.3.1 Nano-Encapsulation of Fixed Platelets

Fixed platelets were successfully coated with different materials. A precursor film of PDDA/PSS multilayers is preferred as a strong substrate for further adsorption of nanoparticles or proteins. In another experiment, polycation PEI was used to build the precursor film alternatively with PSS, but platelet aggregation was found. The reason may be a reaction of the positively charged NH_2^+ group of PSS with the negatively charged COOH^- group of glycoproteins on platelets. A similar aggregation phenomenon was also found in encapsulation of furosemide microcrystals with PEI (Ai, 2002b). The shell thickness could be adjusted by varying the ionic strength of the coating solution. It was reasonable to have a 2-nm bilayer thickness for PDDA/PSS deposited in 0.137 M NaCl solution (Lvov, 1995). Assembly of negatively 78-nm silica or 45-nm fluorescence nanoparticles with positively charged PDDA was observed with the help of TEM and fluorescence microscopy respectively. Usually the addition of an outermost layer of strongly charged polyelectrolyte was preferred to prevent loss of nanoparticles from platelets. Here, a PDDA layer was used as the final treatment.

A layer of IgG adsorption density on QCM electrodes was 3.7 mg/m^2 , which is similar to a previous study (Caruso, 1997). IgG adsorbed on the electrode was still

bioactive to bind an anti-IgG-FITC layer with a coverage of 5.6 mg/m^2 . Greater IgG adsorption was found on electrodes when assembling with polyanion PSS than polycation PDDA. Assembly of IgG was at pH 7.4, slightly higher than its isoelectric point (Caruso, 1997; Buijs, 1995). Thus, the protein surface was approximately neutral in charge, and some additional interaction facilitated the stronger interaction of IgG with anionic PSS rather than with cationic PDDA. Probably, hydrophobic forces between PSS and IgG play an important role (Caruso, 1997). Also PSS may exhibit more roughness than PDDA, which may improve IgG adherence. The orientation of IgG molecules on the film surface is not definite. An upright position would be helpful for binding of anti-IgG.

IgG assembled on the platelet surface was specifically recognized and bound by anti-IgG-FITC, and vice versa. Therefore, most antibodies demonstrated the bio-specific binding ability even in a flow condition. This result may bring possible applications in drug delivery and targeting in treating tumors.

4.3.2 Nano-Encapsulation of Live Platelets

Live platelets were coated with polycation PDDA and polysaccharide heparin. The total time of the assembly procedure was kept short to ensure platelet viability and function after the encapsulation. From a Live/Dead Cell Viability/Cytotoxicity test, most cells were alive and not damaged by the PDDA/heparin shell. Heparin was chosen for the assembly procedure because of other major anticoagulant materials, such as citric acid, have small molecular weights that preclude LbL assembly. Heparin is a negatively charged polysaccharide (PI: 9.5) at pH 7.4. In contrast to the encapsulation procedure for fixed platelets, fewer layers were used in assembly. One important reason is that the biocompatibility and cytotoxicity of PDDA is unknown. A biocompatible polyion,

strongly positively charged, that does not cause platelet activation, is preferable for assembling multilayers on platelets with heparin.

4.4 Thromboxane B₂ Release from Platelets

The Poiseuille value for shear stress at the throat of the stenosis in the silicone model is 23 dynes/cm². This is a lower estimate because the start of the stenosis is a contracting flow the true shear stress will be substantially higher. Shear stress higher than 50 dynes/cm² can lead to platelet activation and aggregation (Huang, 1993). Encapsulation of platelets with the nanofilm may modify platelet α granule and dense granule release upon shear stress activation.

Thromboxane B₂ is an important indicator for platelet activation and aggregation. Here, TXB₂ released from platelets was measured through ELISA. All samples were prepared from pure platelets instead of platelet rich plasma (PRP). Encapsulated platelets released significantly less TXB₂ (1.60 ± 0.09 ng/ml) than did unmodified platelets (1.17 ± 0.22 ng/ml) ($p < 0.01$). The reason is unclear. High shear stress could cause a special platelet quick-release reaction called granule-membrane-fused lytic release (GFLR) (Song, 1990). It is possible that the heparin on the outermost layer limited shear-induced platelet secretion, thus reducing the amount of platelet recruitment. From previous studies, platelets release much more TXB₂ in the presence of ECM (Eldor, 1989). Also, the encapsulated shell on a platelet might limit TXB₂ release and lead to a lower TXB₂ concentration. The amount of TXB₂ release in PRP due to matrix-platelet interaction was much higher than the release in these studies (32.4 ng/ml) (Eldor, 1989).

4.5 Platelet Adhesion

The interaction of platelets with collagens of the vessel wall is a critical event in primary hemostasis. Collagen-platelet interaction is a two-step process of adhesion and activation involving the sequential recognition of distinct receptors. Adhesion involves first the reversible recognition of collagen-bound vWF by the platelet receptor complex GP Ib/IX/V, followed by direct interaction between collagen and the platelet integrin receptor $\alpha_2\beta_1$ (Barnes, 1998). In our study, collagen type I was used in assembly of multilayers in film coating on the inner surface of the silicone model. Collagen fibrils and immobilized collagen could bind strongly to platelets (Moroi *et al.*, 1997). Collagen type I can induce α -granule secretion and up-regulation of cell surface GPIIb-IIIa (Alberio *et al.*, 1998). Platelet adhesion and aggregation on collagen VI are different in shear rate dependence from collagen I (Ross *et al.*, 1995b). Chiang *et al.* (1993) suggested that type I collagen and type III collagen interact with platelets at separate sites.

It has been shown that heparin, by inhibiting the thrombin-GPIb interaction, is able to interfere with thrombin-induced platelet activation (De Candia, 1999). An increased surface expression of GPIIb-IIIa stimulated by HSS has been found from a previous study (Song, 1990). Heparin coating on the cardiopulmonary bypass oxygenator membrane can reduce platelet adhesion and activation (Niimi, 1999). Here, heparin coating on platelets may function as a shield to prevent external force activation and reduce platelet surface glycoprotein expression. After going through the high shear stress site at the stenosis, platelets were activated and “sticky.” In our study, much less encapsulated platelet adhesion on collagen was observed compared with unmodified platelets. The outermost layer heparin blocked platelet surface glycoprotein binding to

collagen nanofilm to a high degree. The encapsulation provided a protective shell to prevent platelet adhesion on collagen under high shear stress. So only 3.84% encapsulated platelets adhered to the collagen substrate compared with a much higher binding rate of 36.84% for unmodified platelets. Still, 3.84% platelets were adhered on collagen substrate and this adhesion is possibly due to the binding effect between collagen and heparin (Keller, 1986).

4.6 Measuring Nitric Oxide Release from Endothelial Cells

No nitric oxide release signal was detected from DAF-FM diacetate labeling in our study. The basal level of NO release from 10^5 endothelial cells was in the range of 140 – 504 pmol (Guo, 1996). The theoretical detection limit of DAF-FM diacetate was about 3 nM (Kojima, 1999). A fluorescence intensity of 2200 corresponded to a NO concentration of 1.2 μ M (Kojima, 1999). In his study, endothelial cells incubated with DAF-FM diacetate did not give off a fluorescence signal without bradykinin stimulation. On the contrary, an electrochemical sensor was sufficiently sensitive to detect the basal NO release from endothelial cells (Guo, 1996). It is possible that the dye may not be sensitive enough to detect normal NO release from endothelial cells. In our study, the flow treatment might be too short (< 1 hour) to cause large amount of NO release from endothelial cells. The small amount of NO release as well as the low sensitivity of dye led to the failure of NO detection.

CHAPTER 5

CONCLUSIONS AND RECOMMENDATIONS

5.1 Conclusions

5.1.1 Micro/Nano-Film Coating

Two gelatin glutaraldehyde (GA) crosslinking methods have been used to coat a hydrophilic membrane with micrometer thickness of silicone rubber in this study. In method I, gelatin and GA were mixed in three different proportions (64:1, 128:1 and 256:1) before coating. In method II, a newly formed 5% gelatin membrane was crosslinked with a 2.5% GA solution. All coatings were hydrophilic, as determined from the measurement of contact angle for a drop of water on the surface. Bovine coronary arterial endothelial cells (BCAEC) grew well on the surface modified by method II at 72 hours. In method I, the cells grew well for gelatin:GA proportions of 64:1 and 128:1 at 72 hours. No cell attachment on untreated silicone rubber was observed by the third day of seeding. The results indicated that both methods of gelatin GA crosslinking provided a hydrophilic surface on silicone for endothelial cell adhesion and growth *in vitro*.

Nanofilms of different compositions have been successfully coated on silicone rubber through the electrostatic LbL self-assembly technique. The technique was

successful not only on the planar surfaces in the Petri dishes, but also on the curved surface inside the coronary artery stenosis models. The films were hydrophilic, as determined from contact angle measurements. The film composed of PDL/gelatin multilayers was biocompatible for endothelial cell adhesion and growth.

5.1.2 Nano-Encapsulation of Platelets

Nanoparticles and immunoglobulins were assembled in nano-organized shells on bovine platelets through an electrostatic LbL self-assembly technique. Platelets were the second class of blood cells modified with nano-assembly after erythrocytes (Mohwald, 2000). The coverage of 78-nm silica and 45-nm fluorescent nanospheres on platelets was studied under TEM or fluorescence microscopes. An IgG-layer was adsorbed on platelets in alternation with poly(styrenesulfonate), and its specific immune-recognition and targeting with fluorescent anti-IgG-FITC were demonstrated. The technique makes several platelet modifications possible. First, abnormal receptor-agonist interactions could be blocked by nano-shells. Second, platelet aggregation could be altered due to novel surface properties of the cells. Third, platelet secretion could be controlled by thickness and composition of the nano-shell. Fourth, platelets can be targeted to specific sites in a blood vessel through antibody coating. These results show that it is possible to modify biological cells properties by assembling different materials. The presented approach of organized nano-shell formation can be extended to other cells or microbes for their surface modification or encapsulation.

The method is not limited to fixed platelets. Live platelets were also coated with polyions with a outermost layer of heparin. Most platelets were alive after the coating

procedure and no obvious cytotoxicity was observed. Also, platelets were not activated after encapsulation. Under high shear stress generated by the stenosis in the silicone model, encapsulated platelets released less TXB₂ compared with unmodified platelets. Platelets with a heparin coating did not readily adhere to the collagen substrate. The heparin shell might block the possible binding reactions between collagen and platelet surface glycoproteins. So the nano-engineered platelets reduced shear stress induced activation and adhesion.

5.2 Recommendations

It would be desirable to investigate and understand the detailed shell function during platelet activation and adhesion. Therefore, measuring platelet secretion of serotonin, von Willebrand factor, nitric oxide, ADP and other key materials are interesting and important for future study. In addition to the collagen substrate used here to study platelet adhesion, coatings of fibrinogen or vWF would be useful in studies designed to examine the mechanism by which the shell blocks the interaction between platelets and related ligands.

Shells with different compositions and outermost layers could also be applied onto platelets. The architecture of a shell is dependent on the application. One important procedure is to coat specific antibodies on platelets for tumor targeting.

The geometry of the stenosis or the Reynolds number can be varied for studying platelet reactions under different flow conditions.

Finally, it would be of great use to see how modified platelets interact with other blood components such as red blood cells. This observation may be accomplished by

adding encapsulated platelets into whole blood and measuring related parameters. Both in vitro and in vivo models could be used for these studies.

REFERENCES

Aarts, P. A., van den Broek, S. A., Prins, G. W., Kuiken, G. D., Sixma, J. J., and Heethaar, R. M., Blood platelets are concentrated near the wall and red blood cells, in the center in flowing blood, *Arteriosclerosis*, 8, 819 (1988).

Abbate, R., Marcucci, R., Camacho-Vanegas, O., Pepe, G., Gori, A. M., Capanni, M., Simonetti, I., Prisco, D., and Gensini, G. F., Role of platelet glycoprotein PL(A1/A2) polymorphism in restenosis after percutaneous transluminal coronary angioplasty, *American Journal of Cardiology*, 82, 524 (1998).

Abrams, C. S., Ellison, N., Budzynski, A. Z., and Shattil, S. J., Direct detection of activated platelets and platelet-derived microparticles in humans, *Blood*, 75, 128 (1990).

Abrams, C., and Shattil, S. J., Immunological detection of activated platelets in clinical disorders, *Thrombosis and Haemostasis*, 65, 467 (1991).

Ai, H., M. Fang, Y. M. Lvov, D. K. Mills, and S. A. Jones, "Electrostatic layer-by-layer self-assembly on biological micro/nanotemplates: platelets and tobacco mosaic virus", *Louisiana 2nd MEMS conference*, 2001a.

Ai, H., M. Fang, S. A. Jones, Y. M. Lvov, "Electrostatic Layer-by-Layer Nano-Assembly on Biological Microtemplates: Platelets", *Biomacromolecules*, 2002a.

Ai, H., S. A. Jones, M. M. de Villiers, Y. M. Lvov, "Nano-Encapsulation of Furosemide Microcrystals for Controlled Drug Release", *JACS*, 2002b, submitted.

Ai, H., Mills, D. K., Lvov, Y., Jones, S., "Assembling Biocompatible Nanofilms on PDMS substrate", *Biomaterials*, 2002c, In preparation.

Ai, H., Y. M. Lvov, D. K. Mills, J. S. Alexander, S. A. Jones, "Coating Poly-D-Lysine Nano-Film on PDMS for Endothelial Cell Adhesion and Growth", *The FASEB Journal*, 2002d.

Ai, H., Y. M. Lvov, D. K. Mills, J. S. Alexander, S. A. Jones, "Coating Biocompatible Nanofilms on PDMS", *BMES 2002 Annual Meeting*, October, 2002e.

Ai, H., Y. M. Lvov, D. K. Mills, S. A. Jones, "Micropatterning of micro/nanospheres on PDMS by using layer-by-layer self-assembly", the 2nd IEEE-EMBS Microtechnologies in Medicine and Biology Conference, 2002f.

Ai, H., S. A. Jones, M. M. de Villiers, Y. M. Lvov, "Nano-Encapsulation of Furosemide Microcrystals for Controlled Drug Release", American Chemical Society Annual Meeting, 2002g.

Ai, H., M. Fang, S. A. Jones, Y. M. Lvov, "Electrostatic Layer-by-Layer Nano-Assembly on Biological Microtemplates: Platelets", American Chemical Society Annual Meeting, 2002h.

Ai, H., M. Fang, Y. M. Lvov, D. K. Mills, and S. A. Jones, "Layer-by-Layer Nano-Assembly of Polymers on Silicone Rubber: A New Substrate for Endothelial Cell Growth", Society for Biomaterials 28th Annual Meeting, April, 2002.

Albelda, S. M., Muller, W. A., Buck, C. A., and Newman, P. J., Molecular and cellular properties of PECAM-1 (endoCAM/CD31): a novel vascular cell-cell adhesion molecule, *Journal of Cell Biology*, 114, 1059 (1991).

Alberio, L. and G. L. Dale (1998). "Flow cytometric analysis of platelet activation by different collagen types present in the vessel wall." *British Journal of Haematology* 102(5): 1212-8.

Ambrose, J. A., Tannenbaum, M. A., Alexopoulos, D., Hjendahl-Monsen, C. E., Leavy, J., Weiss, M., Borrico, S., Gorlin, R., and Fuster, V., Angiographic progression of coronary artery disease and the development of myocardial infarction, *Journal of the American College of Cardiology*, 12, 56 (1988).

Andrews, N. P., Gralnick, H. R., Merryman, P., Vail, M., and Quyyumi, A. A., Mechanisms underlying the morning increase in platelet aggregation: a flow cytometry study, *Journal of the American College of Cardiology*, 28, 1789 (1996).

Antipov, A.A., G. B. Sukhorukov, G.B., Donath, E., and Möhwald, H., "Sustained Release Properties of Polyelectrolyte Multilayer Capsules", *The Journal of Physical Chemistry B*, 2001; 105(12); 2281-2284.

Arcidi, J. M., Powelson, S. W., King, S. B., Douglas, J. S., Jones, E. L., Craver, J. M., Landolt, C. C., Jackson, E. R., Hatcher, C. R., and Guyton, R. A., Trends in invasive treatment of single-vessel and double-vessel coronary disease., *Journal of Thoracic and Cardiovascular Surgery*, 95, 773 (1988).

Ariga, K.; Lvov, Y.; Kunitake, T. Assembling alternate dye-polyion molecular films by electrostatic layer-by-layer adsorption. *J. Am. Chem. Soc.*, 1997, 119, 2224-2231.

Ault, K. A. and J. Mitchell (1994). "Analysis of platelets by flow cytometry." *Methods in Cell Biology* 42 Pt B: 275-94.

Badimon, L., Badimon, J. J., Galvez, A., Chesebro, J. H., and Fuster, V., Influence of arterial damage and wall shear rate on platelet deposition. Ex vivo study in a swine model, *Arteriosclerosis*, 6, 312 (1986).

Badimon, L., B., J. J., Turitto, V. T., Vallabhajosula, S., Fuster, V. (1988). "Platelet Thrombus Formation on collagen Type I a model of deep vessel injury influence of blood rheology, von Willebrand factor, and blood coagulation." *Circulation* 78(6): 1431-1442.

Baker, A., Saltik, M., Lehrmann, H., Killisch, I., Mautner, V., Lamm, G., Christofori, G., and Cotten, M., Polyethylenimine (PEI) is a simple, inexpensive and effective reagent for condensing and linking plasmid DNA to adenovirus for gene delivery., *Gene Therapy*, 4, 773 (1997).

Bar, F., Vainer, J., Stevenhagen, J., Neven, K., Aalbrecht, R., Ophuis, T. O., van Ommen, V., de Swart, H., de Muinck, E., Dassen, W., and Wellens, H., Ten-year experience with early angioplasty in 759 patients with acute myocardial infarction, *Journal of the American College of Cardiology*, 36, 51 (2000).

Baumgartner, H. R., Tschopp, T. B., and Meyer, D., Shear rate dependent inhibition of platelet adhesion and aggregation on collagenous surfaces by antibodies to human factor VIII/von Willebrand factor, *British Journal of Haematology*, 44, 127 (1980).

Belval, T., Hellums, J. D., and Solis, R. T., The kinetics of platelet aggregation induced by fluid-shearing stress, *Microvascular Research*, 28, 279 (1984).

Bennett, J. S., Hoxie, J. A., Leitman, S. F., Vilaire, G., and Cines, D. B., Inhibition of fibrinogen binding to stimulated human platelets by a monoclonal antibody, *Proceedings of the National Academy of Sciences of the United States of America*, 80, 2417 (1983).

Bennett, J. S., Shattil, S. J., Power, J. W., and Gartner, T. K., Interaction of fibrinogen with its platelet receptor. Differential effects of alpha and gamma chain fibrinogen peptides on the glycoprotein IIb-IIIa complex, *Journal of Biological Chemistry*, 263, 12948 (1988).

Biotrak. (1994). Thromboxane B2 enzymeimmunoassay (EIA) system. Amersham Life Science.

Bluestein, D., Niu, L., Schoepfoerster, R. T., and Dewanjee, M. K., Fluid mechanics of arterial stenosis: relationship to the development of mural thrombus, *Annals of Biomedical Engineering*, 25, 344 (1997).

Born, G. V. (1970). "Observations on the change in shape of blood platelets brought about by adenosine diphosphate." *Journal of Physiology* 209(2): 487-511.

Borrione, M., Hall, P., Almagor, Y., Maiello, L., Khat, B., Finci, L., and Colombo, A., Treatment of simple and complex coronary stenosis using rotational ablation followed by low pressure balloon angioplasty, *Catheterization and Cardiovascular Diagnosis*, 30, 131 (1993).

Bottiger, C., Kastrati, A., Koch, W., Mehilli, J., von Beckerath, N., Dirschinger, J., Gawaz, M., and Schomig, A., Polymorphism of platelet glycoprotein IIb and risk of thrombosis and restenosis after coronary stent placement, *American Journal of Cardiology*, 84, 987 (1999).

Bredt, D. S. and S. H. Snyder (1990). "Isolation of nitric oxide synthetase, a calmodulin-requiring enzyme." *Proceedings of the National Academy of Sciences of the United States of America* 87(2): 682-5.

Broekman, M. J., Eiroa, A. M., and Marcus, A. J., Inhibition of human platelet reactivity by endothelium-derived relaxing factor from human umbilical vein endothelial cells in suspension: blockade of aggregation and secretion by an aspirin-insensitive mechanism, *Blood*, 78, 1033 (1991).

Brown, C. H. d., Leverett, L. B., Lewis, C. W., Alfrey, C. P. J., and Hellums, J. D., Morphological, biochemical, and functional changes in human platelets subjected to shear stress, *Journal of Laboratory and Clinical Medicine*, 86, 462 (1975).

Bruckdorfer, K. R., Jacobs, M., and Rice_Evans, C., Endothelium-derived relaxing factor (nitric oxide), lipoprotein oxidation and atherosclerosis., *Biochemical Society Transactions*, 18, 1061 (1990).

Brynda, E.; Houska, M. Ordered multilayer assemblies: Albumin / heparin for biocompatible coating and monoclonal antibodies for optical immunosensors. In book: *Protein Architecture: Interfacial Molecular Assembly and Immobilization Biotechnology*, Ed: Y. Lvov and H. Möhwald, M. Dekker Publ., New York, 2000, 251-286.

Buchwald, A., Werner, G., Unterberg, C., Voth, A., and Wiegand, V., Malignant restenosis after primary successful excimer laser coronary angioplasty, *Clinical Cardiology*, 13, 397 (1990).

Buijs, J.; Lichtenbelt, J. W. Th.; Norde, W.; Lyklema, J. *Colloids Surf. B: Biointer.*, 1995, 5, 11.

Burlet, S. and R. Cespuglio (1997). "Voltammetric detection of nitric oxide (NO) in the rat brain: its variations throughout the sleep-wake cycle." *Neuroscience Letters* 226(2): 131-5.

Caruso, F.; Niikura, K.; Furlong, N.; Okahata, Y. Assembly of alternating polyelectrolyte and protein multilayer films for immunosensing. *Langmuir*, 1997, 13, 3427-3433.

Caruso, F.; Caruso, R.; Möhwald, H. Fabrication of hollow, spherical silica and composite shells via electrostatic self-assembly of nanocomposite multilayers on decomposable colloidal templates. *Science*, 1998, 282, 1111-1114.

Caruso, F.; Furlong, N.; Ariga, K.; Ichinose, I.; Kunitake, T. Characterization of polyelectrolyte-protein multilayer films by atomic force microscopy, scanning electron microscopy and Fourier-transform infrared reflection - absorption spectroscopy. *Langmuir*, 1998a, 14, 4559-4565.

Caruso, F.; Möhwald, H. Protein multilayer formation on colloids through a step-wise self-assembly technique. *J. Am. Chem. Soc.*, 1999, 121, 6039-6045.

Caruso, F.; Trau, D.; Möhwald, H.; Renneberg, R. Encapsulation of enzyme crystals in molecularly engineered multilayer capsules. *Langmuir*, 2000, 16, 1485-1488.

Caspary, E. A., Kekwick, R. A. (1957). "Some physicochemical properties in human fibrinogen." *Biochem. J.* 67: 41.

Cheung, J.; Fou, A.; Rubner, M. Molecular Self-Assembly of conducting polymers. *Thin Solid Films*, 1994, 244, 985-989.

Chiang, T. M., Seyer, J. M., and Kang, A. H., Collagen-platelet interaction: separate receptor sites for types I and III collagen, *Thrombosis Research*, 71, 443 (1993).

Chow, T. W., Hellums, J. D., Moake, J. L., and Kroll, M. H., Shear stress-induced von Willebrand factor binding to platelet glycoprotein Ib initiates calcium influx associated with aggregation, *Blood*, 80, 113 (1992).

Clark, R. A., Horsburgh, C. R., Hoffman, A. A., Dvorak, H. F., Mosesson, M. W., and Colvin, R. B., Fibronectin deposition in delayed-type hypersensitivity. Reactions of normals and a patient with afibrinogenemia, *Journal of Clinical Investigation*, 74, 1011 (1984).

Conti, C. R. (1991). "Coronary stenosis after successful angioplasty: clinical observations [editorial]." *Clinical Cardiology* 14(11): 863-4.

Cohen, N., Zaidenstein, R., Blatt, A., Sarafian, D. A., Litinsky, I., and Modai, D., Unrecognized major bleeding following thrombolysis for acute myocardial infarction presenting with syncope, *Clinical Cardiology*, 21, 599 (1998).

Coherent, Inc., Operator's Manual INNOVA 70C Series Ion Laser, 1997.

Coller, B. S. (1985). "A new murine monoclonal antibody reports an activation-dependent change in the conformation and/or microenvironment of the platelet glycoprotein IIb/IIIa complex." *Journal of Clinical Investigation* 76(1): 101-8.

Daniel, J. L., Dangelmaier, C., Strouse, R., and Smith, J. B., Collagen induces normal signal transduction in platelets deficient in CD36 (platelet glycoprotein IV), *Thrombosis and Haemostasis*, 71, 353 (1994).

Dardik, A., Liu, A., and Ballermann, B. J., Chronic in vitro shear stress stimulates endothelial cell retention on prosthetic vascular grafts and reduces subsequent in vivo neointimal thickness., *Journal of Vascular Surgery*, 29, 157 (1999).

De_Candia, E., De_Cristofaro, R., and Landolfi, R., Thrombin-induced platelet activation is inhibited by high- and low-molecular-weight heparin., *Circulation*, 99, 3308 (1999).

de Bono, D. P. and R. S. More (1993). "Prevention and management of bleeding complications after thrombolysis." *International Journal of Cardiology* 38(1): 1-6.

Decher, G.; Hong, J-D. Buildup of ultrathin multilayer films by self-assembly process: Consecutive adsorption of anionic and cationic bipolar amphiphiles and polyelectrolytes on charged surfaces. *Ber. Bunsenges. Phys. Chem.*, 1991, 95, 1430-1434.

Decher, G.; Essler, F.; Hong, J.-D.; Lowack, K.; Schmitt, J.; Lvov, Y. Layer-by-layer adsorbed films of polyelectrolytes, proteins or DNA. *Polymer Preprints*, 1993, 34, 745-746.

Decher, G.; Lvov, Y.; Schmitt, J. Proof of multilayer structural organization of polycation/ polyanion self-assembled films. *Thin Solid Films*, 1994a, 244, 772-777.

Decher, G.; Lehr, B.; Lowack, K.; Lvov, Y.; Schmitt, J. New nanocomposite films for biosensors: layer-by-layer adsorbed films of polyelectrolytes, proteins or DNA. *Biosensors and Bioelectronics*, 1994b, 9, 677-684.

Decher, G. Fuzzy nanoassemblies: Toward layered polymeric multicomposites. *Science*, 1997, 227, 1232-1237.

Dewitz, T. S., Martin, R. R., Solis, R. T., Hellums, J. D., and McIntire, L. V., Microaggregate formation in whole blood exposed to shear stress, *Microvascular Research*, 16, 263 (1978).

Du, X., Beutler, L., Ruan, C., Castaldi, P. A., and Berndt, M. C., Glycoprotein Ib and glycoprotein IX are fully complexed in the intact platelet membrane, *Blood*, 69, 1524 (1987).

Duguid J.B., Thrombosis as a factor in the pathogenesis of aortic atherosclerosis, *J Pathol Bacteriol*, , 1985;58:207-212.

Elbert, D.; Herbert, C.; Hubbell, J. Thin polymer layers formed by polyelectrolyte multilayer techniques on biological surfaces. *Langmuir*, 1999, 15, 5355-5362.

- Eldor, A., Fuks, Z., Levine, R. F., and Vlodaysky, I., "Measurement of platelet and megakaryocyte interaction with the subendothelial extracellular matrix", *Methods in Enzymology*, 169, 76 (1989).
- Ellis, S. G., O'Neill, W. W., Bates, E. R., Walton, J. A., Nabel, E. G., and Topol, E. J., Coronary angioplasty as primary therapy for acute myocardial infarction 6 to 48 hours after symptom onset: report of an initial experience, *Journal of the American College of Cardiology*, 13, 1122 (1989).
- Ellis, S. G., Roubin, G. S., King, S. B. d., Douglas, J. S. J., and Cox, W. R., Importance of stenosis morphology in the estimation of restenosis risk after elective percutaneous transluminal coronary angioplasty, *American Journal of Cardiology*, 63, 30 (1989).
- Erlemeier, H. H., Zangemeister, W., Burmester, L., Schofer, J., Mathey, D. G., and Bleifeld, W., Bleeding after thrombolysis in acute myocardial infarction, *European Heart Journal*, 10, 16 (1989).
- Estavillo, D., Ritchie, A., Diacovo, T. G., and Cruz, M. A., Functional analysis of a recombinant glycoprotein Ia/IIa (Integrin alpha(2)beta(1)) I domain that inhibits platelet adhesion to collagen and endothelial matrix under flow conditions, *Journal of Biological Chemistry*, 274, 35921 (1999).
- Fang, M., P. S. Grant, M. J. McShane, G. B. Sukhorukov, V. O. Golub and Y. M. Lvov, "Magnetic Bio/Nanoreactor with Multilayer Shells of Glucose Oxidase and Inorganic Nanoparticles", *Langmuir*, 2002a.
- Fang, M., H. Ai, R. Cush, P. Russo, Y. M. Lvov, "Layer-by-Layer Electrostatic Assembly of Biocolloids: Encapsulation of Tobacco Mosaic Virus and Fabrication of Glucose Oxidase Nano-Reactor", *ACS*, 2002b.
- Fardale, R. W., Winkler, A. B., Martin, B. R., and Barnes, M. J., Inhibition of human platelet adenylate cyclase by collagen fibres. Effect of collagen is additive with that of adrenaline, but interactive with that of thrombin, *Biochemical Journal*, 282 (Pt 1), 25 (1992).
- Faull, R. J., Du, X., Ginsberg, M. H., Ed. (1994). *Receptors on Platelets. Methods In Enzymology*, Academic Press, Inc.
- Febbraio, M. and R. L. Silverstein (1990). "Identification and characterization of LAMP-1 as an activation-dependent platelet surface glycoprotein." *Journal of Biological Chemistry* 265(30): 18531-7.
- Fijnheer, R., Modderman, P. W., Veldman, H., Ouwehand, W. H., Nieuwenhuis, H. K., Roos, D., and de Korte, D., Detection of platelet activation with monoclonal antibodies and flow cytometry. Changes during platelet storage, *Transfusion*, 30, 20 (1990).

Fitzgerald, L. A., Steiner, B., Rall, S. C. J., Lo, S. S., and Phillips, D. R., Protein sequence of endothelial glycoprotein IIIa derived from a cDNA clone. Identity with platelet glycoprotein IIIa and similarity to α IIb β 3 integrin, *Journal of Biological Chemistry*, 262, 3936 (1987).

Fitzpatrick, F. A., Gorman, R. R., Mc Guire, J. C., Kelly, R. C., Wynalda, M. A., and Sun, F. F., A radioimmunoassay for thromboxane B₂, *Analytical Biochemistry*, 82, 1 (1977).

Forstermann, U., Pollock, J. S., Schmidt, H. H., Heller, M., and Murad, F., Calmodulin-dependent endothelium-derived relaxing factor/nitric oxide synthase activity is present in the particulate and cytosolic fractions of bovine aortic endothelial cells., *Proceedings of the National Academy of Sciences of the United States of America*, 88, 1788 (1991).

Fox, J. E., Aggerbeck, L. P., and Berndt, M. C., Structure of the glycoprotein Ib-IX complex from platelet membranes, *Journal of Biological Chemistry*, 263, 4882 (1988).

Freeman, G., Dyer, R. L., Juhos, L. T., St_John, G. A., and Anbar, M., Identification of nitric oxide (NO) in human blood., *Archives of Environmental Health*, 33, 19.

Frelinger, A. L. d., Lam, S. C., Plow, E. F., Smith, M. A., Loftus, J. C., and Ginsberg, M. H., Occupancy of an adhesive glycoprotein receptor modulates expression of an antigenic site involved in cell adhesion, *Journal of Biological Chemistry*, 263, 12397 (1988).

Frelinger, A. L. d., Cohen, I., Plow, E. F., Smith, M. A., Roberts, J., Lam, S. C., and Ginsberg, M. H., Selective inhibition of integrin function by antibodies specific for ligand-occupied receptor conformers, *Journal of Biological Chemistry*, 265, 6346 (1990).

Fressinaud, E., Baruch, D., Girma, J. P., Sakariassen, K. S., Baumgartner, H. R., and Meyer, D., von Willebrand factor-mediated platelet adhesion to collagen involves platelet membrane glycoprotein IIb-IIIa as well as glycoprotein Ib, *Journal of Laboratory and Clinical Medicine*, 112, 58 (1988).

Fujikawa, L. S., Foster, C. S., Gipson, I. K., and Colvin, R. B., Basement membrane components in healing rabbit corneal epithelial wounds: immunofluorescence and ultrastructural studies, *Journal of Cell Biology*, 98, 128 (1984).

Fuster, V., Steele, P. M., and Chesebro, J. H., Role of platelets and thrombosis in coronary atherosclerotic disease and sudden death, *Journal of the American College of Cardiology*, 5, 175B (1985).

Fuster, V., Stein, B., Ambrose, J. A., Badimon, L., Badimon, J. J., and Chesebro, J. H., Atherosclerotic plaque rupture and thrombosis. Evolving concepts, *Circulation*, 82, II47 (1990).

Fuster, V., Badimon, J., Chesebro, J. H., and Fallon, J. T., Plaque rupture, thrombosis, and therapeutic implications, *Haemostasis*, 26 Suppl 4, 269 (1996).

Fuster, V., Mechanisms of arterial thrombosis: foundation for therapy, *American Heart Journal*, 135, S361 (1998).

Garthwaite, J., Charles, S. L., and Chess_Williams, R., Endothelium-derived relaxing factor release on activation of NMDA receptors suggests role as intercellular messenger in the brain., *Nature*, 336, 385 (1988).

Gatter, K. C., Cordell, J. L., Turley, H., Heryet, A., Kieffer, N., Anstee, D. J., and Mason, D. Y., The immunohistological detection of platelets, megakaryocytes and thrombi in routinely processed specimens [see comments], *Histopathology*, 13, 257 (1988).

Gautam, A., Densmore, C. L., Xu, B., and Waldrep, J. C., Enhanced gene expression in mouse lung after PEI-DNA aerosol delivery., 2, 63 (2000).

George, J. N. (2000). "Platelets." *Lancet* 355(9214): 1531-9.

Ginsberg, M. H., Forsyth, J., Lightsey, A., Chediak, J., and Plow, E. F., Reduced surface expression and binding of fibronectin by thrombin-stimulated thrombasthenic platelets, *Journal of Clinical Investigation*, 71, 619 (1983).

Ginsberg, M. H., Frelinger, A. L., Lam, S. C., Forsyth, J., McMillan, R., Plow, E. F., and Shattil, S. J., Analysis of platelet aggregation disorders based on flow cytometric analysis of membrane glycoprotein IIb-IIIa with conformation-specific monoclonal antibodies, *Blood*, 76, 2017 (1990).

Glynn, MF, "The role of the platelet membrane in platelet function. II. 5-Hydroxytryptamine (serotonin) uptake," *Am J Clin Pathol*, 60(5):636-643 (1973).

Goel, P. K., Shahi, M., Agarwal, A. K., Srivastava, S., and Seth, P. K., Platelet aggregability and occurrence of restenosis following coronary angioplasty, *International Journal of Cardiology*, 60, 227 (1997).

Goto, S. and S. Handa (1998). "Coronary thrombosis. Effects of blood flow on the mechanism of thrombus formation." *Japanese Heart Journal* 39(5): 579-96.

Gralnick, H. R., Williams, S., McKeown, L., Connaghan, G., Shafer, B., Hansmann, K., Vail, M., and Fenton, J., Endogenous platelet fibrinogen surface expression on activated platelets, *Journal of Laboratory and Clinical Medicine*, 118, 604 (1991).

Gralnick, H. R., Williams, S. B., McKeown, L., Shafer, B., Connaghan, G. D., ansmann, K., Vail, M., and Magruder, L., Endogenous platelet fibrinogen: its modulation after surface expression is related to size-selective access to and conformational changes in the bound fibrinogen, *British Journal of Haematology*, 80, 347 (1992).

Grines, C. L., Cox, D. A., Stone, G. W., Garcia, E., Mattos, L. A., Giambartolomei, A., Brodie, B. R., Madonna, O., Eijgelshoven, M., Lansky, A. J., O'Neill, W. W., and Morice, M. C., Coronary angioplasty with or without stent implantation for acute myocardial infarction. Stent Primary Angioplasty in Myocardial Infarction Study Group., *New England Journal of Medicine*, 341, 1949 (1999).

Guo, J., Murohara, T., Buerke, M., Direct measurement of nitric oxide release from vascular endothelial cells, *the American Physiological Society*, 774 (1996).

Guyton, A. C., Hall, J. E. (1996). Muscle blood flow and cardiac output during exercises; the coronary circulation and ischemic heart disease. *Textbook of Medical Physiology*. Philadelphia, W.B. Saunders Company: 253-264.

Guyton, A. C. and Hall, J. E. (1996). Hemostasis and Blood Coagulation. *Textbook of Medical Physiology*. Philadelphia, W.B. Saunders Company: 463-473.

Hamberg, M., Svensson, J., and Samuelsson, B., Prostaglandin endoperoxides. A new concept concerning the mode of action and release of prostaglandins, *Proceedings of the National Academy of Sciences of the United States of America*, 71, 3824 (1974).

Hamburger, S. A. and R. P. McEver (1990). "GMP-140 mediates adhesion of stimulated platelets to neutrophils." *Blood* 75(3): 550-4.

Hanson SR, Francesco I, Zaverio P, Ruggeri M, Marzec UM, Kunicki TJ, Montgomery RR, Zimmerman TS and Harker LA, "Effects of monoclonal antibodies against the platelet glycoprotein IIb/IIIa complex on thrombosis and hemostasis in the baboon," *J Clin Invest*, 81, 149-158, 1988.

Hawiger, J. (1991). "Adhesive interactions of platelets and their blockade." *Annals of the New York Academy of Sciences* 614: 270-8.

Hayward, C. P., Bainton, D. F., Smith, J. W., Horsewood, P., Stead, R. H., Podor, T. J., Warkentin, T. E., and Kelton, J. G., Multimerin is found in the alpha-granules of resting platelets and is synthesized by a megakaryocytic cell line, *Journal of Clinical Investigation*, 91, 2630 (1993).

He, J-A.; Samuelson, L.; Li, L.; Kumar, J.; Tripathy, S. Oriented bacteriorhodopsin / polycation multilayers by electrostatic layer-by-layer assembly. *Langmuir*, 1998, 14, 1674-1679.

Henrita_van_Zanten, G., Saelman, E. U., Schut_Hese, K. M., Wu, Y. P., Slootweg, P. J., Nieuwenhuis, H. K., de_Groot, P. G., and Sixma, J. J., Platelet adhesion to collagen type IV under flow conditions., *Blood*, 88, 3862 (1996).

Hodak, J.; Etchenique, R.; Calvo, E.; Singhal, K.; Bartlett, P. Layer-by-layer self-assembly of glucose oxidase with a poly(allylamine) ferrocene redox mediator. *Langmuir*, 1997, 13, 2708-2716.

Holmsen, H. (1990a). Biochemistry and function of platelets: Composition of platelets. *Hematology* Fourth edition. W. J. Williams, Beutler, E., Erslev, A. J., Lichtman, M. A. New York, McGraw-Hill, Inc.: 1182-1200.

Holmsen, H. (1990b). Metabolism of platelets. *Hematology* Fourth edition. W. J. Williams, Beutler, E., Erslev, A. J., Lichtman, M. A. New York, McGraw-Hill, Inc.: 1200-1233.

Holmsen, H. a. D., C. A. (1992). Measurement of Secretion of Lysosomal Acid Glycosidases. *Platelets: Receptors, Adhesion, Secretion Part A*. J. Hawiger. San Diego, Academic Press, Inc. 169: 336-351.

Hong, J.-D.; Lowack, K.; Schmitt, J.; Decher, G. Layer-by-layer deposited multilayer assemblies of polyelectrolytes and proteins: from ultrathin films to protein arrays. *Progr. Colloid Polym. Sci.*, 1993, 93, 98-102.

Honour, A. J., Carter, R. D., and Mann, J. I., The effects of changes in diet on lipid levels and platelet thrombus formation in living blood vessels, *British Journal of Experimental Pathology*, 59, 390 (1978).

Horak, E. R., Leek, R., Klenk, N., LeJeune, S., Smith, K., Stuart, N., Greenall, M., Stepniewska, K., and Harris, A. L., Angiogenesis, assessed by platelet/endothelial cell adhesion molecule antibodies, as indicator of node metastases and survival in breast cancer, *Lancet*, 340, 1120 (1992).

Hourdille, P., Heilmann, E., Combrie, R., Winckler, J., Clemetson, K. J., and Nurden, A. T., Thrombin induces a rapid redistribution of glycoprotein Ib-IX complexes within the membrane systems of activated human platelets, *Blood*, 76, 1503 (1990).

Hoylaerts, M. F. (1997). "Platelet-vessel wall interactions in thrombosis and restenosis role of von Willebrand factor." *Verhandelingen - Koninklijke Academie Voor Geneeskunde Van Belgie* 59(3): 161-83.

Hsu-Lin, S., C. L. Berman., (1984). "A platelet membrane protein expressed during platelet activation and secretion. Studies using a monoclonal antibody specific for thrombin-activated platelets." *Journal of Biological Chemistry* 259(14): 9121-6.

Huang, P. Y., Hellums, J. David, "Aggregation and Disaggregation Kinetics of Human Blood Platelets: Part II. Shear-induced Platelet Aggregation." *Biophysical Journal* 65: 344-353, (1993).

Huang, T. C., Graham, D. A., Nelson, L. D., and Alevriadou, B. R., Fibrinolytic agents inhibit platelet adhesion onto collagen type I-coated surfaces at high blood flow conditions., *Blood Coagulation and Fibrinolysis*, 9, 213 (1998).

Ikeda, Y., Handa, M., Kawano, K., Kamata, T., Murata, M., Araki, Y., Anbo, H., Kawai, Y., Watanabe, K., Itagaki, I., The role of von Willebrand factor and fibrinogen in platelet aggregation under varying shear stress, *Journal of Clinical Investigation*, 87, 1234 (1991).
Iler, R. Multilayers of colloidal particles. *J. Colloid Interface Sci.*, 21, 569-594 (1966).

Jacobsen, M. D., Weil, M., and Raff, M. C., Role of Ced-3/ICE-family proteases in staurosporine-induced programmed cell death., *Journal of Cell Biology*, 133, 1041 (1996).

Jaffe, E. A., Hoyer, L. W., and Nachman, R. L., Synthesis of von Willebrand factor by cultured human endothelial cells, *Proceedings of the National Academy of Sciences of the United States of America*, 71, 1906 (1974).

Jennings, L. K., Ashmun, R. A., Wang, W. C., and Dockter, M. E., Analysis of human platelet glycoproteins IIb-IIIa and Glanzmann's thrombasthenia in whole blood by flow cytometry, *Blood*, 68, 173 (1986).

Kaplan, D. R., Chao, F. C., Stiles, C. D., Antoniades, H. N., and Scher, C. D., Platelet alpha granules contain a growth factor for fibroblasts, *Blood*, 53, 1043 (1979).

Kaplan, K. L., Broekman, M. J., Chernoff, A., Lesznik, G. R., and Drillings, M., Platelet alpha-granule proteins: studies on release and subcellular localization, *Blood*, 53, 604 (1979).

Kastrati, A., Schomig, A., Seyfarth, M., Koch, W., Elezi, S., Bottiger, C., Mehilli, J., Schomig, K., and von Beckerath, N., PLA polymorphism of platelet glycoprotein IIIa and risk of restenosis after coronary stent placement, *Circulation*, 99, 1005 (1999).

Kastrati, A., Schomig, A., Seyfarth, M., Koch, W., Elezi, S., Bottiger, C., Mehilli, J., Schomig, K., and von Beckerath, N., PLA polymorphism of platelet glycoprotein IIIa and risk of restenosis after coronary stent placement, *Circulation*, 99, 1005 (1999).

Kehrel, B. (1995). "Platelet-collagen interactions." *Seminars in Thrombosis and Hemostasis* 21(2): 123-9.

Klein, L. W. and J. Rosenblum (1990). "Restenosis after successful percutaneous transluminal coronary angioplasty." *Progress in Cardiovascular Diseases* 32(5): 365-82.

Kleinfeld, E.; Ferguson, G. Stepwise formation of multilayered nanostructural films from macromolecular precursors. *Science*, 1994, 265, 370-373.

Kojima, H., Nakatsubo, N., Kikuchi, K., Kawahara, S., Kirino, Y., Nagoshi, H., Hirata, Y., and Nagano, T., Detection and imaging of nitric oxide with novel fluorescent indicators: diaminofluoresceins., *Analytical Chemistry*, 70, 2446 (1998).

Kojima, H., Urano, Y., Kikuchi, K., Higuchi, T., Hirata, Y., Nagano, T., "Fluorescent Indicators for Imaging Nitric Oxide Production", *Angewandte Chemie International Edition*, pp. 3209-3212, Vol. 38, Issue 21, 1999.

Kong, W.; Wang, L.; Gao, M.; Zhou, H.; Zhang, X.; Li, W.; Shen, J. Immobilized bilayer glucose isomerase in porous trimethylamine polystyrene based on molecular deposition. *J. Chem. Soc., Chem. Commun.*, 1994, 1297-1298.

Kong, J.; Lu, Z.; Lvov, Y.; Desamero, R.; Frank, H.; Rusling, J. Direct electrochemistry of cofactor redox sites in bacterial photosynthetic reaction center protein. *J. Am. Chem. Soc.*, 1998, 120, 7371-7372.

Kong, J.; Sun, W.; Wu, X.; Deng, J.; Lvov, Y.; Desamero, R.; Frank, H.; Rusling, J. Fast reversible electron transfer from photosynthetic reaction center from wild type *Rhodobacter spheroides* re-constituted in polycation sandwiched monolayer film. *Bioelectrochem. Bioenerg.*, 1999, 48, 101-107.

Konstantopoulos, K., Wu, K. K., Udden, M. M., Banez, E. I., Shattil, S. J., and Hellums, J. D., Flow cytometric studies of platelet responses to shear stress in whole blood, *Biorheology*, 32, 73 (1995).

Korneev, D.; Lvov, Y.; Decher, G.; Schmitt, J. Neutron reflectivity analysis of self-assembled film superlattices with alternate layers of deuterated and hydrogenated polystyrenesulfonate and polyallylamine. *Physica B*, 1995, 213 / 214, 954-956.

Kotov, N.; Dekany, I.; Fendler, J. Layer-by-layer self-assembly of polyelectrolyte-semiconductor nanoparticle composite. *J. Phys. Chem.*, 1995, 99, 13065-13069.

Lake_Bruse, K. D., Faraci, F. M., Shesely, E. G., Maeda, N., Sigmund, C. D., and Heistad, D. D., Gene transfer of endothelial nitric oxide synthase (eNOS) in eNOS-deficient mice., *American Journal of Physiology*, 277, H770 (1999).

Lakowicz, J. R. (1999). *Fluorophores. Principles of Fluorescence Spectroscopy*, Plenum Pub Corp: 63-91.

Lam, SC-T, *JBC* 260:11107, 1985.

Lane, G. E. and D. R. J. Holmes (2000). "Primary angioplasty for acute myocardial infarction in the elderly." *Coronary Artery Disease* 11(4): 305-13.

Lantoine, F., Trevin, S., Bedioui, F., Devynck, J. (1995). "Selective and sensitive electrochemical measurement of nitric oxide in aqueous solution: discussion and new results." *Journal of Electroanalytical Chemistry* 392: 85-89.

Lantoine, F., Brunet, A., Bedioui, F., Devynck, J., and Devynck, M. A., Direct measurement of nitric oxide production in platelets: relationship with cytosolic Ca²⁺ concentration., *Biochemical and Biophysical Research Communications*, 215, 842 (1995).

Leasche, M.; Schmitt, J.; Decher, G.; Bouwman, W.; Kjaer, K. Detailed structure of molecularly thin polyelectrolyte multilayer films on solid substrates as revealed by neutron reflectometry. *Macromolecules*, 1998, 31, 8893-8906.

Li M., H. Ai, D. K. Mills, Y. M. Lvov, B. K. Gale, "Increasing the Alignment of Smooth Muscle Cells by 100 μm Channels with Micro- and Nano- Technology", IEEE, 2002 Meeting.

Lindahl, T. L., Festin, R., and Larsson, A., Studies of fibrinogen binding to platelets by flow cytometry: an improved method for studies of platelet activation., *Thrombosis and Haemostasis*, 68, 221 (1992).

Liska, J., Jonsson, A., Lockowandt, U., Herzfeld, I., Gelinder, S., and Franco-Cereceda, A., Arterial patch angioplasty for reconstruction of proximal coronary artery stenosis, *Annals of Thoracic Surgery*, 68, 2185 (1999).

Liska, J., A. Jonsson, (1999). "Arterial patch angioplasty for reconstruction of proximal coronary artery stenosis." *Annals of Thoracic Surgery* 68(6): 2185-9; discussion 2190.

Little, W. C., Applegate, R. J. (1996). "Role of Plaque Size And Degree of Stenosis in Acute Myocardial Infarction." *Cardiology Clinics* 14(2): 221-228.

Looney, R. J., Abraham, G. N., and Anderson, C. L., Human monocytes and U937 cells bear two distinct Fc receptors for IgG, *Journal of Immunology*, 136, 1641 (1986).

Lowenstein, C. J., Dinerman, J. L., and Snyder, S. H., Nitric oxide: a physiologic messenger., *Annals of Internal Medicine*, 120, 227 (1994).

Lvov, Y., Decher, G; Möhwald, H. Assembly, structural characterization and thermal behavior of layer-by-layer deposited ultrathin films of polyvinylsulfate and polyallylamine. *Langmuir*, 1993d, 9, 481-486.

Lvov, Y., Decher, G., Sukhorukov, G. Assembly of thin films by means of successive deposition of alternate layers of DNA and poly(allylamine). *Macromolecules*, 1993a, 26, 5396-5399.

Lvov, Y., Haas, H.; Decher, G.; Möhwald, H.; Kalachev, A. Assembly of polyelectrolyte molecular films onto plasma treated glass. *J. Phys. Chemistry*, 1993b, 97, 12835-12841.

Lvov, Y.; Essler, F.; Decher, G. The combination of polyanion/polycation self-assembly and Langmuir-Blodgett transfer for the construction of superlattice films. *J. Phys. Chemistry*, 1993c, 97, 13773-13777.

Lvov, Y.; Ariga, K.; Kunitake, T. Layer-by-layer assembly of alternate protein / polyion ultrathin films. *Chemistry Letters*, 1994c, 2323-2326.

Lvov, Y.; Haas, H.; Decher, G.; Möhwald, H.; Mikhailov, A.; Mtchedlishvily, B.; Morgunova, E.; Vainshtein, B. Successive deposition of alternate layers of polyelectrolytes and charged virus. *Langmuir*, 1994a, 10, 4232-4236.

Lvov, Y., Decher, G. Assembly of multilayer ordered films by alternating adsorption of oppositely charged macromolecules. *Crystallography Reports*, 1994b, 39, 696-716.

Lvov, Y.; Ariga, K.; Ichinose, I.; Kunitake, K. Assembly of multicomponent protein films by means of electrostatic layer-by-layer adsorption. *J. Am. Chem. Soc.*, 1995, 117, 6117-6123.

Lvov, Y.; Ariga, K.; Ichinose, I.; Kunitake, T. Molecular film assembly via layer-by-layer adsorption of oppositely charged macromolecules (linear polymer, protein, and clay) and of concanavalin A / glycogen pair. *Thin Solid Films*, 1996, 284, 797-801.

Lvov, Y.; Ariga, K.; Ichinose, I.; Kunitake, T. Alternate assembly of ordered multilayers of SiO₂ and other nanoparticles and polyions. *Langmuir*, 1997, 13, 6195-6203.

Lvov, Y.; Rusling, J.; Thomsen, D.; Papadimitrakopoulos, F.; Kawakami, T.; Kunitake, T. High-speed multilayer assembly by alternate adsorption of silica nanoparticles and linear polycation. *J. Chem. Soc., Chem. Commun.*, 1998a, 1229-1230.

Lvov, Y., Onda, M.; Ariga, K.; Kunitake, T. Ultrathin films of charged polysaccharides assembled alternately with linear polyions. *J. Biomater. Sci., Polym. Ed.*, 1998b, 9, 345-355.

Lvov, Y. Electrostatic layer-by-layer assembly of proteins and polyions. In book: *Protein Architecture: Interfacial Molecular Assembly and Immobilization Biotechnology*, Ed: Y. Lvov and H. Möhwald, M. Dekker Publ., New York, 2000, 125-167.

Lvov, Y.; Caruso, F. *Anal. Chem.*, 2001a, 73, 4212.

Lvov, Y., A. Antipov, A. Mamedov, H. Möhwald, and G. B. Sukhorukov, "Urease Encapsulation in Nanoorganized Microshells" *Nano Letters*, 2001b, Vol. 1, No. 3

MacIntyre, I., Zaidi, M., Alam, A. S., Datta, H. K., Moonga, B. S., Lidbury, P. S., Hecker, M., and Vane, J. R., Osteoclastic inhibition: an action of nitric oxide not mediated by cyclic GMP., *Proceedings of the National Academy of Sciences of the United States of America*, 88, 2936 (1991).

Malek, A. M., Alper, S. L., and Izumo, S., Hemodynamic shear stress and its role in atherosclerosis, *JAMA*, 282, 2035 (1999).

Malinski, T. and Z. Taha (1992). "Nitric oxide release from a single cell measured in situ by a porphyrinic-based microsensor [see comments]." *Nature* 358(6388): 676-8.

Malinski, T., Radomski, M. W., Taha, Z., and Moncada, S., Direct electrochemical measurement of nitric oxide released from human platelets, *Biochemical and Biophysical Research Communications*, 194, 960 (1993).

Malinski, T., Radomski, M. W., Taha, Z., and Moncada, S., Direct electrochemical measurement of nitric oxide released from human platelets., *Biochemical and Biophysical Research Communications*, 194, 960 (1993).

Mao, G.; Tsao, Y.; Tirrell, M.; Davis, H. T.; Hessel, V.; Ringsdorf, H. Self-assembly of photopolymerizable bolaform amphiphile mono and multilayers. *Langmuir*, 1993, 9, 3461-3470.

Marzocchi, A., Marrozzini, C., Piovaccari, G., Fattori, R., Castriota, F., D'Anniballe, G., Branzi, A., and Magnani, B., [Restenosis after coronary angioplasty: its pathogenesis and prevention], *Cardiologia*, 36, 309 (1991).

Mazzucato, M., Spessotto, P., Masotti, A., De Appollonia, L., Cozzi, M. R., Yoshioka, A., Ferris, R., Colombatti, A., and De Marco, L., Identification of domains responsible for von Willebrand factor type VI collagen interaction mediating platelet adhesion under high flow., *Journal of Biological Chemistry*, 274, 3033 (1999).

McCann, D. S., Tokarsky, J., and Sorkin, R. P., Radioimmunoassay for plasma thromboxane B₂, *Clinical Chemistry*, 27, 1417 (1981).

McEver, R. P. and M. N. Martin (1984). "A monoclonal antibody to a membrane glycoprotein binds only to activated platelets." *Journal of Biological Chemistry* 259(15): 9799-804.

McEver, R. P. (1990). "Properties of GMP-140, an inducible granule membrane protein of platelets and endothelium." *Blood Cells* 16(1): 73-80; discussion 80-3.

McGregor, J.; Clemetson, K.; James, E.; Luscher, E.; Dechavanne, M. *Biochim. Biophys. Acta.*, 1980, 599, 473.

Mellion, B. T., Ignarro, L. J., Ohlstein, E. H., Pontecorvo, E. G., Hyman, A. L., and Kadowitz, P. J., Evidence for the inhibitory role of guanosine 3', 5'-monophosphate in ADP-induced human platelet aggregation in the presence of nitric oxide and related vasodilators., *Blood*, 57, 946 (1981).

Mendelsohn, M. E., O'Neill, S., George, D., and Loscalzo, J., Inhibition of fibrinogen binding to human platelets by S-nitroso-N-acetylcysteine, *Journal of Biological Chemistry*, 265, 19028 (1990).

Michelson, A. D., Ellis, P. A., Barnard, M. R., Matic, G. B., Viles, A. F., and Kestin, A. S., Downregulation of the platelet surface glycoprotein Ib-IX complex in whole blood stimulated by thrombin, adenosine diphosphate, or an in vivo wound [see comments], *Blood*, 77, 770 (1991).

Michelson, A. D., Benoit, S. E., Furman, M. I., Breckwoldt, W. L., Rohrer, M. J., Barnard, M. R., and Loscalzo, J., Effects of nitric oxide/EDRF on platelet surface glycoproteins, *American Journal of Physiology*, 270, H1640 (1996).

Michelson, A. D., Barnard, M. R., Krueger, L. A., Frelinger, A. L. r., and Furman, M. I., Evaluation of platelet function by flow cytometry, *Methods*, 21, 259 (2000).

Modderman, P. W., Admiraal, L. G., Sonnenberg, A., and von dem Borne, A. E., Glycoproteins V and Ib-IX form a noncovalent complex in the platelet membrane, *Journal of Biological Chemistry*, 267, 364 (1992).

Möhwald, H. *Colloids Surf.*, 2000, 171, 25.

Moncada, S., Palmer, R. M., and Higgs, E. A., Biosynthesis of nitric oxide from L-arginine. A pathway for the regulation of cell function and communication., *Biochemical Pharmacology*, 38, 1709 (1989).

Moritz, M. W., Reimers, R. C., Baker, R. K., Sutura, S. P., and Joist, J. H., Role of cytoplasmic and releasable ADP in platelet aggregation induced by laminar shear stress, *Journal of Laboratory and Clinical Medicine*, 101, 537 (1983).

Moroi, M., Jung, S. M., Shinmyozu, K., Tomiyama, Y., Ordinas, A., and Diaz_Ricart, M., Analysis of platelet adhesion to a collagen-coated surface under flow conditions: the involvement of glycoprotein VI in the platelet adhesion., *Blood*, 88, 2081 (1996).

Moroi, M. and S. M. Jung (1997). "Platelet receptors for collagen." *Thrombosis and Haemostasis* 78(1): 439-44.

Murad, F. (1999). "Discovery of some of the biological effects of nitric oxide and its role in cell signaling." *Bioscience Reports* 19(3): 133-54.

Murata, K., Izuka, K., and Furuhashi, T., Effects of chondroitin polysulphate on thrombus-formation and serum lipid levels, *Experientia*, 25, 611 (1969).

Mustard, J. F., Packham, M. A., Kinlough-Rathbone, R. L. (1990). "Platelets, Blood flow, and the vessel wall." *Circulation* 81(suppl I): I-24-I27.

Nakamura, T., Kambayashi, J., Okuma, M., and Tandon, N. N., Activation of the GP IIb-IIIa complex induced by platelet adhesion to collagen is mediated by both $\alpha 2\beta 1$ integrin and GP VI, *Journal of Biological Chemistry*, 274, 11897 (1999).

Naqvi, T. Z., Shah, P. K., Ivey, P. A., Molloy, M. D., Thomas, A. M., Panicker, S., Ahmed, A., Cercek, B., and Kaul, S., Evidence that high-density lipoprotein cholesterol is an independent predictor of acute platelet-dependent thrombus formation, *American Journal of Cardiology*, 84, 1011 (1999).

Nieuwenhuis, H. K., van Oosterhout, J. J., Rozemuller, E., van Iwaarden, F., and Sixma, J. J., Studies with a monoclonal antibody against activated platelets: evidence that a secreted 53,000-molecular weight lysosome-like granule protein is exposed on the surface of activated platelets in the circulation, *Blood*, 70, 838 (1987).

NIH, 2000. <http://rsb.info.nih.gov/nih-image/>

Niimi, Y., Ichinose, F., Ishiguro, Y., Terui, K., Uezono, S., Morita, S., and Yamane, S., The effects of heparin coating of oxygenator fibers on platelet adhesion and protein adsorption., *Anesthesia and Analgesia*, 89, 573 (1999).

O'Brien, J. R. (1990). "Shear-induced platelet aggregation." *Lancet* 335(8691): 711-3.

Onda, M.; Ariga, K.; Kunitake, T. Activity and stability of glucose oxidase in molecular films assembled alternately with polyions. *J. Biosci. Bioeng.*, 1999, 87, 69-75.

Oura, Y. (1994). "[The effects of platelet-activating factor (PAF) on the collagen-induced whole blood aggregation]." *Rinsho Byori. Japanese Journal of Clinical Pathology* 42(1): 63-9.

Palmer, R. M., Ferrige, A. G., and Moncada, S., Nitric oxide release accounts for the biological activity of endothelium-derived relaxing factor., *Nature*, 327, 524 (1987).

Papadopoulos, N. G., Dedoussis, G. V., Spanakos, G., Gritzapis, A. D., Baxevanis, C. N., and Papamichail, M., An improved fluorescence assay for the determination of lymphocyte-mediated cytotoxicity using flow cytometry., *Journal of Immunological Methods*, 177, 101 (1994).

Patton, S. R. (1997) Nitric Oxide in the Cardiovascular System. Ph. D Dissertation, Oakland University. 53-53.

Pigazzi, A., Heydrick, S., Folli, F., Benoit, S., Michelson, A., and Loscalzo, J., Nitric oxide inhibits thrombin receptor-activating peptide-induced phosphoinositide 3-kinase activity in human platelets, *Journal of Biological Chemistry*, 274, 14368 (1999).

Pitrowski, J. J., Hunter, G. C., Eskelson, C. D., Sethi, G. K., Copeland, J. C., McIntyre, K. E., Cottrell, E. D., Aguirre, M. L., and Bernhard, V. M., Lipid peroxidation: a possible factor in late graft failure of coronary artery bypass grafts., *Journal of Vascular Surgery*, 13, 652 (1991).

Plow, E. F., Srouji, A. H., Meyer, D., Marguerie, G., and Ginsberg, M. H., Evidence that three adhesive proteins interact with a common recognition site on activated platelets, *Journal of Biological Chemistry*, 259, 5388 (1984).

Pommersheim, R.; Schrezenmeir, J.; Vogt, W. Immobilization of enzymes by multilayer microcapsules. *Macromol. Chem. Phys.*, 1994, 195, 1557-1567.

Prentice, C. R. (1990). "Pathogenesis of thrombosis." *Haemostasis* 20 Suppl 1: 50-9.

Pytela, R., Pierschbacher, M. D., Ginsberg, M. H., Plow, E. F., and Ruoslahti, E., Platelet membrane glycoprotein IIb/IIIa: member of a family of Arg-Gly-Asp--specific adhesion receptors, *Science*, 231, 1559 (1986).

Qiu, X., S. Leporatti, E. Donath, and H. Möhwald, "Studies on the Drug Release Properties of Polysaccharide Multilayers Encapsulated Ibuprofen Microparticles", *Langmuir*, 2001; 17(17); 5375-5380.

Radomski, M. W., Palmer, R. M., and Moncada, S., Endogenous nitric oxide inhibits human platelet adhesion to vascular endothelium, *Lancet*, 2, 1057 (1987).

Rasmussen, C., Thiis, J. J., Clemmensen, P., Efsen, F., Arendrup, H. C., Saunamaki, K., Madsen, J. K., and Pettersson, G., Significance and management of early graft failure after coronary artery bypass grafting: feasibility and results of acute angiography and re-vascularization., *European Journal of Cardio-Thoracic Surgery*, 12, 847 (1997).

Rosenblum, W. I (1997). "Platelet adhesion and aggregation without endothelial denudation or exposure of basal lamina and/or collagen." *Journal of Vascular Research* 34(6): 409-17.

Rosenfeld, S. I., Looney, R. J., Leddy, J. P., Phipps, D. C., Abraham, G. N., and Anderson, C. L., Human platelet Fc receptor for immunoglobulin G. Identification as a 40,000-molecular-weight membrane protein shared by monocytes, *Journal of Clinical Investigation*, 76, 2317 (1985).

Ross, M. H., Romrell, L. J., Kaye, G. I. (1995a). *Connective Tissue. Histology A Text and Atlas*. Baltimore, Williams & Wilkins: 94-115.

Ross, J. M., McIntire, L. V., Moake, J. L., and Rand, J. H., Platelet adhesion and aggregation on human type VI collagen surfaces under physiological flow conditions, *Blood*, 85, 1826 (1995).

Ruggeri, Z. M., Bader, R., and de Marco, L., Glanzmann thrombasthenia: deficient binding of von Willebrand factor to thrombin-stimulated platelets, *Proceedings of the National Academy of Sciences of the United States of America*, 79, 6038 (1982).

Ruggeri, Z. M. (1991). "The platelet glycoprotein Ib-IX complex." *Progress in Hemostasis and Thrombosis* 10: 35-68.

Saelman, E. U., Nieuwenhuis, H. K., Hese, K. M., de Groot, P. G., Heijnen, H. F., Sage, E. H., Williams, S., McKeown, L., Gralnick, H. R., and Sixma, J. J., Platelet adhesion to collagen types I through VIII under conditions of stasis and flow is mediated by GPIa/IIa (alpha 2 beta 1-integrin)., *Blood*, 83, 1244 (1994).

Salvemini, D., de Nucci, G., Gryglewski, R. J., and Vane, J. R., Human neutrophils and mononuclear cells inhibit platelet aggregation by releasing a nitric oxide-like factor, *Proceedings of the National Academy of Sciences of the United States of America*, 86, 6328 (1989).

Samuelsson, B., Hamberg, M., Malmsten, C., and Svensson, J., The role of prostaglandin endoperoxides and thromboxanes in platelet aggregation, *Advances in Prostaglandin and Thromboxane Research*, 2, 737 (1976).

Sander, H. J., Slot, J. W., Bouma, B. N., Bolhuis, P. A., Pepper, D. S., and Sixma, J. J., Immunocytochemical localization of fibrinogen, platelet factor 4, and beta thromboglobulin in thin frozen sections of human blood platelets, *Journal of Clinical Investigation*, 72, 1277 (1983).

Sato, J., Nair, K., Hiddinga, J., Eberhardt, N. L., Fitzpatrick, L. A., Katusic, Z. S., and O'Brien, T., eNOS gene transfer to vascular smooth muscle cells inhibits cell proliferation via upregulation of p27 and p21 and not apoptosis., *Cardiovascular Research*, 47, 697 (2000).

Sauerbrey, G. Z. *Physik.*, 1959, 155, 206.

Schmitt, J.; Grünwald, T.; Krajer, K.; Pershan, P.; Decher, G.; Lösche, M. The internal structure of layer-by-layer adsorbed polyelectrolyte films: a neutron and X-ray reflectivity study. *Macromolecules*, 1993, 26, 7058-7063.

Schmitt, J.; Decher, G.; Dressik, W.; Brandow, S.; Geer, R.; Shashidhar, R.; Calvert, J. Metal nanoparticles / polymer superlattice films: Fabrication and control of layer structure. *Adv. Materials*, 1997, 9, 61-65.

Schwartz, R. S., Murphy, J. G., Edwards, W. D., Camrud, A. R., Vliestra, R. E., and Holmes, D. R., Restenosis after balloon angioplasty. A practical proliferative model in porcine coronary arteries, *Circulation*, 82, 2190 (1990).

Sekimoto, H. (1980). “[Lipid metabolism and atherosclerosis--especially on ultrastructure of endothelial free surface in human arteries related to thrombus and atherosclerosis (author's transl)].” *Nippon Naika Gakkai Zasshi. Journal of Japanese Society of Internal Medicine* 69(10): 1250-5.

Senogles, SE, and Nelsestuen, GL, (1983). von Willebrand factor. A protein which binds at the cell surface interface between platelets *J. Biol. Chem.* 258: 12327-12333.

Shattil, S. J., Hoxie, J. A., Cunningham, M., and Brass, L. F., Changes in the platelet membrane glycoprotein IIb.IIIa complex during platelet activation, *Journal of Biological Chemistry*, 260, 11107 (1985).

Shattil, S. J., Cunningham, M., and Hoxie, J. A., Detection of activated platelets in whole blood using activation-dependent monoclonal antibodies and flow cytometry, *Blood*, 70, 307 (1987).

Shattil, S. J., Regulation of platelet anchorage and signaling by integrin alpha IIb beta 3, *Thrombosis and Haemostasis*, 70, 224 (1993).

Shattil, S. J. and M. H. Ginsberg (1997). “Perspectives series: cell adhesion in vascular biology. Integrin signaling in vascular biology.” *Journal of Clinical Investigation* 100(1): 1-5.

Shattil, S. J., Kashiwagi, H., and Pampori, N., Integrin signaling: the platelet paradigm, *Blood*, 91, 2645 (1998).

Shin, H., Katogi, T., Yozu, R., and Kawada, S., Surgical angioplasty of left main coronary stenosis complicating supraaortic stenosis, *Annals of Thoracic Surgery*, 67, 1147 (1999).

Sixma, J. J. and P. G. de Groot (1991). “von Willebrand factor and the blood vessel wall.” *Mayo Clinic Proceedings* 66(6): 628-33.

Smith, J. B. (1987a). Formation of prostaglandins and thromboxanes. Platelet Responses and Metabolism. II. Receptors and Metabolism. H. Holmsen. Boca Raton, CRC Press: 287.

Smith, J. B. (1987b). “Pharmacology of thromboxane synthetase inhibitors.” *Federation Proceedings* 46(1): 139-43.

Smith, C. C., Stanyer, L., Cooper, M. B., and Betteridge, D. J., Platelet aggregation may not be a prerequisite for collagen-stimulated platelet generation of nitric oxide, *Biochim Biophys Acta*, 1473, 286 (1999).

Sneddon, J. M. and J. R. Vane (1988). "Endothelium-derived relaxing factor reduces platelet adhesion to bovine endothelial cells." *Proceedings of the National Academy of Sciences of the United States of America* 85(8): 2800-4.

Song, M., Li, J., and Yang, F. C., Studies of human platelet ultrastructure and quantitative analyses of membrane glycoprotein IIB/IIIA in shear stress-induced platelet quick release reaction., , 103, 166 (1990).

Steg, P. G., D. Himbert. (1999). "[Angioplasty in acute myocardial infarction]." *Archives Des Maladies Du Coeur Et Des Vaisseaux* 92(11 Suppl): 1627-35.

Stenberg, P. E., Shuman, M. A., Levine, S. P., and Bainton, D. F., Redistribution of alpha-granules and their contents in thrombin-stimulated platelets, *Journal of Cell Biology*, 98, 748 (1984).

Stenberg, P. E., McEver, R. P., Shuman, M. A., Jacques, Y. V., Bainton, D. F. (1985). "A platelet alpha-granule membrane protein (GMP-140) is expressed on the plasma membrane after activation." *Journal of Cell Biology* 101: 880.

Stuehr, D. J., Cho, H. J., Kwon, N. S., Weise, M. F., and Nathan, C. F., Purification and characterization of the cytokine-induced macrophage nitric oxide synthase: an FAD- and FMN-containing flavoprotein., *Proceedings of the National Academy of Sciences of the United States of America*, 88, 7773 (1991).

Sukhorukov, G.; Möhwald, H.; Decher, G.; Lvov, Y. Layer-by-layer assembly of DNA and polynucleotides films by means of alternate adsorption with polycations. *Thin Solid Films*, 1996, 284, 220-223.

Sukhorukov, G.; Moroz, N.; Larionova, N.; Donath, E.; Möhwald, H. Encapsulation of proteins by layer-by-layer adsorption of polyelectrolytes. *J. Microencapsulation*, 2000, 17, 418 -522.

Turitto, V. T., Weiss, H. J., and Baumgartner, H. R., Decreased platelet adhesion on vessel segments in von Willebrand's disease: a defect in initial platelet attachment, *Journal of Laboratory and Clinical Medicine*, 102, 551 (1983).

Turitto, V. T., Weiss, H. J., Zimmerman, T. S., and Sussman, I. I., Factor VIII/von Willebrand factor in subendothelium mediates platelet adhesion, *Blood*, 65, 823 (1985).

Venturini, C. M. and J. E. Kaplan (1992). "Thrombin induces platelet adhesion to endothelial cells." *Seminars in Thrombosis and Hemostasis* 18(2): 275-83.

Wagner, D. D. and V. J. Marder (1984). "Biosynthesis of von Willebrand protein by human endothelial cells: processing steps and their intracellular localization." *Journal of Cell Biology* 99(6): 2123-30.

Wagner, C. L., Mascelli, M. A., Neblock, D. S., Weisman, H. F., Collier, B. S., and Jordan, R. E., Analysis of GPIIb-IIIa receptor number by quantification of 7E3 binding to human platelets, *Blood*, 88, 907 (1996).

Warkentin, T. E., Powling, M. J., and Hardisty, R. M., Measurement of fibrinogen binding to platelets in whole blood by flow cytometry: a micromethod for the detection of platelet activation, *British Journal of Haematology*, 76, 387 (1990).

Weigensberg, B. I., More, R. H., and Sumiyoshi, A., Lipid profile in the evolution of experimental atherosclerotic plaques from thrombus, *Laboratory Investigation*, 33, 43 (1975).

Weiss, H. J., Turitto, V. T., and Baumgartner, H. R., Platelet adhesion and thrombus formation on subendothelium in platelets deficient in glycoproteins IIb-IIIa, Ib, and storage granules, *Blood*, 67, 322 (1986).

White, J. G. (1968). "The dense bodies of human platelets. Origin of serotonin storage particles from platelet granules." *American Journal of Pathology* 53(5): 791-808.

Wu, Y. P., van Breugel, H. H., Lankhof, H., Wise, R. J., Handin, R. I., de Groot, P. G., and Sixma, J. J., Platelet adhesion to multimeric and dimeric von Willebrand factor and to collagen type III preincubated with von Willebrand factor, *Arteriosclerosis, Thrombosis, and Vascular Biology*, 16, 611 (1996).

Yang, Z., Ruschitzka, F., Rabelink, T. J., Noll, G., Julmy, F., Joch, H., Gafner, V., Aleksic, I., Althaus, U., and Luscher, T. F., Different effects of thrombin receptor activation on endothelium and smooth muscle cells of human coronary bypass vessels. Implications for venous bypass graft failure., *Circulation*, 95, 1870 (1997).

Yano, Y., Kambayashi, J., Kawasaki, T., and Sakon, M., Quantitative determination of circulating platelet microparticles by flow cytometry, *International Journal of Cardiology*, 47, S13 (1994).

Yoo, D.; Lee, J.; Rubner, M. Investigations of new self-assembled multilayer thin films based on alternately adsorbed layers of polyelectrolytes and functional dye molecules. *Mat. Res. Symp. Proc.*, 1996, 413, 395-400.

Yoo, D.; Shiratori, S.; Rubner, M. Controlling bilayer composition and surface wettability of sequentially adsorbed multilayers of weak polyelectrolytes. *Macromolecules*, 1998, 31, 4309-4318.

Zeher, A. M. (1996). "Endothelial vasodilator dysfunction: pathogenetic link to myocardial ischaemia or epiphenomenon?" *Lancet* 348 Suppl 1: s10-2.

Zucker-Franklin, D. (1990). Platelet morphology and function. *Hematology*. W. J. Williams, Beutler, E., Erslev, A. J. and Lichtman, M. A. New York, McGraw-Hill, Inc.: 1172-118.